

**UNDERSTORY VARIABILITY OF PHOTOSYNTHETICALLY ACTIVE  
RADIATION IN A MID-ATLANTIC DECIDUOUS FOREST AND ITS  
EFFECTS ON LINDERA BENZOIN L. BLUME (NORTHERN SPICEBUSH)**

by

Janice E. Hudson

A thesis submitted to the Faculty of the University of Delaware in partial fulfillment  
of the requirements for the degree of Master of Science in Geography

Spring 2015

© 2015 Janice E. Hudson  
All Rights Reserved

ProQuest Number: 1596859

All rights reserved

INFORMATION TO ALL USERS

The quality of this reproduction is dependent upon the quality of the copy submitted.

In the unlikely event that the author did not send a complete manuscript and there are missing pages, these will be noted. Also, if material had to be removed, a note will indicate the deletion.



ProQuest 1596859

Published by ProQuest LLC (2015). Copyright of the Dissertation is held by the Author.

All rights reserved.

This work is protected against unauthorized copying under Title 17, United States Code  
Microform Edition © ProQuest LLC.

ProQuest LLC.  
789 East Eisenhower Parkway  
P.O. Box 1346  
Ann Arbor, MI 48106 - 1346

**UNDERSTORY VARIABILITY OF PHOTOSYNTHETICALLY ACTIVE  
RADIATION IN A MID-ATLANTIC DECIDUOUS FOREST AND ITS  
EFFECTS ON LINDERA BENZOIN L. BLUME (NORTHERN SPICEBUSH)**

by

Janice E. Hudson

Approved: \_\_\_\_\_  
Delphis F. Levia, Ph.D.  
Professor in charge of thesis on behalf of the Advisory Committee

Approved: \_\_\_\_\_  
Tracy L. DeLiberty, Ph.D.  
Chair of the Department of Geography

Approved: \_\_\_\_\_  
Nancy M. Targett, Ph.D.  
Dean of the College of Earth, Ocean, and Environment

Approved: \_\_\_\_\_  
James G. Richards, Ph.D.  
Vice Provost for Graduate and Professional Education

## ACKNOWLEDGMENTS

I would like to extend my sincerest gratitude to my advisor Dr. Levia. Without his guidance, assistance and friendship, this thesis would have never been, and I look forward to many more collaborations. I would like to thank: Dr. Bais and his lab for their invaluable instruction and assistance in all aspects of my growth chamber and lab experiments; Dr. Legates for his good humor and his assistance in all things statistics, including the many hours spent working for his multivariate and spatial statistics classes; Fair Hill Natural Resource Management Area for the use of their property; Dr. David Francis for his assistance with plant identification; Bill Bartz for his direction and support at the Fischer Greenhouse Laboratory; Sandra Mather, for her generosity and financial support through the Mather Graduate Fellows Research Grant; the University of Delaware department of Geography faculty, staff, and graduate students, for their unending support and friendship; the staff at DEOS for their assistance with instrumentation, and for allowing me to bumble around with them on field work excursions; Nathaly Rodriguez for her assistance with PAR collection and the ecological survey; and the undergraduates of Dr. Levia's field methods class, who assisted in the collection of the four consecutive hours of PAR measurements in September. I'd like to thank my family for their love, support, and tolerance through this endeavor. I want to acknowledge Oliver, our field assistant in utero, and my post-partum writing buddy. And last but not least, to Sean Hudson, whose assistance in all aspects of this thesis and whose loving partnership in all aspects of my life have been awesomely immeasurable, thank you, thank you, thank you, and I love you more.

## TABLE OF CONTENTS

LIST OF TABLES .....	vii
LIST OF FIGURES .....	ix
ABSTRACT .....	xiv

### Chapter

1	PHYSIOLOGICAL PLANT ECOLOGY: EFFECTS OF VARIATION IN SUBCANOPY PHOTOSYNTHETICALLY ACTIVE RADIATION ON UNDERSTORY PLANTS .....	1
1.1	Phenology and Climate.....	1
1.2	Plant Ecology.....	3
1.3	Photosynthetically Active Radiation .....	4
1.4	Research Question and Rationale .....	10
2	SPATIOTEMPORAL VARIABILITY OF PHOTOSYNTHETICALLY ACTIVE RADIATION AND SPICEBUSH ECOLOGY: A REVIEW OF THE LITERATURE.....	13
2.1	Measurement of PAR .....	13
2.2	PAR and its variability .....	18
2.3	Ecology of <i>Lindera benzoin</i> .....	21
2.4	Beer's Law, pigments, and absorbance .....	27
2.5	Contribution to the Literature .....	29
3	CHARACTERISTICS OF THE STUDY PLOT AT THE FAIR HILL NATURAL RESOURCE MANAGEMENT AREA .....	31
3.1	Location.....	31
3.2	Climate and Weather .....	32
3.3	Plot Description .....	36
4	MATERIALS AND METHODS .....	39
4.1	PAR Collection in the Field .....	39
4.2	Ecological Survey and Mensurational Data .....	45
4.3	<i>Lindera benzoin</i> Treatments .....	45

4.4	Data Analysis.....	51
4.4.1	PAR .....	51
4.4.2	Ecological Survey.....	52
4.4.3	<i>Lindera benzoin</i> Treatments .....	53
5	RESULTS.....	55
5.1	PAR Collection in the Field .....	55
5.1.1	Winter Leafless Phenoseason (November to February) .....	57
5.1.2	Spring Leafless Phenoseason (February to April).....	60
5.1.3	Spring Leafing Phenoseason (April to May).....	63
5.1.4	Summer Leafing Phenoseason (May to June).....	68
5.1.5	Summer Fully-leafed Phenoseason (June to August).....	71
5.1.6	Autumnal Fully-Leafed Phenoseason (August to October) .....	75
5.1.7	Autumnal Partially-Leafed Phenoseason (October to November).....	79
5.1.8	Shrub Layer .....	83
5.1.9	Comparative analysis of PAR across phenoseasons .....	87
5.1.10	Comparative analysis of PAR among locations .....	90
5.1.11	Temporal variation in PAR over the course of an afternoon.....	98
5.2	Ecological Survey.....	100
5.3	<i>Lindera benzoin</i> Treatments .....	103
5.3.1	Physical Results.....	104
5.3.1.1	Comparison of plants grown at 350 $\mu\text{mol m}^{-2} \text{s}^{-1}$ .....	106
5.3.1.2	Comparison of plants grown at 150 $\mu\text{mol m}^{-2} \text{s}^{-1}$ .....	107
5.3.1.3	Comparison of all plants from Experiments 1 and 2..	107
5.3.2	Spectrophotometry Results.....	114
5.3.2.1	Comparison of plants grown at 350 $\mu\text{mol m}^{-2} \text{s}^{-1}$ .....	117
5.3.2.2	Comparison of plants grown at 150 $\mu\text{mol m}^{-2} \text{s}^{-1}$ .....	117
5.3.2.3	Comparison of all plants from Experiments 1 and 2, and Field Plant .....	118
6	DISCUSSION AND CONCLUSION .....	132
6.1	Spatial and temporal distribution of PAR in the field .....	132
6.1.1	Discussion of the Spring Leafless phenoseason .....	133

6.2	<i>Lindera benzoin</i> response to changes in PAR .....	134
6.3	Future research & factors not considered .....	138
REFERENCES .....		139
Appendix		
A	FAIR HILL (DFHM) DEOS STATION INSTRUMENTATION .....	144
B	COMPLETED FIELD SHEET EXAMPLE .....	145
C	COPYRIGHT PERMISSIONS .....	147
D	L. BENZOIN ILLUSTRATION .....	154

## LIST OF TABLES

Table 1: Studies of PAR by forest and sensor type. ....	15
Table 2: Some examples of light values at the forest floor by differing canopy species, expressed as a percent of the total above canopy light. ....	17
Table 3: Temperature and Precipitation for the Study Period Compared to 30-yr Climate Norms .....	35
Table 4: Number of times readings were collected during a 15 minute period during each phenoseason.....	43
Table 5: Summary descriptive statistics of understory PAR ( $\mu\text{mol m}^{-2} \text{s}^{-1}$ ) for each phenoseason.....	57
Table 6: Summary descriptive statistics of PAR ( $\mu\text{mol m}^{-2} \text{s}^{-1}$ ) for selected days of the winter leafless phenoseason. ....	59
Table 7: Summary descriptive statistics of PAR ( $\mu\text{mol m}^{-2} \text{s}^{-1}$ ) for selected days of the spring leafless phenoseason.....	62
Table 8: Summary descriptive statistics of PAR ( $\mu\text{mol m}^{-2} \text{s}^{-1}$ ) for selected days of the spring leafing phenoseason.....	67
Table 9: Summary descriptive statistics of PAR ( $\mu\text{mol m}^{-2} \text{s}^{-1}$ ) for selected days of the summer leafing phenoseason.....	70
Table 10: Summary descriptive statistics of PAR ( $\mu\text{mol m}^{-2} \text{s}^{-1}$ ) for selected days of the summer fully-leafed phenoseason. ....	74
Table 11: Summary descriptive statistics of PAR ( $\mu\text{mol m}^{-2} \text{s}^{-1}$ ) for selected days of the autumnal fully-leafed phenoseason. ....	78
Table 12: Summary descriptive statistics of PAR ( $\mu\text{mol m}^{-2} \text{s}^{-1}$ ) for selected days of the autumnal partially-leafed phenoseason. ....	82
Table 13: Descriptive statistics of PAR by phenoseason. ....	86

Table 14: Comparison of winter and summer clear and overcast days, showing that winter overcast conditions increased subcanopy radiation, while summer overcast conditions decreased subcanopy radiation ( $\mu\text{mol m}^{-2} \text{s}^{-1}$ ).	90
Table 15: Descriptive statistics of annual PAR ( $\mu\text{mol m}^{-2} \text{s}^{-1}$ ) for each location.*	91
Table 16: Descriptive statistics of PAR in $\mu\text{mol m}^{-2} \text{s}^{-1}$ for each location during four consecutive hours on September 26, 2014.	99
Table 17: Trees and shrubs in the Fair Hill NRMA plot.	101
Table 18: Descriptive statistics of measured physical characteristics by experiment.	105
Table 19: Standardized coefficients for canonical variables of physical attributes.	112
Table 20: Classification functions of measured physical attributes.	112
Table 21: Mahalanobis distances between groups.	113
Table 22: Posterior probabilities of cases of physical attributes. Incorrectly classified cases are marked with a *.	114
Table 23: Descriptive statistics for chemical attribute variables.	115
Table 24: Foliar sample weights used for spectrophotometry.	115
Table 25: Standardized coefficients for canonical variables of chemical attributes.	123
Table 26: Classification functions of measured chemical attributes.	123
Table 27: Squared Mahalanobis distances from group centroid for chemical attribute discriminant analysis. Incorrectly classified cases are marked with a *.	126
Table 28: Posterior probabilities for cases from chemical attribute discriminant analysis. Incorrectly classified cases are marked with a *.	129
Table 29: Fair Hill (DFHM) DEOS station instrumentation.	144

## LIST OF FIGURES

Figure 1: From Hutchison & Matt (1977); “Phenoseasons in the tulip poplar forest.” .....	2
Figure 2: The absorption spectrum of chlorophyll a, chlorophyll b, and carotenoids and the rate of photosynthesis at a corresponding wavelength.....	6
Figure 3: From Hutchison & Matt (1977); “Synthesized annual course of average daily total solar radiation received within and above a tulip poplar forest. Langleys x $4.184 \times 10^4 = \text{J/m}^2$ .” .....	8
Figure 4: Spicebush on April 10, 2014 and April 19, 2015. ....	21
Figure 5: Spicebush drupes in June (left) and early September (right). ....	22
Figure 6: Spicebush present under <i>L. tulipifera</i> . ....	23
Figure 7: Spicebush leaves senescing to yellow in autumn. ....	24
Figure 8: Spicebush Swallowtail ( <i>Papilio troilus</i> ). Photo by J. Hudson, near field site. ....	25
Figure 9: Female Spicebush silkmoth ( <i>Callosamia promethea</i> ). Photo by S. Hudson, field site.....	26
Figure 10: Personal illustration of <i>L. benzoin</i> seedling. ....	27
Figure 11: Fair Hill NRMA in relation to the greater Mid-Atlantic region. ....	32
Figure 12: Map showing the distance between the PAR collection site and the DEOS station where meteorological variables are measured. ....	33
Figure 13: DEOS Station at Fair Hill NRMA .....	34
Figure 14: Seasonal changes in the study plot from upper left: winter, spring, late summer, and autumn. ....	37
Figure 15: Aspect map of PAR collection site. ....	37

Figure 16: Slope (%) map of PAR collection site. ....	38
Figure 17: Aerial view of the plot, with observation points. ....	40
Figure 18: Path taken through the field site to collect readings. ....	41
Figure 19: Example of a field sheet used to record PAR observation data. ....	44
Figure 20: Spectral distribution of MH400, courtesy of Philips Lighting North America. ....	46
Figure 21: Workflow diagram of the <i>L. benzoin</i> experiments. Seeds germinated and grew for 60 days in the lab, were transferred to the growth chamber and kept under experimental conditions for ~35 days, were harvested and measured, then finally the fourth and fifth leaves were used for spectrophotometry. ....	48
Figure 22: Workflow diagram of fatal measurements and spectrophotometry. ....	50
Figure 23: Line plot of collected field data for open readings (Open PAR) plotted next to PAR and solar radiation data from the meteorological station nearby. ....	55
Figure 24: Box plot of PAR values at each location for the winter leafless phenoseason. ....	58
Figure 25: Distributions of PAR for varying sky conditions in the winter leafless phenoseason. ....	60
Figure 26: Box plot of PAR values at each location for the spring leafless phenoseason. ....	61
Figure 27: Distribution of PAR values for three sky conditions during the spring leafless phenoseason. ....	63
Figure 28: Box plot of PAR values at each location for the spring leafing phenoseason. ....	64
Figure 29: Leaf-out canopy changes: a one month period spanning the end of the spring leafing phenoseason and beginning of the summer leafing phenoseason. From left to right: April 24, May 6, and May 24, 2014. ...	65
Figure 30: Line plot of leaf area index versus the ln of Average PAR for a ten week period from March 27 <sup>th</sup> to May 24 <sup>th</sup> . Trend shows that as leaf out occurs, and LAI increases, average subcanopy PAR decreases. ....	66

Figure 31: Distribution of PAR values for three sky conditions during the spring leafing phenoseason. ....	68
Figure 32: Box plot of PAR values at each location for the summer leafing phenoseason.....	69
Figure 33: Distributions of PAR values for three sky conditions during the summer leafing phenoseason. ....	71
Figure 34: Box plot of PAR values on a log scale at each location for the summer fully-leafed phenoseason. ....	72
Figure 35: Canopy on June 29, 2014.....	73
Figure 36: Distribution of PAR values for three sky conditions during the summer fully-leafed phenoseason. ....	75
Figure 37: Box plot of PAR values on a log scale at each location for the autumnal fully-leafed phenoseason. ....	76
Figure 38: Canopy on September 20, 2014.....	77
Figure 39: Distribution of PAR values for three sky conditions during the autumnal fully-leafed phenoseason. ....	79
Figure 40: Box plot of PAR values at each location for the autumnal partially-leafed phenoseason. ....	80
Figure 41: Canopy on November 2, 2014.....	81
Figure 42: Distribution of PAR values for three sky conditions during the autumnal partially-leafed phenoseason. ....	83
Figure 43: Mean annual PAR (by day of the year in $\mu\text{mol m}^{-2} \text{s}^{-1}$ ) in the open and at three levels beneath the canopy. ....	84
Figure 44: Results of an ANOVA of mean PAR by phenoseason; means and confidence intervals (95%) of understory, shrub mid-level and shrub low-level PAR. ....	85
Figure 45: Contour plot of annual course of average daily total PAR received within and above our plot canopy. Contours represent $\mu\text{mol m}^{-2} \text{s}^{-1}$ . ....	88
Figure 46: Box plot of PAR by phenoseason. ....	89

Figure 47: PAR ( $\mu\text{mol m}^{-2} \text{s}^{-1}$ ) on a log scale by phenoseason for locations 0 (open), 1, 2, and 3.....	92
Figure 48: PAR ( $\mu\text{mol m}^{-2} \text{s}^{-1}$ ) on a log scale by phenoseason for locations 4, 5, 6, and 7. ....	93
Figure 49: PAR ( $\mu\text{mol m}^{-2} \text{s}^{-1}$ ) on a log scale by phenoseason for locations 8, 9, 10, and 11. ....	94
Figure 50: PAR ( $\mu\text{mol m}^{-2} \text{s}^{-1}$ ) one a log scale by phenoseason for locations 12, 13, 14, and 15. ....	95
Figure 51: PAR ( $\mu\text{mol m}^{-2} \text{s}^{-1}$ ) on a log scale by phenoseason for locations 16, 17, 18, and 19. ....	96
Figure 52: PAR ( $\mu\text{mol m}^{-2} \text{s}^{-1}$ ) on a log scale by phenoseason for locations 20, 21, 22, and 23. ....	97
Figure 53: PAR ( $\mu\text{mol m}^{-2} \text{s}^{-1}$ ) on a log scale by phenoseason for locations 24 and 25. ....	98
Figure 54: Scatterplot of subcanopy PAR and the adjusted PAR from the Fair Hill DEOS station PAR (adjusted) in the open over a 4 hour period, showing the “arc” of the sun across the sky and the only slight decrease in subcanopy PAR. ....	100
Figure 55: Tree locations with respect to <i>L. benzoin</i> locations represented as a binary “present” or “not present” using 2m cells. ....	102
Figure 56: Results of a Ripley’s K analysis, showing the observed significant clustering of <i>L. benzoin</i> within the plot. ....	103
Figure 57: Subset of plants grown for experiment 1, with lower level PAR plants shown on the left, and upper level PAR plants shown on the right. ....	106
Figure 58: Subset of plants grown for experiment 1, with upper level PAR plants shown on the left, and lower level PAR plants shown on the right. ....	107
Figure 59: Box plot of means of dry root-shoot ratios for all experiments .....	108
Figure 60: Box plot of means of total dry weight (mg) for all experiments. ....	109
Figure 61: Box plot of means of initial stomatal conductance ( $\text{mmol m}^{-2} \text{s}^{-1}$ ) for all experiments .....	109

Figure 62: Box plot of means of secondary stomatal conductance ( $\text{mmol m}^{-2} \text{s}^{-1}$ ) for all experiments.....	110
Figure 63: Scatterplot of the canonical scores of the physical attributes. ....	113
Figure 64: Graphical representation of the results of the Tukey-Kramer All Pairs test of significance for chlorophyll a, and its associated ordered differences report.....	119
Figure 65: Box plot and mean diamonds of chlorophyll b results for all experiments. ....	120
Figure 66: Box plot and mean diamonds of total carotenoid (%) results for all experiments. ....	120
Figure 67: Box plot and mean diamonds of carotenoid to chlorophyll ratio for all experiments. ....	121
Figure 68: Box plots and mean diamonds for chlorophyll a to b ratio results for all experiments. ....	121
Figure 69: Scatterplot of the canonical scores of the chemical attributes for Root 1 vs Root 2.....	124
Figure 70: Scatter plot of the canonical scores of the chemical attributes for Root 1 vs Root 3.....	125
Figure 71: Scatter plot of the canonical scores of the chemical attributes for Root 2 vs Root 3.....	126
Figure 72: Photograph of plant “U6”, a plant on the upper level of Experiment 1, showing evidence of viral infection. ....	137

## ABSTRACT

Photosynthetically active radiation (PAR, 400-700 nm) is of critical importance to the physiological ecology of plants, partially governing photosynthesis and the carbon balance of forest ecosystems. The spatiotemporal variability of PAR is particularly critical for understory shrub species which rely on uneven PAR inputs for their survival. Employing a combination of field and laboratory techniques over the seven phenoseasons of deciduous forests, this research sought to better understand the spatial and temporal dynamics of subcanopy PAR and link differences in the length and intensity of PAR to the physiological ecology of *Lindera benzoin* L. Blume (northern spicebush).

Nearly 4,600 individual observations of PAR were made under a Mid-Atlantic deciduous forest canopy to quantify the effect of phenoseason on the spatial and temporal distribution of light reaching the subcanopy and how this distribution of light impacted *L. benzoin* within the plot. Additionally, laboratory experiments were conducted to assist in the quantification of the effect of various photointensities on the physiological ecology of *L. benzoin*. Health was determined by monitoring physical growth and biomass, as well as the amount of chlorophyll a, chlorophyll b, and carotenoid by way of UV-vis spectrophotometry.

The leafless subcanopy PAR values were almost 10 times higher than leafed season PAR. Sunflecks and sun patches could be three orders of magnitude higher than the subcanopy mean during the leafed season. Phenoseason (i.e. the combination of canopy state and celestial geometry) is responsible for nearly three-quarters of the

variation between levels in this mid-Atlantic deciduous forest. Understory PAR is typically less than 40% of open PAR, values of PAR in the shrub canopy are often ~5% lower than the subcanopy.

Growth of spicebush in the field is significantly clustered. Locations with spicebush growth are in the top 36% of annual PAR receipt. UV-vis spectrophotometry showed significant differences in Root to shoot ratios, biomass, initial stomatal conductance, and all chemical attributes. Changes in photointensity resulted in significant changes in biomass. Spicebush under lab conditions do significantly alter their individual pigments and pigment ratios in response to high intensity light conditions. Temporal light sequences in the field may be a very important factor in the health of northern spicebush.

This work represents a novel approach to measuring photosynthetic photon flux density. By utilizing instruments capable of providing the user with a 15 second spatially integrated one meter linear average of the PPFD, obtaining measurements at multiple locations and elevations in the subcanopy over a full year for all cloud conditions, and coupling our research with detailed laboratory experiments, we are able to synthesize our understanding of PAR and its impact on the ecology and physiology of a common and significant regional understory plant.

## Chapter 1

# PHYSIOLOGICAL PLANT ECOLOGY: EFFECTS OF VARIATION IN SUBCANOPY PHOTOSYNTHETICALLY ACTIVE RADIATION ON UNDERSTORY PLANTS

### 1.1 Phenology and Climate

Most living organisms will experience many physical changes throughout their lifespan, many of which may be cyclical. The study of this periodic change in biota (including hibernation, migration, and metamorphosis) as related to climate, is called phenology. For example, in a temperate forest, deciduous plants experience a change in phenological state - also called a phenophase - as the energy of solar radiation changes throughout the year causing budding, flowering and fruiting, and leaf growth, leaf senescence, and leaf fall. Hutchison and Matt (1977) defined these seasonal radiation conditions as phenoseasons – "...segment[s] of the year during which the prevailing earth-sun geometry and phenological state of the forest create a unique set of conditions which determine forest radiation regimes." By combining the timing of the primary seasonal solar conditions with that of canopy phenophase, seven unique phenoseasons were created for a temperate deciduous forest. The phenoseasons, in chronological order from full leaf-off conditions are: winter leafless, spring leafless, spring leafing, summer leafing, summer fully-leafed, autumnal fully-leafed, and autumnal partially leafed. These phenoseasons can be seen, for a mid-latitude deciduous forest, in Figure 1. While these dates work well for a study in a mid-latitude

deciduous forest, it would be necessary to adjust these phenoseasons by latitude, and likely by species as well.

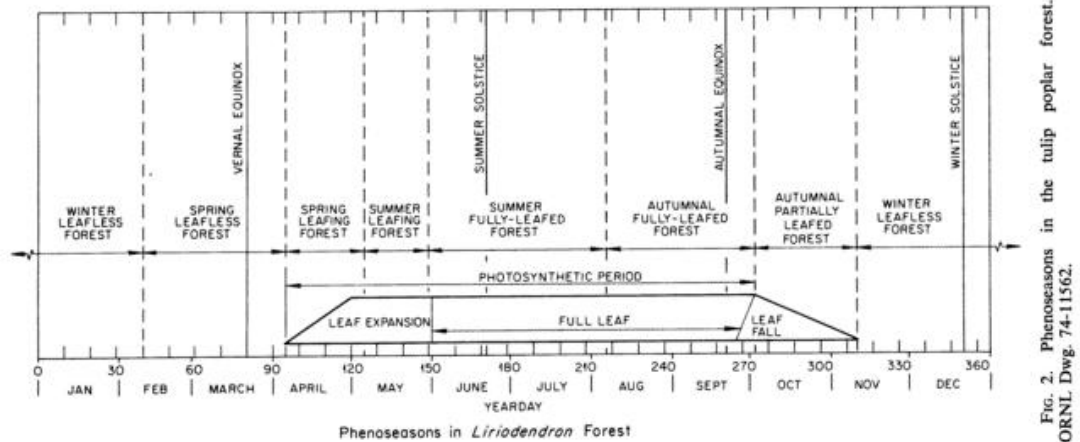


Figure 1: From Hutchison & Matt (1977); “Phenoseasons in the tulip poplar forest.”<sup>1</sup>

These differences in the amount of insolation by latitude due to Earth-Sun geometry, in conjunction with atmospheric thickness and global, regional, and synoptic circulations – which can affect the receipt of this energy at the surface – have a profound impact on the ecology of a location (Baldochi *et al.* 1984; Hutchison and Matt 1977; Richardson *et al.* 2013). For example, soil moisture, evapotranspiration, precipitation and plant species will all be affected by these variables (Hanson and Wullschleger 2003).

---

<sup>1</sup> Republished with permission of Ecological Society of America from “The Distribution of Solar Radiation within a Deciduous Forest,” Hutchison and Matt, Ecological Monographs, 47(2), 1977; permission conveyed through Copyright Clearance Center, Inc.

Conditions influencing forest species composition and plant growth and phenophase are not strictly limited to solar radiation; additional variables include temperature, precipitation, soil type and terrain, among others. As Earth's climate continues to change, so will the regional species composition of canopy trees, and therefore the sub-canopy climate and radiation regime and the understory plants which thrive in it. Studies such as the Walker Branch Throughfall Displacement Experiment, as highlighted by Hanson and Wullschleger (2003) emphasize that temperate deciduous forests will experience both ecological and physiological changes in response to even just one climatic variable (precipitation), and that without further impact studies, we cannot understand the magnitude of these regional changes.

## **1.2 Plant Ecology**

In a forested area, the distribution and physical characteristics of individual trees can greatly affect water inputs, nutrient quality, nutrient quantity, and rates of photosynthetic photon flux density at the forest floor. Bark storage capacity and texture, as well as canopy structure have been shown to affect hydrologic and nutrient inputs at the forest floor (Levia and Herwitz 2005; Levia and Herwitz 2002; Levia and Herwitz 2000; Parker 1983). The smooth bark of an American beech has been shown to quickly direct a large amount of intercepted precipitation down its bole as stemflow, whereas the furrowed bark of a yellow poplar will reduce stemflow (Levia *et al.* 2010; Siegert and Levia 2014). Andersson (1991) demonstrated that the physiology and growth strategy of old growth oaks influenced soil nutrition via stemflow and throughfall, and thus the species growing directly beneath. Canopy trees redistribute the temporal and spatial quantity and quality of light that can be

utilized by understory species (de Castro 2000; Chazdon and Pearcy 1991; Gendron *et al.* 2001; Leuchner *et al.* 2007). Being such modifying factors in the ecosystem, canopy trees can profoundly alter the species composition, abundance, and success of understory plants (Andersson 1991; Canham *et al.* 1999; Chazdon and Pearcy 1991; Leuchner *et al.*, 2011). Plants and shrubs adapted to forest understories must be able to acquire the resources necessary for their own survival in the limiting environments created by such large interspecific competitors as trees (Hojjati *et al.*, 2008; Perry *et al.*, 1969; Pukkala *et al.*, 1991; Richardson *et al.*, 2013), while also competing against other understory plants for resources and preserving themselves against herbivory. These environments present a very specific set of challenges for understory plants whose growth strategies must modify for both short and long term changes in understory microclimate.

Seasonality is particularly important to understory plants, which must utilize solar energy and available nutrients in shade environments for growth and reproduction while these very factors are constantly changed by canopy species. Acquisition and allocation of resources, and efficient use of those resources, is of the utmost importance in the survival of understory plants.

### **1.3 Photosynthetically Active Radiation**

Taiz and Zeiger (2010) explain photosynthesis as the process by which plants use solar energy to convert carbon dioxide and water into carbohydrates and oxygen ( $\text{CO}_2 + \text{H}_2\text{O} + \text{light} \rightarrow \text{CH}_2\text{O} + \text{O}_2$ ). This process takes place inside plant cells, inside a structure called a chloroplast. Within the chloroplasts are the chlorophylls and carotenoids that funnel high energy light down an energy staircase of antenna pigments, reducing the energy each time so that it is at a usable level when it reaches

the specialized chlorophylls that make up the reaction center. In the reaction center, a redox reaction (carbon dioxide is reduced, water is oxidized) takes place that creates the energy storage molecules that plants use to complete all their other functions.

Photosynthetically active radiation, or PAR, is the spectral range of light from 400-700 nm (Leuchner *et al.*, 2007). These wavelengths, which correspond closely with what we see as our visible light spectrum, are available to plants for photosynthesis. Chlorophyll, a critical pigment in plant photosynthesis, easily absorbs wavelengths of blue (450-495 nm) and red (620-700 nm), and reflects green wavelengths (495-570 nm) (Figure 2). All chlorophyllic plants require light in the range of 400-700 nm to conduct photosynthesis (Taiz & Zeiger, 2010). Many understory plants have acquired shade tolerance or have even become shade-loving. These plants require less light energy, fewer hours of daylight, less intense daylight, or can thrive in highly variable PAR conditions by adapting physically and chemically. They typically have broader, thinner leaves, grow laterally, and become more efficient in their use of the photons that reach them via the adjustment of carotenoids and chlorophylls in the leaves.

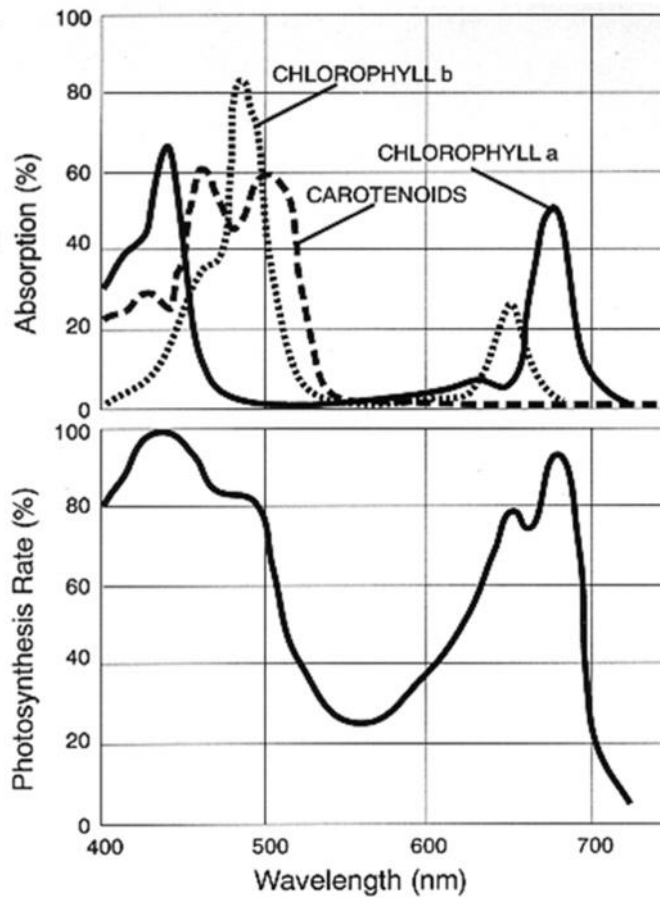


Figure 2: The absorption spectrum of chlorophyll a, chlorophyll b, and carotenoids and the rate of photosynthesis at a corresponding wavelength.<sup>2</sup>

PAR is variable at all spatial and temporal scales (Chazdon and Pearcy 1991; Gendron *et al.* 2001; Gross 1982; Hutchison and Matt 1977; Leuchner *et al.* 2007; Pukkala *et al.* 1991). PAR varies annually with the seasons due to changes in canopy

---

<sup>2</sup> By John Whitmarsh and Govindjee. Jasonphollinger at en.wikipedia [CC BY-SA 2.0 (<http://creativecommons.org/licenses/by-sa/2.0>)], from Wikimedia Commons.

condition, day length, solar altitude, and solar azimuth (Anderson 1964; Baldocchi *et al.* 1984; Gendron *et al.* 2001; Hutchison and Matt 1977; Richardson *et al.* 2013).

Although measured in Langley's per day, Figure 3 demonstrates how higher amounts of solar energy reach the forest floor during leafless conditions due to leaf-off canopy state while overall solar energy is lower during this time due to solar position. In the summer, overall energy increases above the canopy due to a more direct sun angle, but decreases beneath the canopy due to the fully-leafed canopy state.

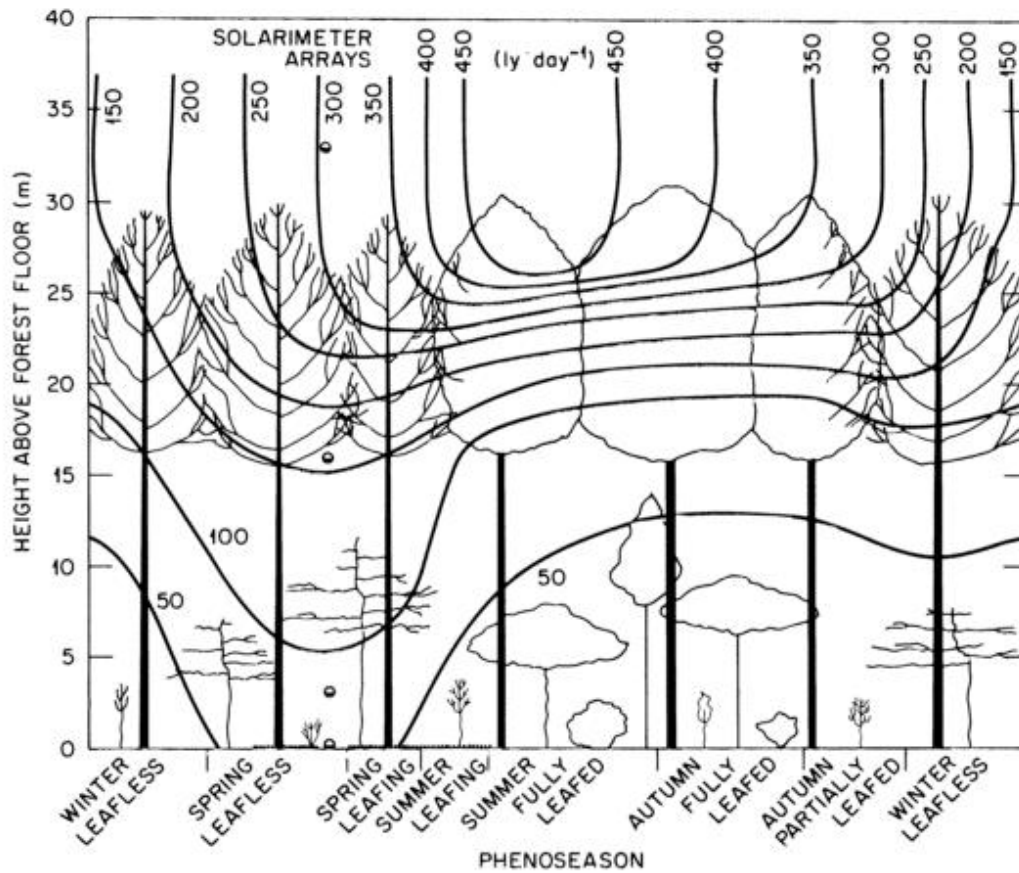


Fig. 24. Synthesized annual course of average daily total solar radiation received within and above a tulip poplar forest. Langleys  $\times 4.184 \times 10^4 = \text{J/m}^2$ . ORNL Dwg. 76-7581.

Figure 3: From Hutchison & Matt (1977); “Synthesized annual course of average daily total solar radiation received within and above a tulip poplar forest. Langleys  $\times 4.184 \times 10^4 = \text{J/m}^2$ .”<sup>3</sup>

<sup>3</sup> Republished with permission of Ecological Society of America from “The Distribution of Solar Radiation within a Deciduous Forest,” Hutchison and Matt, Ecological Monographs, 47(2), 1977; permission conveyed through Copyright Clearance Center, Inc.

PAR also varies diurnally as the sun rises and sets, as well as with sky conditions (Chazdon and Pearcy 1991; Gendron *et al.* 2001; Hutchison and Matt 1977). The solar angle in the morning and evening in conjunction with atmospheric thickness at the horizon causes lower values of PAR. Individual clouds can temporarily reduce PAR as they move in front of the sun. On a breezy day, when the sky is full of cumulus clouds, PAR values will be highly variable due to both cloud and tree movement (Chazdon and Pearcy 1991). Full overcast conditions scatter all photons and can reduce overall light energy and reduce variability at the same time (Anderson 1964; Chazdon and Pearcy 1991; Gendron *et al.* 2001; Hutchison and Matt 1977; Wilson 1967).

The attenuation and dispersion of light that occurs due to full overcast conditions can be attributed to the Beer-Lambert Law. This law describes the attenuation of light as a function of the properties of the material through which the light is traveling. This law has also often been applied to light attenuation by forest canopies, with varying success (Gholz *et al.* 1991; Perry *et al.* 1969; du Toit 2008) due to assumptions regarding homogeneity of leaf distribution, which cannot be met for most forest canopy types, and the fact that shading by woody areas is ignored (Holst *et al.* 2004; Pukkala *et al.* 1991). Other models derived from the Beer-Lambert Law have been more successful in their results by incorporating leaf area index into the calculation. De Castro (2000) lists a number of alternative attenuation models developed for these purposes including Federer (1971), Oker-Blom *et al.* (1991), and Pukkala *et al.* (1991).

Spatial variations occur with variations in terrain. Aspect can affect how long light reaches plants on a slope as well as where the light reaches as the sun moves over

the slope. Additionally the locations of individual trees and their canopies will determine where light can penetrate to the forest floor and where the forest floor will be shaded (Kuuluvainen and Pukkala 1987).

Historically, studies of PAR have employed individual spot quantum sensors (Proe *et al.* 2002), spherical fiber optic cable sensors (Leuchner *et al.* 2007) and further in the past, solarimeters (Hutchison and Matt 1977), spectroradiometers (Kinerson 1973) and chemical light meters (Perry *et al.* 1969). Sensors have typically been placed at multiple depths along the canopy-subcanopy gradient, often at less than three locations (Hutchison and Matt 1977; Kinerson 1973). Often these sensors would be turned on for only a few days during a season, typically the growing season, or for one day of each cloud condition (Kinerson 1973; Leuchner *et al.* 2007; Proe *et al.* 2002; and others). While some studies have taken millions of PAR readings in a field site (Leuchner *et al.* 2011), the readings are often stationary and therefore limited spatially (Kinerson 1973). Published work of such large datasets often is only inclusive of particular days. Most studies often included sensors located above the canopy or in the open to observe the photosynthetic photon flux.

#### **1.4 Research Question and Rationale**

The aim of this study is to understand (1) how PAR varies spatially and temporally within and among phenoseasons in a mid-Atlantic deciduous forest and (2) how this PAR variability affects woody understory shrubs, specifically *Lindera benzoin* L. Blume (northern spicebush), within the same plot. The author postulates that (1) as phenoseasons progress from leafless to fully-leafed, subcanopy PAR will be significantly decreased while PAR in the open will increase, and that canopy closure will affect the amount and distribution of PAR by creating sunflecks and sun patches

that are temporally variable, (2) this re-distribution of PAR will affect the growth and distribution of the shrub *L. benzoin* in the subcanopy by limiting a primary growth-limiting resource, and that (3) spatial distribution of canopy species may also affect the spatial distribution of PAR, and therefore *L. benzoin*. The author also postulates that light quality and quantity will not only affect the ‘growth’ of *L. benzoin*, but will also affect the health of *L. benzoin* and its ability to thrive.

This work is novel in both the length of study and number of observations ( $n=4,614$ ). To our knowledge, no other study of subcanopy PAR has obtained so many unique measurements during all daylight hours, all cloud conditions, and all phenoseasons over an entire year. Instrumentation is also novel; no other known study of this kind and length conducted with this instrumentation could be found. Lastly, the inclusion of the laboratory component of this study has improved our understanding of the impact of PAR on plant strategy and physiology in the field. The work of this thesis may contribute to gaps in the literature pertaining to (1) our understanding of PAR variability both spatially and temporally, especially as it relates to phenoseason, and (2) its effect on the physiology of ecologically significant understory plants, particularly their health and the responses of chlorophyll a, chlorophyll b, and carotenoids to changes in photoperiod and photointensity, (3) photosynthesis research such as refining stomatal conductance models and photosynthesis models and approximating subcanopy light dynamics at the microscale (Dietze 2014) and (4) instrumentation and measurement of photosynthetic photon flux density. This thesis will help to tease out subtleties in the way understory PAR varies by season based on leaf phenology, and how understory plants utilize, or compensate for, a limited amount of a hugely important growth limiting variable like solar radiation by broadening the

temporal and spatial scales and increasing the temporal and spatial resolutions of previous work.

In combination, the photosynthesis of these canopy and subcanopy plants plays a large role in the carbon and water cycles. In our changing climate, it is important to understand the subtleties of these processes and how they may change in the future, as well as how this may affect species composition, plant structure, function, production, and even periodicity of phenophases, to better understand the larger role plants play in the future of the Earth's climate.

## Chapter 2

### SPATIOTEMPORAL VARIABILITY OF PHOTOSYNTHETICALLY ACTIVE RADIATION AND SPICEBUSH ECOLOGY: A REVIEW OF THE LITERATURE

#### 2.1 Measurement of PAR

PAR is the portion of the electromagnetic spectrum available to plants for photosynthesis. This region aligns approximately with our visible spectrum (red, orange, yellow, green, blue, indigo, and violet) and can be found at the 400-700 nm wavelength range. This radiation is typically measured in two ways: by either an energy system or a photon system (Taiz & Zeiger, 2010). Energy units are  $\text{W m}^{-2}$ , while photon units or quanta are  $\mu\text{mol m}^{-2} \text{s}^{-1}$ . Measurement of quanta is called the photosynthetic photon flux density (PPFD), or, the number of photosynthetically active photons passing through one square meter per second (Taiz & Zeiger, 2010). As a reminder, here we are considering the photon properties of light, and not the wave properties. Additionally, differences in terminology also exist depending on the shape of the sensor surface; energy measured as it is received on a plane is called irradiance, and energy reaching a sphere is called the fluence rate (Taiz & Zeiger, 2010). Measurement of radiation is at the discretion of the researcher, their intended purpose for the data, and the sensors they have available to them.

Studies of PAR have employed individual spot quantum sensors (Proe *et al.* 2002), light sensing diodes (Gholz *et al.* 1991), spherical fiber optic cable sensors (Leuchner *et al.* 2007), solarimeters (Hutchison and Matt 1977), spectroradiometers

(Kinerson 1973) and chemical light meters (Perry *et al.* 1969). Sensors have typically been placed at multiple depths along the canopy-subcanopy gradient, often at less than three locations (Hutchison and Matt 1977; Kinerson 1973) (Table 1). Sensors might be turned on for only a few days during a season or for moments of each cloud condition for growing seasons only (Kinerson 1973; Leuchner *et al.* 2007; Proe *et al.* 2002; and others). In a few studies, readings were taken for only one day in each season. While some studies have taken millions of PAR readings in a field site (Leuchner *et al.* 2011), the readings have often stationary and constrained by sensor diameter and therefore limited spatially (Kinerson 1973) or, when using a larger diameter or fish-eye sensor, precision is compromised (Chazdon 1988). Published work of such large datasets often are only inclusive of particular days. Most studies typically include sensors located above the canopy or in the open to observe differences in the flux of radiation as it is attenuated by the forest canopy.

Table 1: Studies of PAR by forest and sensor type.

Forest type	Sensor	Frequency	Duration	Reference
<i>P. virginiana</i>	Chemical light meter	-	24 hours	Perry <i>et al.</i> 1969
<i>P. menziesii</i>	Spectroradiometer	-	-	Kinerson 1973
<i>L. tulipifera</i>	Solarimeter	5-20 minutes	2 years	Hutchison & Matt 1977
<i>Quercus sp., Cary asp.</i>	Pyranometer	Hourly	7 months	Baldocchi <i>et al.</i> 1984
<i>P. elliotii</i>	Light sensing diode arrays & remotely sensed data	Hourly	2 years	Gholz <i>et al.</i> 1991
<i>S. viminalis, Populus sp., A. rubra</i>	Spot quantum sensors	1 day each 1-3 weeks	5 years	Proe <i>et al.</i> 2002
<i>F. sylvatica, P. abies</i>	Spherical fiber optic cable sensor	2 minutes	5 months	Leuchner 2007 & 2011
<i>L. benzoin</i>	Quantum light sensor	Hourly	7 days	Niesenbaum & Kluger 2006
<i>A. saccharum, L. tulipifera, Q. alba, Q. nigra</i>	BF3 sensor	2-16 sec	2 years	Oliphant <i>et al.</i> 2011

Each of these sensors has its unique advantages; the cost effectiveness of a chemical light meter, for example, or the extent of coverage of spherical fiber optic cable sensors. It becomes distinctly clear though, that each of these sensors has only a small diameter and is therefore measuring only a small fraction of light reaching the forest floor. For this study, we employed the LI-COR LI-191 Line Quantum (PAR) Sensor in conjunction with a LI-COR LI-250A light meter (LI-COR, Lincoln, NE, USA; calibrated February 15, 2011). The LI-191 sensor consists of a 1 m quartz rod conductor under an acrylic diffuser. The conductor is connected to a high stability blue enhanced silicon photovoltaic light sensor, and the line quantum sensor is then connected to the calibrated LI-250A. Together the instruments are capable of

providing the user with a 15 second spatially integrated one meter linear average of the PPFD reaching the quartz rod in  $\mu\text{mol m}^{-2} \text{s}^{-1}$ . When light environment can vary orders of magnitude in less than half a meter distance (Chazdon and Pearcy 1991) it is essential to be able to integrate measurements over a larger area. Other benefits of using a line quantum sensor include its portability, accuracy, efficiency, and ease of maintaining calibration on a single instrument. It is uncomplicated and relatively quick to collect many measurements over a large distance rather quickly and independently, which is key when field conditions relating to incoming solar radiation can change in a matter of moments, and a large data set is needed to represent reality.

There can be no question that much of the research relating to radiation in forests has found this particular aspect of the system to be complex, dynamic, and difficult to measure. Many studies which have attempted to quantify PAR in varying forest types have found that it often represents between 1 and 30% of the above canopy radiation. Table 2 illustrates a number of these studies and the corresponding cover types and light levels as a percent of the total above canopy radiation. Table 2 also indicates that subcanopy PAR is commonly lower in forest types where species may grow more densely and higher in forest types that are sparsely populated. Species is a significant factor influencing the variability of PAR. Other factors, both biotic and abiotic, influencing PAR variability are discussed in Section 2.2.

Table 2: Some examples of light values at the forest floor by differing canopy species, expressed as a percent of the total above canopy light.

Species	Approx. of total light beneath canopy (%)	Reference
Slash pine	31	Gholz <i>et al.</i> 1991
Red alder	26	Proe <i>et al.</i> 2002
Gray birch	20	Horn 1971
Bigtooth aspen	19	Horn 1971
Sassafras	15	Horn 1971
Virginia pine	11	Perry <i>et al.</i> 1969
Red oak	10	Horn 1971
Sweetgum	8.6	Horn 1971 Hutchison and Matt
Yellow poplar	7.8	1977
Red maple	7.8	Horn 1971
White oak	7.7	Horn 1971
Black oak	7.2	Horn 1971
Hickory	7	Horn 1971
Blackgum	6.9	Horn 1971
American beech	3.1	Horn 1971
'Hardwood' stand	1.4	Perry <i>et al.</i> 1969

While it may seem quite obvious now, older studies often found that the amount of light reaching the forest floor was only enough to permit growth of the particular species that can exist within that light environment (Perry *et al.* 1969). These light environments are key to succession, especially in mid-Atlantic deciduous forests (Horn, 1971).

Our study expands on this past research by collecting readings two to three times a week for a full year, during all daylight hours, capturing all cloud and canopy conditions during all seven phenoseasons using instrumentation that is novel for this type of study. By capturing field conditions at twenty-five subcanopy locations, five

shrub canopy locations, five forest floor locations, and essentially two open locations, and by pairing our findings with detailed laboratory experiments, we refine our understanding of plant physiology and how plants use photosynthetically active radiation in the field.

## **2.2 PAR and its variability**

The study of cyclical change in biota as related to climate, is called phenology. In a temperate forest, deciduous plants experience a change in phenological state - also called a phenophase - as the energy of solar radiation changes throughout the year causing budding, flowering and fruiting, and leaf growth, leaf senescence, and leaf fall. Hutchison & Matt (1977) defined these seasonal radiation conditions as phenoseasons – "...segment[s] of the year during which the prevailing earth-sun geometry and phenological state of the forest create a unique set of conditions which determine forest radiation regimes." Many of the phenological changes in trees are dependent on the quality and quantity of solar radiation reaching plants. In response, light environments beneath plant canopies are altered due to changing solar angles and elevations, canopy geometry, canopy leaf state, canopy closure, and cloud conditions, as well as the distribution of canopy trees, tree height and meteorological conditions such as wind (Hutchison and Matt 1977; Chazdon and Pearcy 1991).

Hutchison and Matt (1977) defined the seven unique phenoseasons of a temperate deciduous forest by superimposing the timing of the primary seasonal solar conditions, what they call celestial geometry, with that of canopy phenophase. The phenoseasons, in chronological order from complete leaf-off conditions are: winter leafless (beginning mid-November), spring leafless (beginning early February), spring leafing (beginning early April), summer leafing (beginning early May), summer fully-

leafed (beginning early June), autumnal fully-leafed (beginning early August), and autumnal partially leafed (beginning early October). These phenoseasons can be seen, for a mid-latitude deciduous forest, in Figure 1. While these dates work well for a study in a mid-latitude deciduous forest, it would be necessary to adjust these phenoseasons by latitude, and likely by species as well due to differences in the timing of leaf senescence and abscission.

PAR is variable at all spatial and temporal scales (Chazdon and Pearcy 1991; Gendron et al 2001; Gross 1982; Hutchison and Matt 1977; Leuchner *et al.* 2007; Pukkala *et al.* 1991). Some of these variations follow regular patterns, while others do not (Hutchison and Matt 1977). PAR varies annually with the seasons due to changes in canopy condition, day length, solar altitude, and solar azimuth (Anderson 1964; Baldocchi *et al.* 1984; Gendron *et al.* 2001; Hutchison and Matt 1977; Richardson *et al.* 2013). Although measured in Langley's per day, Figure 3 demonstrates how higher amounts of solar energy reach the forest floor during leafless conditions due to leaf-off canopy state while overall solar energy is lower during this time due to solar position. In the summer, overall energy increases above the canopy due to a more direct sun angle, but decreases beneath the canopy due to the fully-leafed canopy state.

PAR also varies diurnally as the sun rises and sets, as well as with sky conditions (Chazdon and Pearcy 1991; Gendron *et al.* 2001; Hutchison and Matt 1977). The solar angle in the morning and evening in conjunction with atmospheric thickness at the horizon causes lower values of PAR. Individual clouds can temporarily reduce PAR as they move in front of the sun. On a breezy day, when the sky is full of cumulus clouds, PAR values will be highly variable due to both cloud and tree movement (Chazdon and Pearcy 1991). Full overcast conditions scatter all

photons and reduce variability at the same time (Anderson 1964; Chazdon and Pearcy 1991; Gendron *et al.* 2001; Hutchison and Matt 1977; Wilson 1967). Spatial variations occur with variations in terrain. Aspect can affect how long light reaches plants on a slope as well as where the light reaches as the sun moves over the slope. Additionally, the locations of individual trees and their canopies will determine where light can penetrate to the forest floor and where the forest floor will be shaded (Kuuluvainen and Pukkala 1987). Vertically, heights of different canopy and subcanopy species will create additional layers to block light from shorter plants.

Light penetrating a forest canopy can vary in both quantity and quality. Full sunlight may reach to the forest floor for only a second or a number of hours, and may be direct, diffuse, or affected by shadows and leaf absorption. While Chazdon and Pearcy's discussion (1991) pertains specifically to sunflecks, during clear days of the summer and autumnal fully-leaved phenoseasons, these sunflecks and hot spots may be the highest recorded PAR values, sometimes orders of magnitude higher. That being said, most of the variation in PAR occurs in the direct light, rather than the diffuse light simply due to the physical qualities of light as it is distributed through a medium such as water vapor (clouds) or a canopy of leaves (Oliphant *et al.* 2011). Indeed, when all contributing factors have been accounted for, dynamic seems a blasé description of the subcanopy light environment.

According to Chazdon (1988) this dynamism can be highly correlated with plant success even if it cannot be correlated between observation locations. The opposite can also be true, as Oliphant (2011) demonstrates for some shade tolerant plant species, even short episodes of full sun can be a detriment. How can we determine if locations with higher occurrences of *L. benzoin* are actually receiving

greater photon flux density, and if so, do we see a carbon gain in understory vegetation such as *L. benzoin* as a result?

### 2.3 Ecology of *Lindera benzoin*

The dominant understory plant in our field site is the native deciduous perennial shrub *Lindera benzoin* L. Blume (northern spicebush). It flowers, bright yellow, in early April, before leaf-out of the canopy trees (Mooney *et al.* 2010) (Figure 4). Individual plants are present as both male and female (male flowers do not appear on female plants and vice versa) in a 1:1 ratio in natural habitats (Mooney *et al.* 2010). Drupes (the fruit of *L. benzoin*) on female plants grow through the summer before turning red in the autumn (Figure 5).



Figure 4: Spicebush on April 10, 2014 and April 19, 2015.



Figure 5: Spicebush drupes in June (left) and early September (right).

It is shade tolerant, and an indicator of the fertile soils which are common in shade habitats. Many of *L. benzoin* physiological traits including growth, defense, and reproduction have been shown to be greatly affected by light levels (Mooney *et al.* 2010; Mooney and Niesenbaum 2012; Mooney *et al.* 2009; Niesenbaum 1992). For example, spicebush can be found under closed canopies or along forest edges, and while inhibited by light conditions greater than 25% PPFD and less than 1% PPFD (Luken *et al.* 1997), growth of plants for all ages, and flower and fruit production have been shown to more successful in sun patches and along forest edges (Mooney *et al.* 2010). In a short study, observing plasticity in response to light changes, Luken *et al.* (1997) showed that *L. benzoin* had most new stem growth, lower stomatal density, highest photosynthetic rate and lower leaf thickness at light levels between 191 and 391  $\mu\text{mol m}^{-2} \text{s}^{-1}$ . Leaves of spicebush grown in sun conditions are often tougher, with lower water content, than those grown in shade (Niesenbaum 1992). These sun leaves also typically experience less herbivory than shade leaves (Niesenbaum 1992).



Figure 6: Spicebush present under *L. tulipifera*.



Figure 7: Spicebush leaves senescing to yellow in autumn.

Spicebush has ecologically significant associations with many other species. Humans have historically used it for teas and spices due to its distinct flavor and possible medicinal value. It is often found under *L. tulipifera*. The spicebush's drupes are an important food source for songbirds and pheasants, especially during fall migration. Leaves are a food source for white-tailed deer and other herbivorous

mammals, and an invaluable habitat for small to medium sized mammals, songbirds, pheasants, and winged insects – specifically the Spicebush Swallowtail (Figure 8) and Spicebush Silkmoth (Figure 9).

Associations with bird species are especially important for seed dispersion (Meyer and Witmer 1998). Due to its dioecious nature and seed processing and dispersion by mobile species such as birds such as American robins and woodthrush, genetic variation within spicebush is diverse (Meyer and Witmer 1998; Mooney *et al.* 2010).



Figure 8: Spicebush Swallowtail (*Papilio troilus*). Photo by J. Hudson, near field site.



Figure 9: Female Spicebush silkmoth (*Callosamia promethea*). Photo by S. Hudson, field site.

In our changing climate, it is necessary to understand the physiological responses of *L. benzoin* to changes in light conditions, and the impact these changes can have on native species that depend on the shrub for their survival, as well as how *L. benzoin* will adapt to other changes in its ecosystem.



Figure 10: Personal illustration of *L. benzoin* seedling.

#### 2.4 Beer's Law, pigments, and absorbance

The attenuation and dispersion of light that occurs due to full overcast conditions can be attributed to Beer's Law or the Beer-Lambert Law. This law describes the attenuation of light as a function of the properties of the material, typically a fluid, through which the light is traveling using the following equation:

$$A = \epsilon l c$$

Where  $A$  is the absorbance,  $\epsilon$  is the molar extinction coefficient ( $\text{L mol}^{-1} \text{cm}^{-1}$ , determined by the substance),  $l$  is the light path length, and  $c$  is the concentration ( $\text{mol L}^{-1}$ ) (Taiz & Zeiger, 2010).

The Beer-Lambert Law is the basis of UV-visible (UV-vis) spectrophotometry. Within a spectrophotometer, a monochromator allows for the adjustment of the wavelength of light that will be sent through the fluid inside a cuvette through which the light shines. The fluid, measured with no attenuator, will calibrate the spectrophotometer. Then, samples of the fluid containing the attenuator will be placed in front of the monochromatic light of the selected wavelength, and a photodetector on the other side will send the value of the transmitted light, essentially lower energy due to absorbance and reflectance by the particles of attenuator, to the screen for recording (Taiz & Zeiger, 2010).

Using spectrophotometry, it is possible to measure the amount of pigment present in leaf supernatant by setting the wavelength to that which corresponds to that pigment. For this study, amounts of chlorophyll a, chlorophyll b, and carotenoids were measured. Chlorophyll a (primarily red absorption, and the primary electron donor) and chlorophyll b (antenna pigment, primarily blue absorption) molecules absorb red and blue photons, which excite the molecule and initiate photosynthesis (or release heat, fluoresce, or transfer energy to another molecule) (Taiz & Zeiger, 2010). In the case of carotenoids (accessory pigments also useful in photoprotection), absorption of energy from green photons is transferred directly to the chlorophyll for photosynthesis (Taiz & Zeiger, 2010). Absorption wavelengths selected were 450 nm, 470 nm, 645 nm, and 661 nm to measure these pigments (see Figure 2). It has been shown that leaves of woody and herbaceous shade adapted species grown in high light conditions

often have fewer pigments, and higher chlorophyll a to chlorophyll b ratio (Hallik *et al.* 2012; Kitajima and Hogan 2003).

The Beer-Lambert Law has also often been applied to light attenuation by forest canopies, with varying success (Gholz *et al.* 1991; Perry *et al.* 1969; du Toit 2008) due to assumptions regarding homogeneity of leaf distribution, which cannot be met for most forest canopy types, and the fact that shading by woody areas is often ignored (Holst *et al.* 2004; Pukkala *et al.* 1991). This assumption that woody area can be ignored is especially erroneous, especially in deciduous forests, whose woody areas can absorb 50-70% of gross radiation in leaf-off conditions (Hutchison and Matt 1977). Other models derived from the Beer-Lambert Law have been more successful in their results by incorporating leaf area index into the calculation. De Castro (2000) lists a number of alternative attenuation models developed for these purposes including Federer (1971), Oker-Blom *et al.* (1991), and Pukkala *et al.* (1991).

## **2.5 Contribution to the Literature**

As Dietze (2014) states, it is imperative that we continue to refine our understanding of plant physiology as it relates to photosynthesis, the variability of photosynthetic parameters, how this varies across species, and how a changing climate will impact carbon cycling. This thesis attempts to assist in that refinement.

As can be seen from the previous pages as well as by a search of the literature, much of the literature is limited to crop and plantation canopies, or is limited to the temperate mid-latitudes. Future research should expand into alternative climates, both higher and lower latitudes, to more forest cover types and in natural settings, to better understand how carbon gain and photosynthesis are working and changing in nature.

The literature would additionally benefit from larger studies that capture multiple within-canopy elevations at multiple locations, preferably not dependent on human presence. Dependence on humans to conduct these studies leaves open the possibility for large degrees of human error, and technology has come far enough that, given proper funding and instrumentation, data storage and transmission would allow for these large datasets to be collected indefinitely.

Many models also fall short due to the inherent dynamism of photosynthesis and the number of variables involved. Indeed, how does one capture accurately a system with variables that can change three orders of magnitude in a matter of seconds, only to change again seconds later? It is important that we continue to incorporate knowledge gained in the field, especially that from larger long-term studies, into these models so that we can better understand the possibilities held in the future of our climate.

## Chapter 3

### CHARACTERISTICS OF THE STUDY PLOT AT THE FAIR HILL NATURAL RESOURCE MANAGEMENT AREA

#### 3.1 Location

The study area is located 73 m above sea level, within the Fair Hill Natural Resource Management Area (NRMA) in Cecil County, MD, at 39° 42' 36" N, -75° 50' 56" W (Figure 13). Fair Hill NRMA has been the site of a joint National Science Foundation (NSF) and University of Delaware funded watershed study since 2007. During this time, nested watersheds of 12 ha and 79 ha have been monitored for a variety of hydrologic variables including throughfall, stemflow, stream discharge and chemistry, as well as meteorological conditions. Since the establishment of the site, monitoring has also begun on leaf litter chemistry, groundwater, soil moisture, and CH<sub>4</sub> and CO<sub>2</sub> gas exchange.

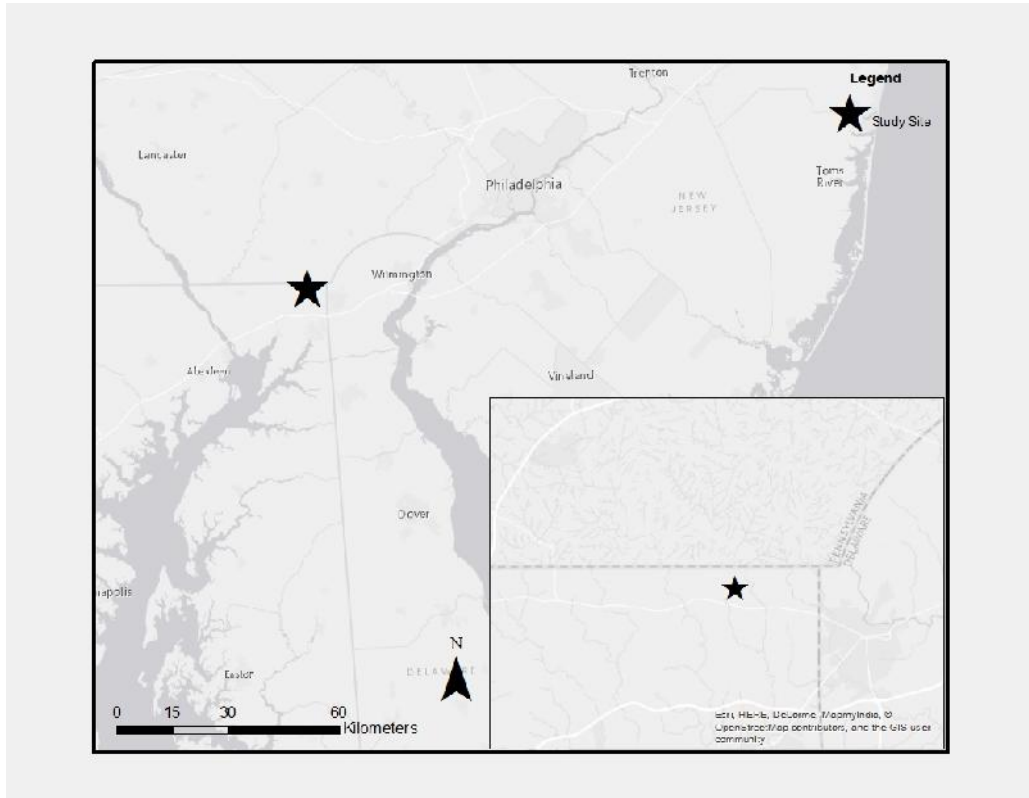


Figure 11: Fair Hill NRMA in relation to the greater Mid-Atlantic region.

### 3.2 Climate and Weather

This region lies within the humid subtropical (Cfa) climate classification of the Köppen system, receiving 1205.23 mm annual mean precipitation, which falls almost evenly throughout the year, having just slightly more precipitation from May to September. The 30-year mean maximum temperature is 19.1°C and the 30-year minimum temperature is 6.78°C (NCDC 2014).

A Delaware Environmental Observing System (DEOS) Network meteorological station (ID: DFHM) sits at 39° 43' N, 75° 50' W, 45.7 m above sea level in an open field approximately 1 km west of the study plot, near Fair Hill Nature

Center (Figures 12 and 13). Data for precipitation, air temperature, dew point temperature, barometric pressure, wind chill, wind and wind gust speed, wind direction, solar radiation, relative humidity, and volumetric water content, was archived at five minute intervals for the study period with the exception of a flooding event at the site in April 2014 and upgrades during June 2014. Readings were not collected during these times. An LI-190 quantum sensor (LI-COR, Lincoln, NE) was installed for direct comparison for this study and began collecting data on April 9, 2014. For additional instrumentation information see Appendix A.



Figure 12: Map showing the distance between the PAR collection site and the DEOS station where meteorological variables are measured.



Figure 13: DEOS Station at Fair Hill NRMA

Weather for this site during the research period was 2.6°C colder than usual, and even with record snowfall in some places, received 212.1 mm less liquid precipitation than the climatological norm. The research period also included some of the coldest recorded daily temperatures during changes in the positioning of the polar vortex (NCDC 2014, DEOS 2014). Additional comparisons can be found in Table 3.

Table 3: Temperature and Precipitation for the Study Period Compared to 30-yr Climate Norms

	<b>Study Year Mean Temp (°C)</b>	<b>30-yr Temp (°C)</b>	<b>Study Year Dev. from Mean (°C)</b>	<b>Study Year Precip (mm)</b>	<b>30-yr Precip (mm)</b>
November	4.8	7.9	3.1	68.8	89.9
December	1.2	2.6	1.4	92.7	102.4
January	-3.4	-0.1	3.3	63.7	87.4
February	-2.2	1.5	3.7	122.1	72.4
March	1.9	6.0	4.1	85.8	108.0
April	10.1	11.9	1.8	84.5	99.8
May	16.4	17.7	1.3	78.9	100.6
June	20.6	23.2	2.6	78.0	106.2
July	22.6	25.7	3.1	93.4	109.0
August	20.8	24.7	3.9	87.8	99.3
September	18.3	20.6	2.3	68.9	125.7
October	13.6	13.8	0.2	68.5	104.6
Average/Total	10.4	13.0	2.6	993.1	1205.2
	<b>Study Year</b>	<b>30 Year</b>			
Max Temp (°C)	34.6	19.2			
Mean Temp (°C)	10.4	13.0			
Min Temp (°C)	-19.5	6.8			
Precip (mm)	993.1	1205.2			
Snow (mm)	759.5	447.0			
Total Precip (mm)	1752.6	1652.3			

### 3.3 Plot Description

Historically a mix of both farm- and woodland, the NRMA is a patchwork of open fields and deciduous forest. Similar to other deciduous forests in the mid-Atlantic, the dominant tree species in the research plot are *Fagus grandifolia* Ehrh. (American beech) and *Liriodendron tulipifera* L. (yellow poplar), with limited numbers of *Acer rubrum* L. (red maple), *Carya* spp. (hickory), and *Quercus* spp. (oak). *L. benzoin* is a dominant understory plant, its canopy covering approximately 27% of the study plot. Its commonality in this and other deciduous forests in the region make it an excellent choice for this study. Other less extensive understory plants include *Anemonella thalictroides* (rue anemone), *Arisaema triphyllum* (jack-in-the-pulpit), *Cardamine impatiens* (narrow-leaved bittercress), *Ethythronium amricanum* (dogtooth violet), *Hamamelis virginiana* (American witch-hazel), *Phegopteris hexagonoptera* (broad beech fern), and *Podophyllum peltatum* (Mayapple). The 1800 m<sup>2</sup> plot, expanded from a previous study, inside Fair Hill NRMA contains 42 trees having diameter at breast height (DBH, measured at 1.37m) >10 cm, and a stand density of 233 trees ha<sup>-1</sup>. The largest trees in the plot are a red oak (102.8 cm DBH) and a yellow poplar (100.3 cm DBH). Based on a plot inventory conducted in October of 2014, canopy height ranges from 5.5 m to 30 m, with a mean height of 23 m. The stand mean DBH is 39.5 ± 28.8 cm. The stand basal area is 43.7 m<sup>2</sup> ha<sup>-1</sup>. The plot has a woody area index of 1.21 ± 0.01 m<sup>2</sup> m<sup>-2</sup> and a leaf area index of 5.12 ± .17 m<sup>2</sup> m<sup>-2</sup>. The plot has northeasterly aspect (Figure 15). Within the plot, slopes range from 0 to 30% (USDA NRCS, 2012; Figure 16).



Figure 14: Seasonal changes in the study plot from upper left: winter, spring, late summer, and autumn.

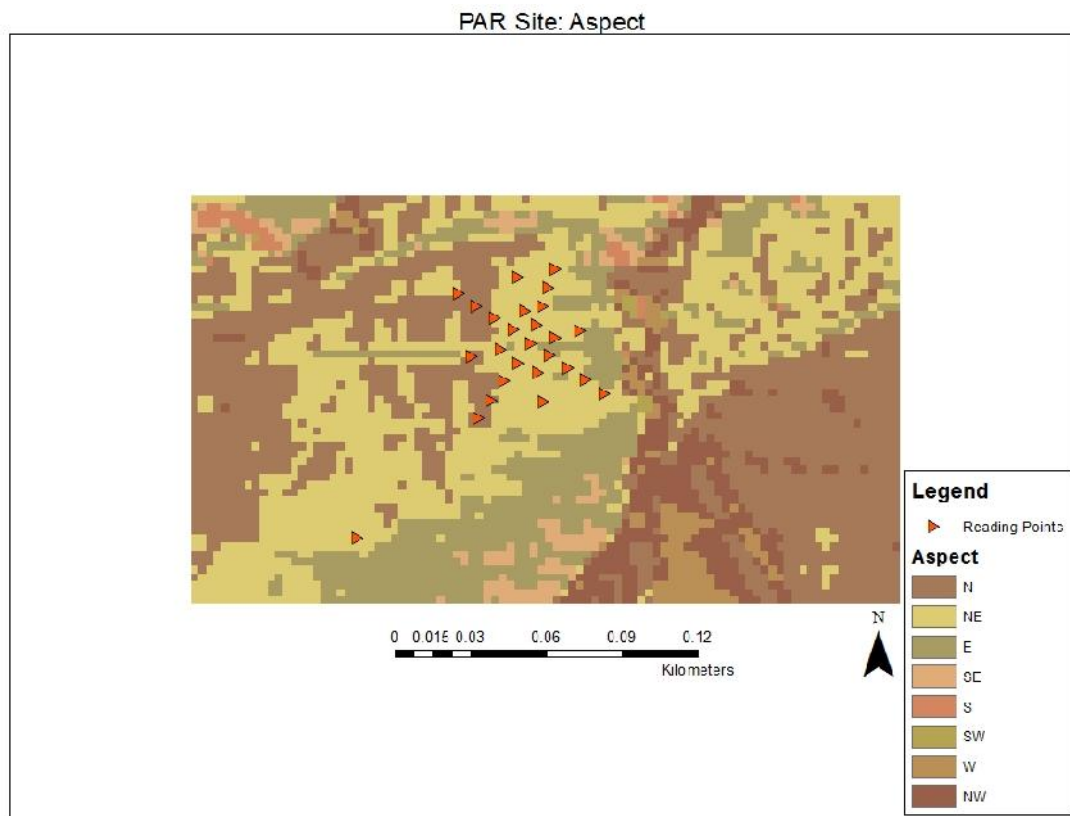


Figure 15: Aspect map of PAR collection site.

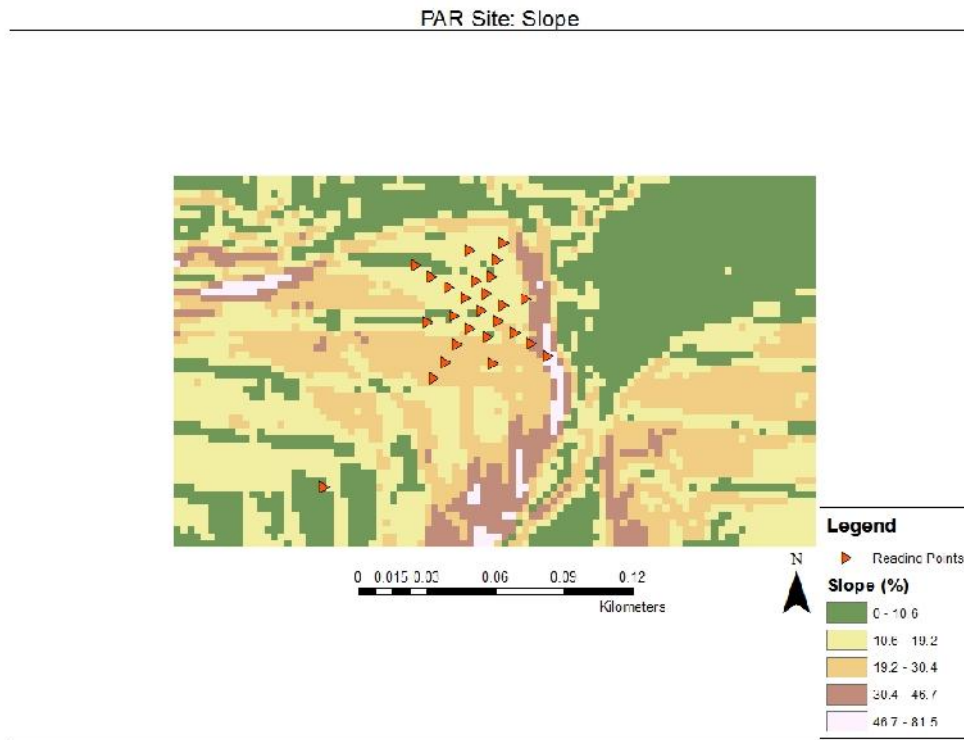


Figure 16: Slope (%) map of PAR collection site.

## Chapter 4

### MATERIALS AND METHODS

#### 4.1 PAR Collection in the Field

The field work component consisted of readings of PAR approximately three times a week, at varying times of day, under varying sky cover conditions for one full year. This full year encompassed all 7 phenoseasons (winter leafless (WL), spring leafless (SL), spring leafing (SLG), summer leafing (SULG), summer fully-leafed (SUFL), autumnal fully-leafed (AFL), and autumnal partially-leafed (APL) (Hutchison and Matt 1977), a broad range of daylight hours, and all sky conditions. To maintain consistency, every attempt was made to acquire all readings within the plot and in the open within a half-hour time frame. A total of 4,592 unique measurements were taken.

PAR was measured using a LI-COR LI-191 Line Quantum Sensor in conjunction with a LI-COR LI-250A light meter. The calibrated LI-191 sensor consists of a 1 m quartz rod under a diffuser, connected to the LI-250A light meter. Together, the instruments are capable of providing the user with a 15 second spatially integrated average of the photosynthetic photon flux density (PPFD) reaching the quartz rod.

For this study, a satisfactory plot (1800 m<sup>2</sup>) was selected at Fair Hill NRMA. The plot was divided by four transects: a north-south transect and an east-west transect, each with 5 equidistant marked points for taking PAR readings, and a NE-SW and NW-SE transect, each with 9 equidistant marked points.

These points were found through an initial survey in November 2013 during which the four corners and center of the plot were located. Coordinates of these first five points were entered into ArcGIS and connected with straight lines. The lines were then bifurcated, and then bifurcated again, creating the multiple mid-points between corners and the center (Figure 17).

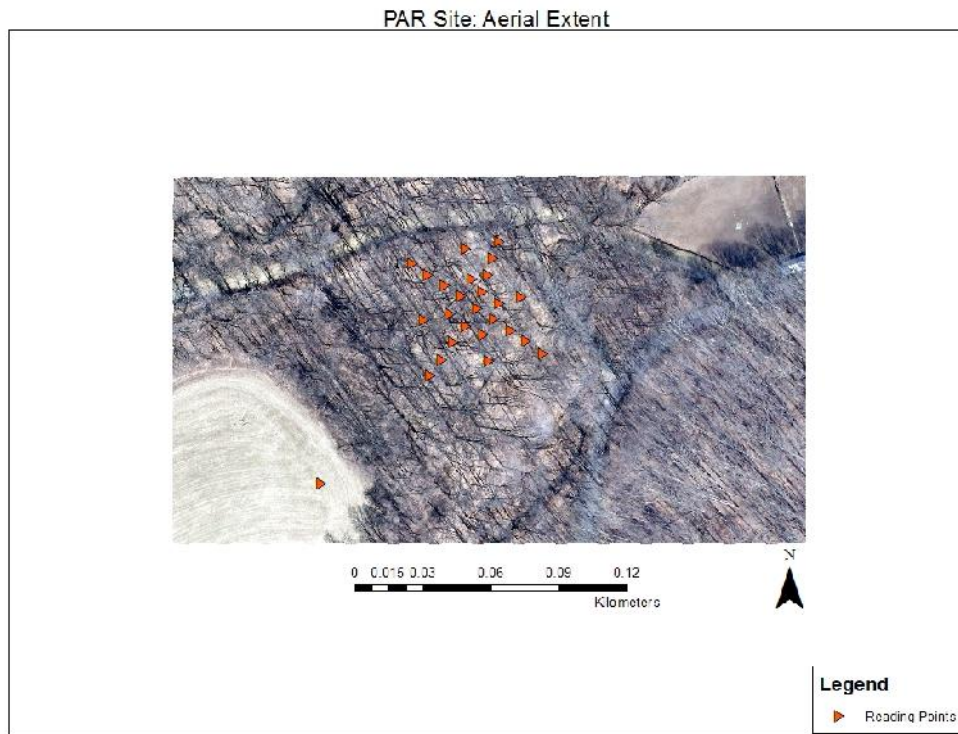


Figure 17: Aerial view of the plot, with observation points.

Each point was arbitrarily assigned a number (1 through 25) with 5 being the center. At each walk of each transect during readings, location 5 was assigned a value (see Figure 18). This meant location 5 had four values for each day readings were



At five of the coordinates within the plot (numbers 5, 8, 14, 15, and 23; see locations marked with ‘\*’ in Figure 22), there is significant growth of *L. benzoin*. At these locations, PAR readings were conducted above the *L. benzoin* canopy, within the *L. benzoin* canopy, and beneath the *L. benzoin* canopy in an attempt to compare how much light is reaching these plants as well as to make some connections between plant strategy and PAR.

Week, year, month, day, 365 day, phenoseason, visual sky condition, and PAR readings and associated times were recorded using a field sheet created for this purpose (Figure 19) before being entered into a database. Phenoseasons were based on those of Hutchison and Matt (1977). Visual sky conditions were described in Oktas, or cloud cover in 1/8<sup>th</sup> increments where 0 is clear, 4 is 50% sky cloudiness, and 8 is completely overcast. An example of a completed field sheet can be found in Appendix B. To capture as many conditions as possible, trips to the field site were tracked using a spreadsheet in which the number of visits to the field site during a 15-minute interval could be recorded (Table 4).

Table 4: Number of times readings were collected during a 15 minute period during each phenoseason

WINTER LEAFLESS		SPRING LEAFLESS				SPRING LEAFING										
<i>Minutes</i>		<i>Minutes</i>				<i>Minutes</i>										
		0	15	30	45											
<i>Hour</i>	7			1	1	7			1	1	7				1	
	8	1			1	8	1	1	1	1	8	1	1			
	9	1	1	1	4	9					9		1	1	1	
	10	4	5	2	2	10		1	1	2	10			1	1	
	11	2	2	1	1	11	1	1			11	1		1	1	
	12	1	3	3	1	12			1	2	12	2	1	1	1	
	13		1	2	2	13	1	1	1	1	13	1	1			
	14	3	4	4	4	14	1	2	2	2	14			2	2	
	15	2	2	1	1	15		1	1	2	15	3	2	2	1	
						16	2	2	1	1	16	1	1	2	4	
					17	1	1			17	2.5	2				
SUMMER LEAFING		SUMMER FULLY-LEAFED				AUTUMNAL FULLY-LEAFED										
<i>Minutes</i>		<i>Minutes</i>				<i>Minutes</i>										
		0	15	30	45											
<i>Hour</i>	7				1	7			1	1	7					
	8	1			1	8	1	1			8					
	9	1				9					9				1	
	10	1	1	1	1	10			1	2	10	2	1	1	2	
	11	1				11	1		1	3	11	1	1	1	1	
	12	1	2	2		12	3	2	3	2	12	1		1	1	
	13	1	1		1	13	2	1	1		13		1	1	1	
	14	1				14		1	1	1	14		1	1	1	
	15	1	1	1		15	1			1	15	1	2	1	2	
	16	1	1	1	1	16	2	1	1	1	16	2	2	2		
17	1	1	2	1	17	1	1			17	1	1	2	2		
18	1	1	1		18		2	3	1	18	0.5					
AUTUMNAL PARTIALLY-LEAFED																
<i>Minutes</i>		<i>Minutes</i>														
		0	15	30	45											
<i>Hour</i>	7															
	8		1	1												
	9		1	1	1											
	10	1	1	1												
	11		1	1	1											
	12	1	2	2	1											
	13		1	1												
	14		1	2	1											
	15	1	1	1	1											
	16	1	1	1												

#1  
Time:  
PAR:

#2  
Time:  
PAR:

#3  
Time:  
PAR:

#4  
Time:  
PAR:

#5  
Time:  
PAR:  
Time:  
PAR:  
Time:  
PAR:

#6  
Time:  
PAR:

#7  
Time:  
PAR:

#8  
Time:  
PAR:

#9  
Time:  
PAR:

#10  
Time:  
PAR:

#11  
Time:  
PAR:

#12  
Time:  
PAR:

#13  
Time:  
PAR:

#14  
Time:  
PAR:

#15  
Time:  
PAR:

#16  
Time:  
PAR:

#17  
Time:  
PAR:

#18  
Time:  
PAR:

#19  
Time:  
PAR:

#20  
Time:  
PAR:

#21  
Time:  
PAR:

#22  
Time:  
PAR:

#23  
Time:  
PAR:

#24  
Time:  
PAR:

#25  
Time:  
PAR:

N

Week: \_\_\_\_\_ Year: \_\_\_\_\_ Month: \_\_\_\_\_ Day: \_\_\_\_\_ 365 Day: \_\_\_\_\_  
 Phenoseason: \_\_\_\_\_  
 Visual sky conditions/time: \_\_\_\_\_  
 NOTES (Record spicebush & open readings here):

OKTA SKY CONDITIONS	
0 - CLEAR	
1	
2 - 25%	
3	
4 - 50%	
5	
6 - 75%	
7	
8 - OVERCAST	
PHENOSEASON	
1 - WINTER LEAFLESS	
2 - SPRING LEAFLESS	
3 - SPRING LEAFING	
4 - SUMMER LEAFING	
5 - SUMMER FULLY-LEAFED	
6 - AUTUMNAL FULLY-LEAFED	
7 - AUTUMNAL PARTIALLY LEAFED	

Figure 19: Example of a field sheet used to record PAR observation data.

## 4.2 Ecological Survey and Mensurational Data

A site survey of all relevant individuals was conducted using GPS locations of canopy trees > 10 cm DBH and *L. benzoin* > 45cm tall (~2 years of age or older). Stand characteristics of DBH, stand density, and basal area were collected in October 2014. DBH was measured using diameter tape from Forestry Suppliers. Standard equations for stand density (Equation 1) and basal area (Equation 2) were used. Canopy heights and mean bark thickness were initially collected for a portion of this field site during the fall of 2012 using a laser range finder and bark gauge on trees >10cm DBH. These measurements were then expanded to include the addition of the southern end of the plot.

$$(1) \quad \frac{\# \text{ trees } > 10\text{cm DBH}}{\text{plot size (m}^2\text{)}} * \frac{10^4\text{m}^2}{\text{ha}}$$

$$(2) \quad \Sigma \left( \frac{\text{DBH}}{200^2\pi} \right) * \frac{10^4\text{m}^2}{\text{plot size (m}^2\text{)}}$$

## 4.3 *Lindera benzoin* Treatments

In the lab, sets of *L. benzoin* seeds purchased from Horizon Herbs (Williams, OR, USA) were germinated in PRO-MIX® and grown in natural light at room temperature for approximately 60 days. After this time, the sets of plants were placed into the base of a Conviron PGC20 Reach-In Plant Growth Chamber (Winnipeg, Manitoba, Canada) programmed at 24°C and 68% relative humidity. At the time of use, the growth chamber was equipped with 400W metal halide light bulbs (MH400/U//ED28, Philips Lighting North America, operational) and 400W high

pressure sodium bulbs (non-operational). A spectral distribution of the MH400/U//ED28 can be found in Figure 20.

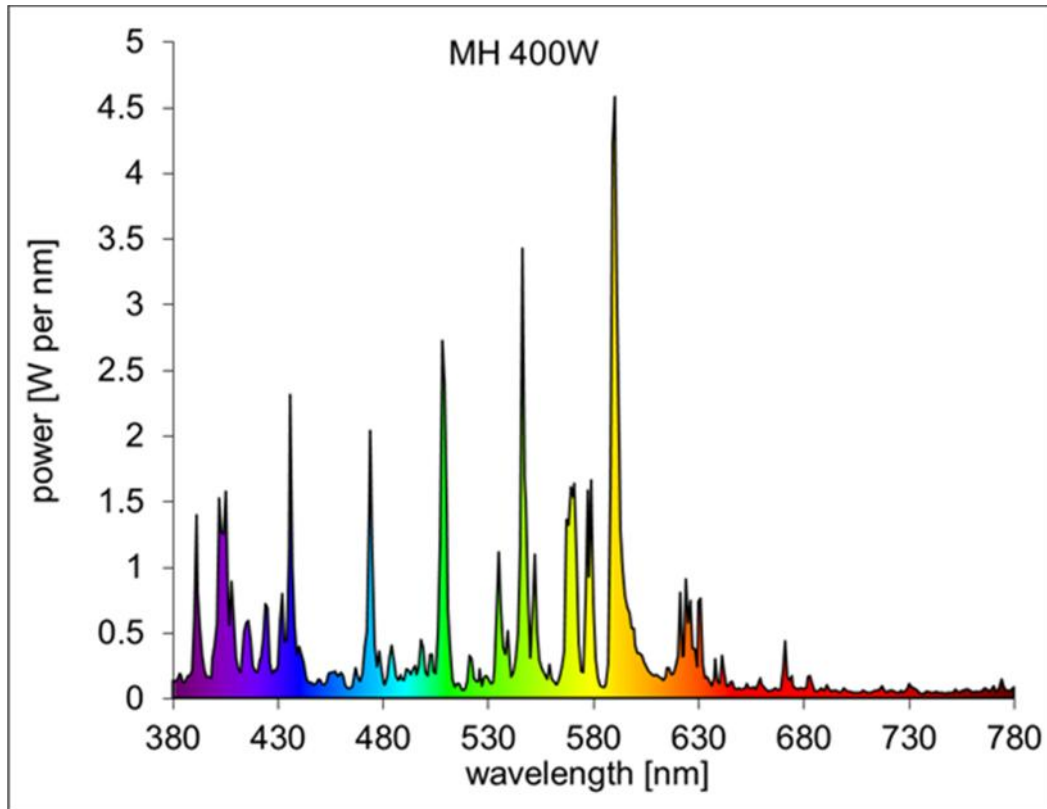


Figure 20: Spectral distribution of MH400, courtesy of Philips Lighting North America.

The growth chamber was arranged for the two treatments of each experiment to receive a different photointensity for a standard photoperiod by elevating one treatment 55cm above the other using a box placed within the growth chamber. Photointensity within the growth chamber was set to  $350 \mu\text{mol m}^{-2}\text{s}^{-1}$ . At this intensity, PAR was manually measured (using an LI-190 Quantum Sensor in conjunction with a

LI-COR LI-250A light meter, LI-COR, Lincoln, NE, USA) at  $517.9 \mu\text{mol m}^{-2}\text{s}^{-1}$  for the upper treatment or “sun” environment and  $366 \mu\text{mol m}^{-2}\text{s}^{-1}$  for the lower treatment or “shade” environment. The program was set to run 16 hours of light and 8 hours of darkness for Experiment #1. Overall, photointensity for the second experiment was set to  $150 \mu\text{mol m}^{-2}\text{s}^{-1}$ . At this intensity, the upper and lower treatments of Experiment #2 were  $164.5 \mu\text{mol m}^{-2}\text{s}^{-1}$  and  $118.06 \mu\text{mol m}^{-2}\text{s}^{-1}$ , respectively, for 12 hours of light and 12 hours of darkness. These values were selected based on our experience in the field, as well as the field work of Niesenbaum and Kluger (2006) who found that, in a deciduous forest in Northampton County, PA, average PAR for a shade environment was  $48.01 \mu\text{mol m}^{-2}\text{s}^{-1}$ , and  $658.3 \mu\text{mol m}^{-2}\text{s}^{-1}$  for a sun environment. While an attempt was made to come as close to these values as possible, the growth chamber was unable to be set for any lower photointensity than  $150 \mu\text{mol m}^{-2}\text{s}^{-1}$ , limiting the lower range of PAR for this aspect of the study. The growth chamber experienced a failure and shut down in the last two days of the end of the second experiment. No negative effects were noted.

Each set was grown under these respective conditions for 35 days. At the end of the 35 day growing period, living plants were sketched (see Appendix D for example), photographed, and measured for leaf area, node height, and internodal distance. Porometer readings were conducted twice, once at during the 2<sup>nd</sup> to last week, and one week later using a Model SC-1 Leaf Porometer (Decagon Devices, Inc., Pullman, WA, USA). All plants were then harvested for the following fatal measurements: dry weight, root-to-shoot ratio, analysis of chlorophyll a, chlorophyll b, carotenoids, and biomass. See Figure 21 for a workflow diagram.

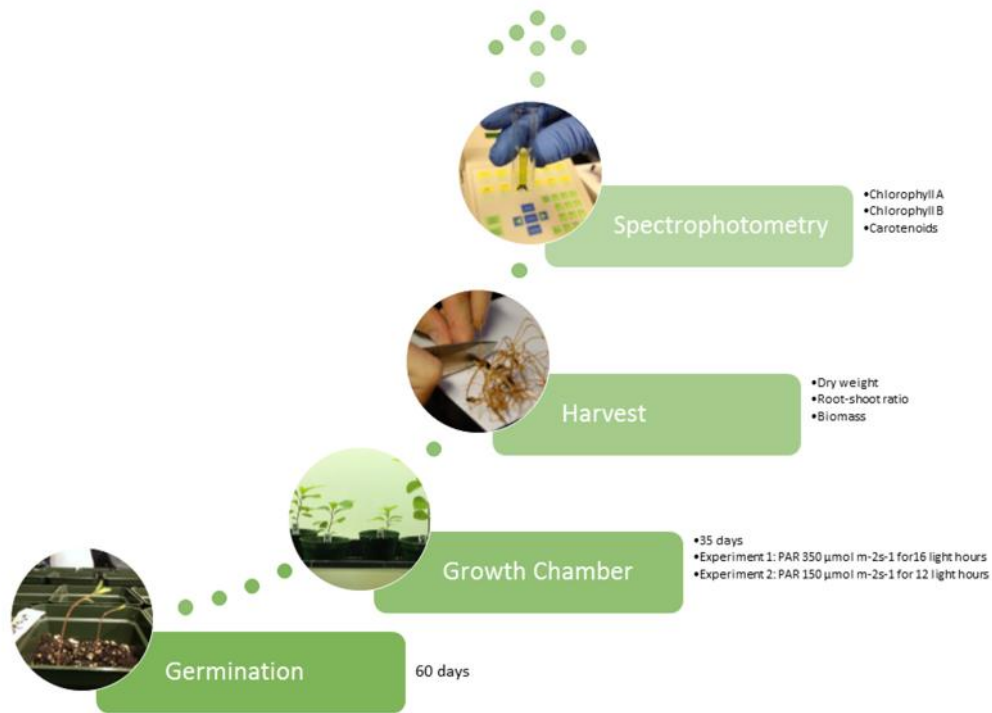


Figure 21: Workflow diagram of the *L. benzoin* experiments. Seeds germinated and grew for 60 days in the lab, were transferred to the growth chamber and kept under experimental conditions for ~35 days, were harvested and measured, then finally the fourth and fifth leaves were used for spectrophotometry.

Additionally, one similarly sized *L. benzoin* was located within the plot at Fair Hill NRMA. This individual was marked with flagging tape and sketched. Porometer readings were conducted in the field twice, one week apart using a Model SC-1 Leaf Porometer (Decagon Devices, Inc., Pullman, WA, USA). Due to restrictions on removal of naturally occurring species within the NRMA, only the fourth and fifth leaves were harvested from the field specimen for spectrophotometry analysis.

Using standard lab protocol, growth chamber specimens were removed from their soil, rinsed, photographed with scale, and bisected at the root-shoot division. Roots and shoots were weighed separately. The fourth and fifth leaves from the top were removed from each plant, weighed, placed into labeled sealed vials, and placed into cold storage at 4°C. To obtain dry weight for roots and shoots, remaining wet mass was oven dried at 60°C for 48 hours and roots and shoots were re-weighed separately.

Fourth and fifth leaves were taken to the Bais Lab at the Delaware Biotechnology Institute for measurement of chlorophylls and carotenoids using spectrophotometry. Samples were prepared by cutting the fourth and fifth leaves into two sets each of approximately 25 mg yielding four samples per plant, two per leaf, and the weight of each sample was recorded (see Table 24, in Chapter 5). Individual samples were placed into a mortar with 500 µL of 90% methanol and crushed to a uniform consistency (acetone was not used for health concerns). Samples were then transferred to a labeled Eppendorf Safe-Lock 1.5 mL tube and placed into an Eppendorf Centrifuge Minispin® (Hamburg, Germany) at 13.2 x 1000 rpm for 5 minutes. After separation the supernatant, or liquid portion, was transferred to a respectively labeled Eppendorf Safe-Lock 1.5 mL tube and another 500µl of 90% methanol was added to the pellet (solid remains). The pellet was re-extracted in the centrifuge at 13.2 x 1000 rpm for 5 minutes. Supernatant was again removed and pooled to 1.0 mL in the secondary Eppendorf Safe-Lock 1.5 mL tube.

Extracted samples were held in cold storage (4°C) for less than 48 hours before spectrophotometry. Using an absorbance blank of 90% methanol, a SmartSpec™ Plus Spectrophotometer (Bio-Rad, CA) was calibrated to zero absorbance. The absorbance

of each sample was then measured at 450 nm, 470 nm, 645 nm, and 661 nm. Calculations for chlorophyll a, chlorophyll b, and total chlorophyll were completed in Excel using equations 3, 4, and 5, respectively, provided by Bais Lab. See Figure 22 for a spectrophotometry workflow diagram.

$$(3) \text{ Chla } (g \text{ l}^{-1}) = 0.0127 (\alpha_{661.5}) - 0.00269 (\alpha_{645})$$

$$(4) \text{ Chlb } (g \text{ l}^{-1}) = 0.0029 (\alpha_{661.5}) - 0.00468 (\alpha_{645})$$

$$(5) \text{ Total Chl } (g \text{ l}^{-1}) = 0.0202 (\alpha_{661.5}) + 0.00802 (\alpha_{645})$$

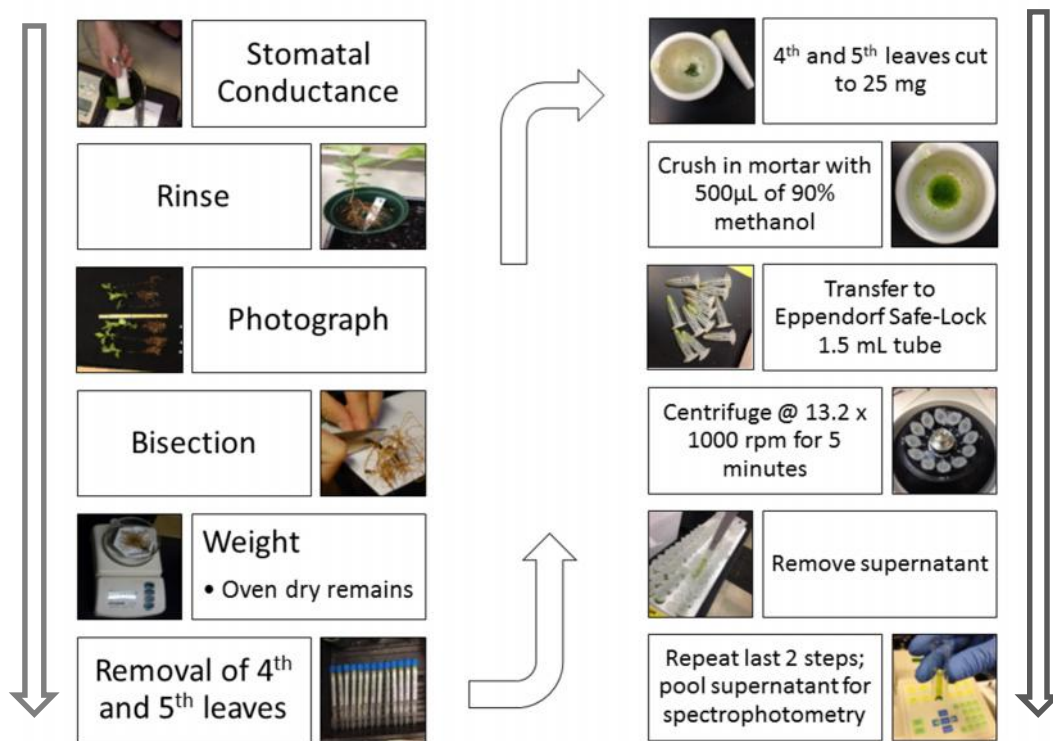


Figure 22: Workflow diagram of fatal measurements and spectrophotometry.

## **4.4 Data Analysis**

### **4.4.1 PAR**

The spreadsheet of data collected throughout the year was used for statistical analysis of annual, whole phenoseason, and individual day data via box plot, line plot, and descriptive statistics procedures. Descriptive statistics (mean, median, max value, min value, lower quartile, upper quartile, and standard deviation) and box plots (median, upper and lower quartile, outliers and extreme cases) were calculated for almost all variables, including: all open and understory PAR observations, understory PAR observations by phenoseason, average understory, shrub mid-level and shrub low-level PAR observations, clear and overcast sky conditions, PAR observations by location, PAR observations for a four hour period on an afternoon in September, and the measured physical and chemical attributes of plants used in the growth chamber experiments.

Additionally, an analysis of variance (ANOVA) was conducted on the values of PAR for the understory, shrub mid-level and shrub low-level to determine if phenoseason was a governing factor in its variation. ANOVA assumes normality, that observations be independent of one another, and that the variances of the groups be similar. ANOVA is a forgiving statistical analysis that can yield significant results with few observations.

An attribute table was assigned to the coordinates of the observation points using the PAR data collected throughout the year by selecting one day from each phenoseason, as close to solar noon as possible, which represented one clear, one overcast, and one partly cloudy sky condition. For some phenoseason-sky condition combinations, no “solar noon” readings are available within the two hour time frame

so other times as near solar noon as possible were selected. Observation points were assigned their unique PAR value at the selected time step. Distributions of these days were created in an attempt to show light quantity changes as a function of phenoseason and sky condition.

#### **4.4.2 Ecological Survey**

Plant locations and measurements collected during the ecological survey conducted in October of 2014 were entered into a database and analyzed using geospatial software. In an attempt to show associations and dependence between species and obtain a detailed picture of how the *L. benzoin* grows, possibly in relation to the spatial distribution of light as a function of canopy trees of varying species, point-pattern analysis was attempted.

Ripley's method of point-pattern analysis allows one to look at the spatial arrangement of points, to determine if clusters exist, or if plants grow randomly within a space, and while the scale of this study is not appropriate for determining clusters of canopy trees using point-pattern analysis (Dale, 1999), it should be appropriate for shrubs, and helpful for making inferences about inhibition processes and the distribution of *L. benzoin* in relation to the canopy trees. This process places a circle with radius  $t$  centered over plant  $n$  for all plants and counts the distance to the number of plants within that circle to determine if points occur randomly as well as the density of plants in a given area (Dale, 1999). To correct of "lack of plants" edge effects, a weighting factor is also calculated, by determining the amount of the roving circle located outside of the study area (Dale, 1999). This feature is called "Multi-distance Spatial Cluster Analysis (Ripley's K Function)" in ArcMap 10.2. The statistic was

calculated using 99 permutations for the confidence interval and a Ripley's Edge Correction Formula.

#### **4.4.3 *Lindera benzoin* Treatments**

Statistical analysis for *L. benzoin* chemistry experiments was conducted. Quantile-Quantile plots were used to determine normality. In addition to Each Pair Student's T test, the Tukey-Kramer comparison of means test was selected to account for type one errors due to small sample sizes. In an attempt to verify if experimental plant groups could be predicted based on the physical and chemical attributes of individual plants, discriminate analysis were performed. Discriminant analysis is useful for separating metric data into categorical groups (Hair Jr. *et al.* 1987). In this case groups represent plants from different levels and experiments, for example, the upper treatment of plants from Experiment 2 or the lower treatment from Experiment 1. Using discriminant analysis, the non-redundant variables can be entered, and using variables that maximize the among-group variance (coefficients), a discriminant score is calculated for each plant which allows it to be grouped with plants most similar to it. Some of the primary assumptions of discriminant analysis are the same as in most multivariate analysis: the data should be normally distributed, relationships should be linear, and multiple independent variables should not be collinear (Afifi *et al.* 2012). Correlations were computed between all variables, allowing detection of linearity and collinearity. By excluding one of the two variables which are highly correlated, collinearity is avoided in the discriminant analysis and all assumptions for this analysis are met. Unfortunately, due to low germination rates as the experiment progressed, it is possible that the small sample sizes in the physical attributes may be inappropriate for discriminant analysis but, all groups are similarly small and it is

hoped that this will not have too much impact on the analysis because it is often large groups which become over-classified (Hair Jr. *et al.* 1995).

## Chapter 5

### RESULTS

#### 5.1 PAR Collection in the Field

PAR collected for this study was compared to DEOS station data for accuracy. The correspondence between all three radiation sensors is visible in Figure 23.

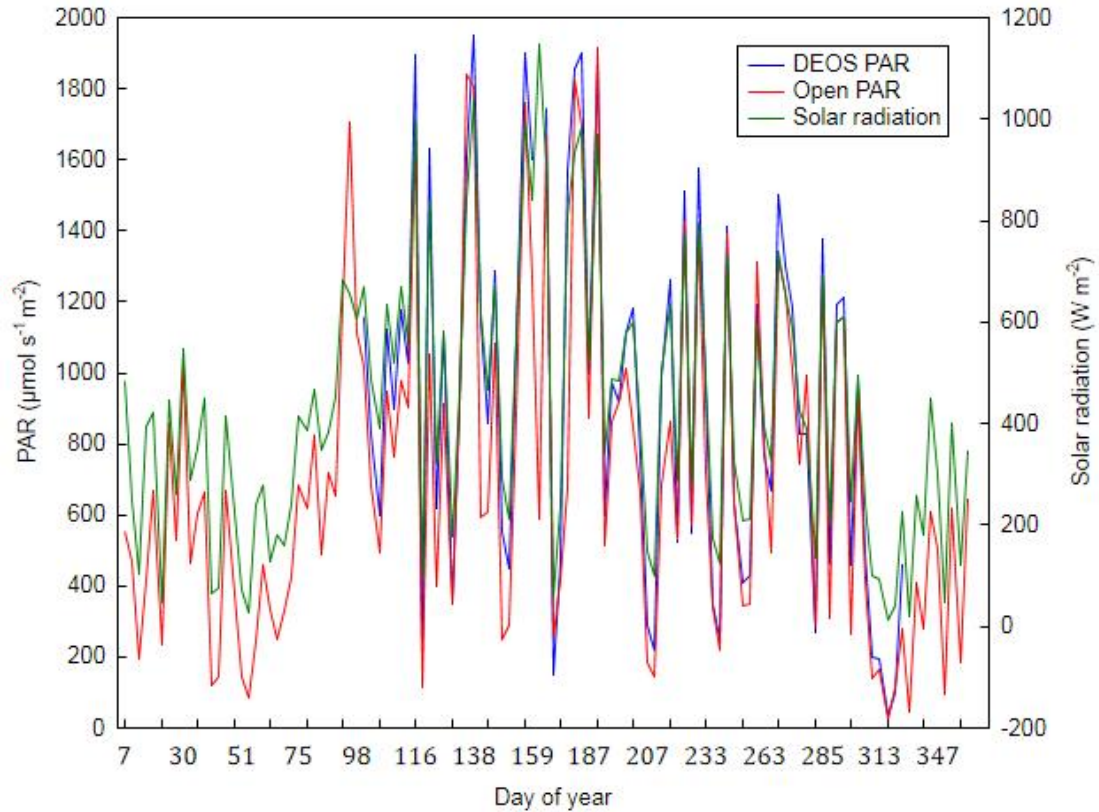


Figure 23: Line plot of collected field data for open readings (Open PAR) plotted next to PAR and solar radiation data from the meteorological station nearby.

Understory PAR values increase in the beginning of the spring as the solar elevation rises, but drop sharply, to near zero, with leaf-out and see only a slight increase after leaf-off occurs in the autumn. Understory PAR has, overall, a greater range of ‘normal’ values during the leaf-off phenoseasons, but extreme cases increase as mean PAR values and the intensity of variability decrease with leaf-on phenoseasons. For all but locations two and three, the spring leafing phenoseason has the greatest range. The summer fully-leafed and autumnal fully-leafed phenoseasons have the greatest instances of extreme values (observations often go from near zero to many hundreds of  $\mu\text{mol m}^{-2} \text{s}^{-1}$ ). The spring leafing and summer leafing phenoseasons have the highest standard deviations, 259.48 and 218.76  $\mu\text{mol m}^{-2} \text{s}^{-1}$ , respectively. A summary of descriptive statistics for each phenoseason can be found in Table 5.

A quantile-quantile plot determined that PAR data is non-normally distributed, but rather follows an exponential curve. This result is expected, per the results of Hutchison and Matt (1977), therefore median values and quartiles are presented for a more complete representation of the data. The following sections contain selected data from each phenoseason.

Table 5: Summary descriptive statistics of understory PAR ( $\mu\text{mol m}^{-2} \text{s}^{-1}$ ) for each phenoseason.

Phenoseason	Valid N	Mean	Median	Min	Max	Lower quartile	Upper quartile	Std. Dev.
Winter Leafless	667	181.15	157.98	8.43	1017.90	87.21	244.90	124.60
Spring Leafless	399	178.74	129.67	21.42	777.60	74.18	286.90	133.28
Spring Leafing	435	415.17	341.70	88.73	1704.70	229.70	520.40	259.48
Summer Leafing	406	105.45	26.47	2.77	1839.00	12.90	98.30	218.76
Summer Fully-leafed	637	56.81	10.77	1.12	1913.30	6.51	18.82	211.28
Autumnal Fully-leafed	493	47.14	11.06	0.53	1428.00	6.30	19.30	174.07
Autumnal Partially-leafed	397	77.04	44.91	0.61	1278.80	22.47	85.08	132.99

### 5.1.1 Winter Leafless Phenoseason (November to February)

The winter leafless phenoseason had a total of 667 observations, not including the tiered readings, and low overall values of subcanopy PAR. 41.5 % of reading days had visual sky conditions greater than 4 oktas and 11.9% of days were fully overcast. The mean subcanopy PAR was  $181.15 \mu\text{mol m}^{-2} \text{s}^{-1}$  and the median subcanopy PAR was  $157.98 \mu\text{mol m}^{-2} \text{s}^{-1}$  (not including the open reading). The interquartile range remains below  $250 \mu\text{mol m}^{-2} \text{s}^{-1}$  with few out outliers or extreme values. For a graphical representation of PAR for the winter leafless phenoseason by location, see Figure 24.

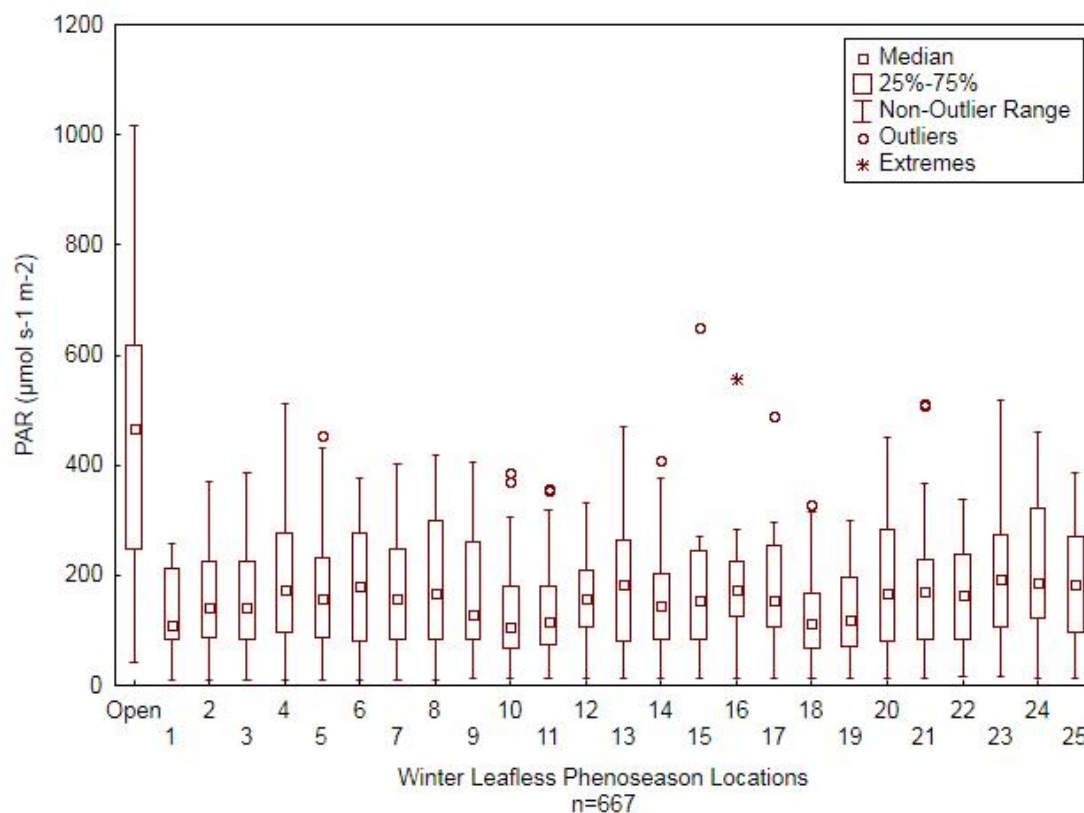


Figure 24: Box plot of PAR values at each location for the winter leafless phenoseason.

### 5.1.1.1 Selected Days

Days selected to highlight the variability of the winter leafless phenoseason were January 16, January 30, and February 4, 2014. A summary of the descriptive statistics is found in Table 6.

Table 6: Summary descriptive statistics of PAR ( $\mu\text{mol m}^{-2} \text{s}^{-1}$ ) for selected days of the winter leafless phenoseason.

<b>Day</b>	<b>Mean</b>	<b>Median</b>	<b>Minimum</b>	<b>Maximum</b>	<b>Lower (Quartile)</b>	<b>Upper (Quartile)</b>	<b>Std.Dev.</b>
16	184.68	180.36	148.77	320.20	170.16	190.56	30.15
30	255.62	225.10	80.53	649.70	117.65	365.95	159.80
35	295.21	288.70	244.10	390.40	263.90	321.40	39.54

January 30, 2014 (Day 30, Figure 25) was a clear day with a visual sky cover of 0% cloudiness. Measurements were taken from 12:21 to 12:51. The open value PAR was  $1017.9 \mu\text{mol m}^{-2} \text{s}^{-1}$ , and snowpack was still leftover on the ground from a recent snow. January 16, 2014 (Day 16, Figure 25) was partly cloudy with a visual sky cover of 4 oktas. Measurements were taken from 13:16 to 13:44. The open value PAR was  $416.10 \mu\text{mol m}^{-2} \text{s}^{-1}$ . February 4, 2014 (Day 35, Figure 25) was mostly overcast with a VSC of 7 oktas. Readings were collected from 11:55 to 12:23. Open value PAR was recorded at  $606.10 \mu\text{mol m}^{-2} \text{s}^{-1}$ . These readings were taken between two ice storms and there was a high, thin overcast. Values of PAR for the overcast day are higher and the range is much smaller than for the partly cloudy day.

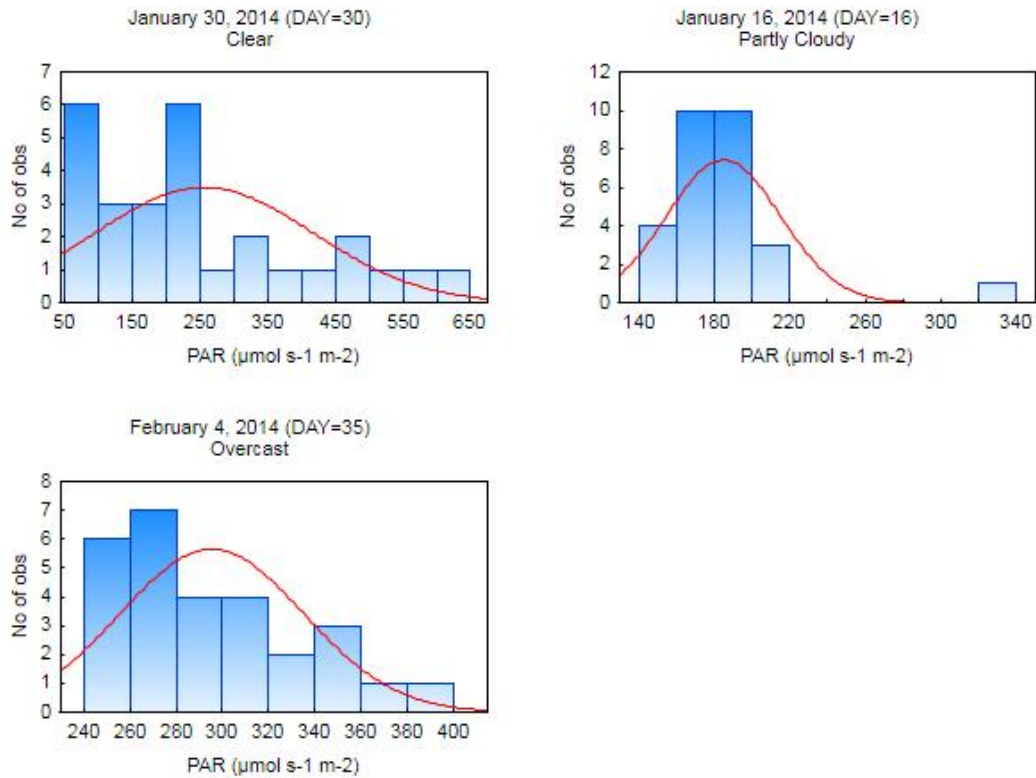


Figure 25: Distributions of PAR for varying sky conditions in the winter leafless phenoseason.

### 5.1.2 Spring Leafless Phenoseason (February to April)

The spring leafless phenoseason had a total of 399 readings, not including tiered readings, 65.1% of which had cloud cover greater than 4 oktas. 43.6% of days were fully overcast. Mean remained below 200 μmol m<sup>-2</sup> s<sup>-1</sup>, at 178.74 μmol m<sup>-2</sup> s<sup>-1</sup>, with the median even lower at 129.67 μmol m<sup>-2</sup> s<sup>-1</sup> but interquartile range shifted upward to 286.9 μmol m<sup>-2</sup> s<sup>-1</sup> and lower to 74.18. Open readings are similarly low for this phenoseason. For a graphical representation of PAR for the spring leafless phenoseason by location, see Figure 26.

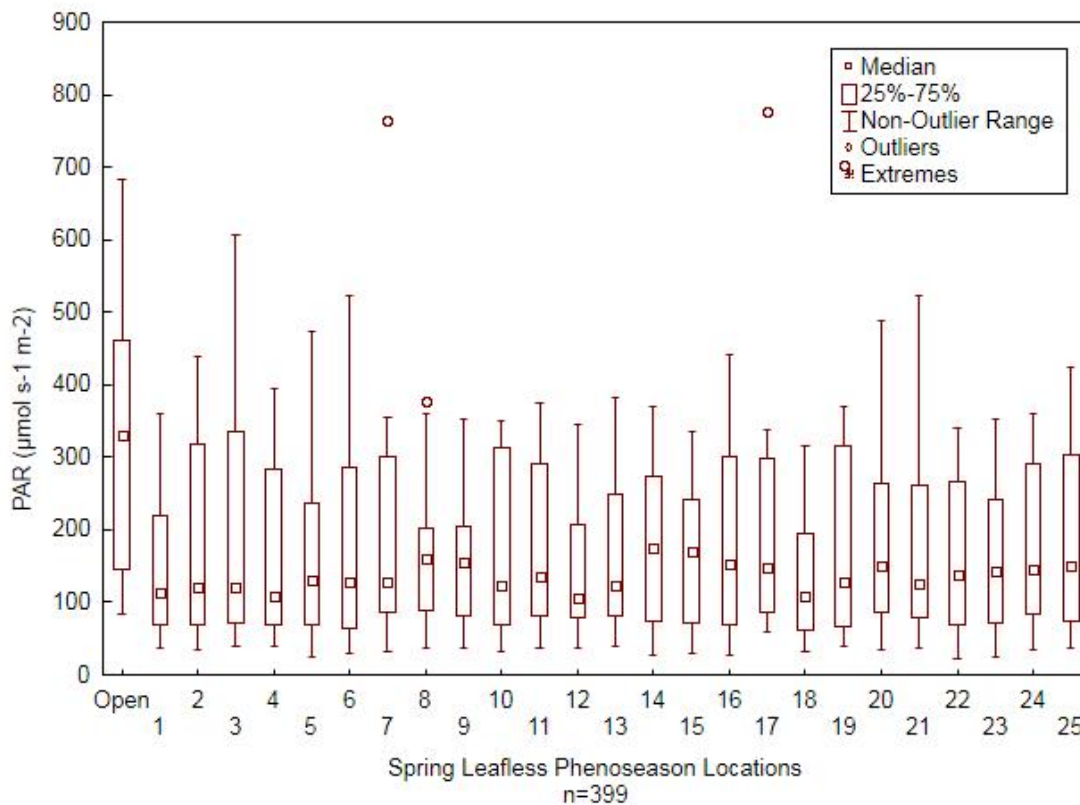


Figure 26: Box plot of PAR values at each location for the spring leafless phenoseason.

### 5.1.2.1 Selected Days

Days selected to highlight variability for the spring leafless phenoseason were February 10 and 28, and March 16, 2014. A summary of the descriptive statistics for these days can be found in Table 7.

Table 7: Summary descriptive statistics of PAR ( $\mu\text{mol m}^{-2} \text{s}^{-1}$ ) for selected days of the spring leafless phenoseason.

Day	Mean	Median	Minimum	Maximum	Lower (Quartile)	Upper (Quartile)	Std.Dev.
41	74.70	74.49	52.64	93.01	65.29	85.44	11.08
59	50.57	44.72	35.63	122.31	40.95	56.01	17.03
75	334.77	334.45	285.30	396.50	314.50	352.00	27.78

February 28, 2014 (Day 59, Figure 27) was clear with a VSC of 0.

Unfortunately, due to the cloudiness of this phenoseason no readings met the solar noon requirement. The closest clear day values were taken between 07:34 and 08:07. Sunrise occurred at 6:36 and so, open value PAR was recorded at  $245.10 \mu\text{mol m}^{-2} \text{s}^{-1}$ . February 10, 2014 (Day 41, Figure 27) represents the partly cloudy day for the spring leafless phenoseason. Measurements were taken from 16:14 to 16:35. Cloud cover was VSC of 5. The open value was  $144.58 \mu\text{mol m}^{-2} \text{s}^{-1}$ , and there were no significant notes. March 16, 2014 (Day 75, Figure 27) was completely overcast with a VSC of 8. Readings were collected between 13:15 and 13:45. Open value PAR was  $682.10 \mu\text{mol m}^{-2} \text{s}^{-1}$ . Distributions in Figure 27 show that increasing cloud cover seems to reduce skewness of the distribution and increase overall energy in the subcanopy.

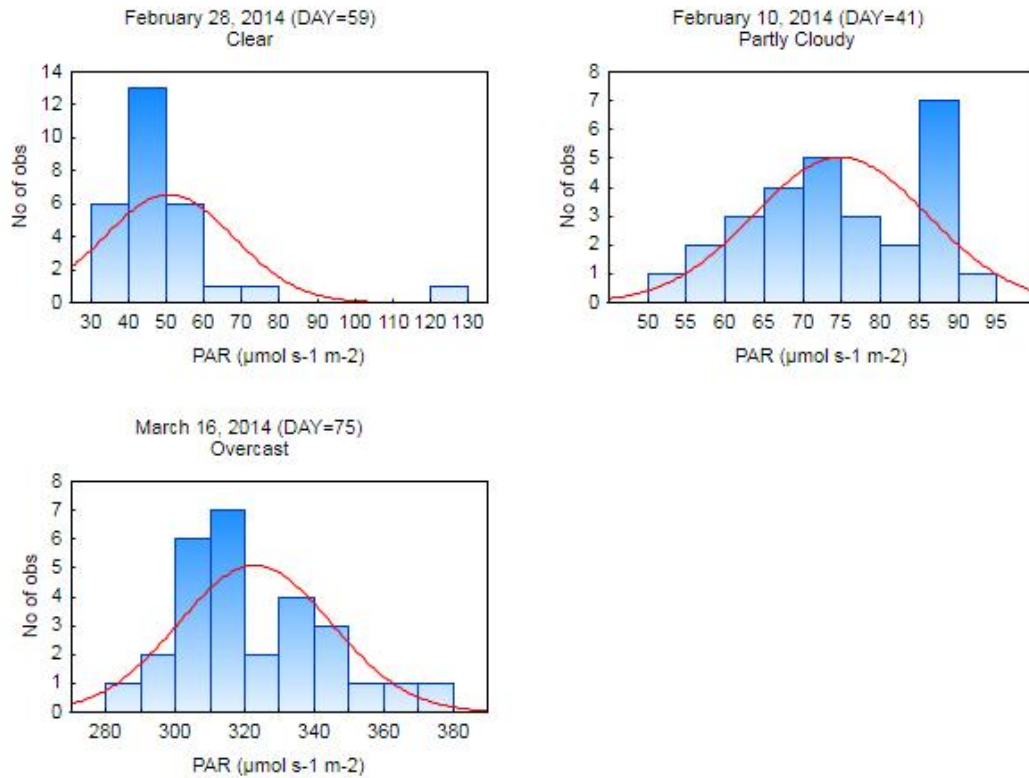


Figure 27: Distribution of PAR values for three sky conditions during the spring leafless phenoseason.

### 5.1.3 Spring Leafing Phenoseason (April to May)

The spring leafing phenoseason shows a peak in open PAR similar to that of the summer fully-leafed phenoseason. A total of 435 readings were collected, not including tiered readings, with 46.7% of days with sky cover greater than 4 oktas and 6.6% fully overcast days. Subcanopy readings increase for all locations by nearly double, to a mean of  $415.17 \mu\text{mol m}^{-2} \text{s}^{-1}$ , while ranges diminish. For a graphical representation of PAR for the spring leafing phenoseason by location, see Figure 28. Figure 29 shows canopy state as leaf-out occurs over a one-month period. Figure 30 shows the relationship between increasing LAI and the natural log of average PAR. A

trend line shows that as leaf out occurs and LAI increases, average subcanopy PAR decreases.

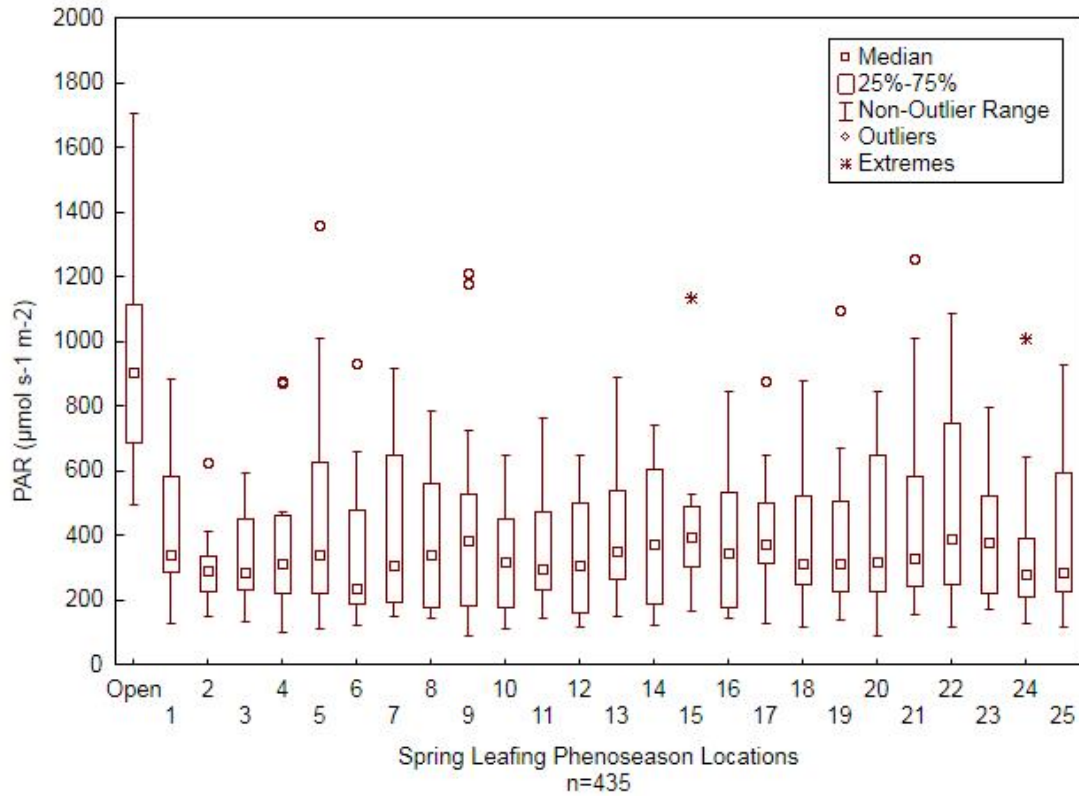


Figure 28: Box plot of PAR values at each location for the spring leafing phenoseason.



Figure 29: Leaf-out canopy changes: a one month period spanning the end of the spring leafing phenoseason and beginning of the summer leafing phenoseason. From left to right: April 24, May 6, and May 24, 2014.

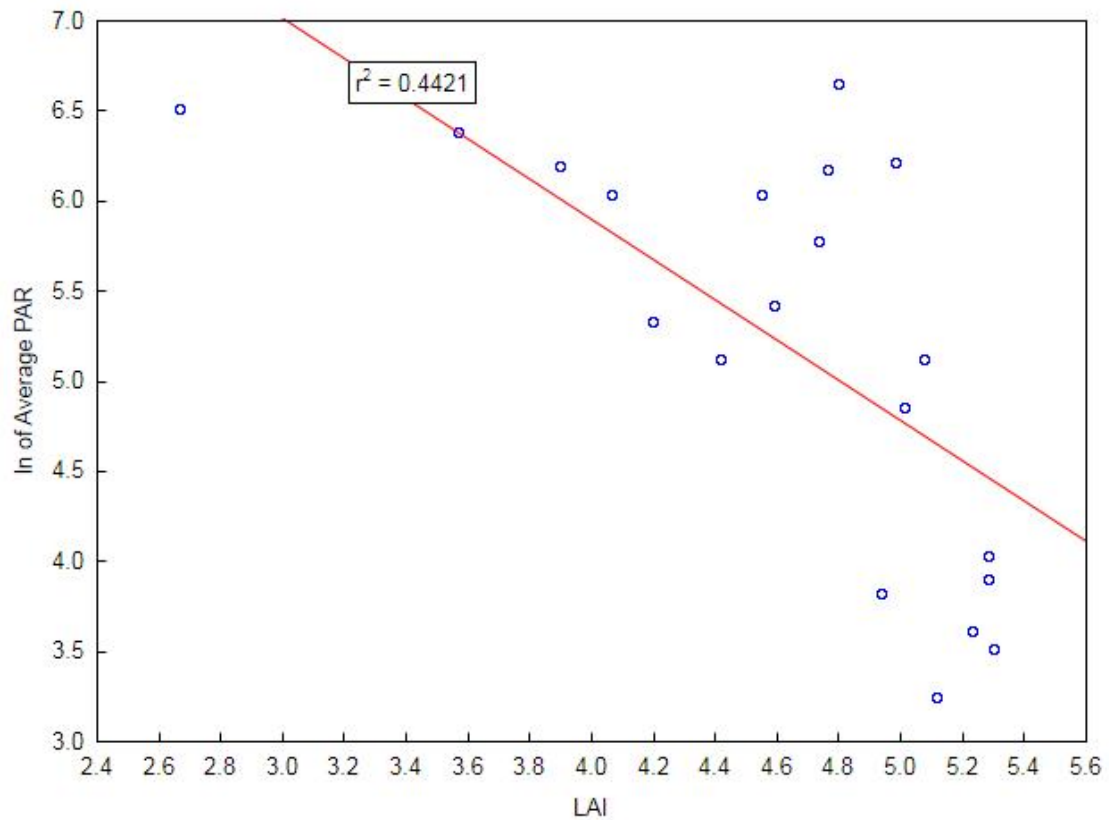


Figure 30: Line plot of leaf area index versus the ln of Average PAR for a ten week period from March 27<sup>th</sup> to May 24<sup>th</sup>. Trend shows that as leaf out occurs, and LAI increases, average subcanopy PAR decreases.

### 5.1.3.1 Selected Days

Days selected to highlight variability for the spring leafing phenoseason were March 23<sup>rd</sup>, April 1<sup>st</sup>, and April 26<sup>th</sup> of 2014. A summary of the descriptive statistics for these days can be found in Table 8.

Table 8: Summary descriptive statistics of PAR ( $\mu\text{mol m}^{-2} \text{s}^{-1}$ ) for selected days of the spring leafing phenoseason.

Day	Mean	Median	Minimum	Maximum	Lower (Quartile)	Upper (Quartile)	Std.Dev.
82	312.34	311.40	256.40	379.70	286.90	336.00	36.16
91	675.98	661.35	98.68	1254.50	507.05	846.05	274.28
116	772.28	768.80	232.20	1357.40	634.80	934.85	268.74

April 26, 2014 (Day 116, Figure 31) was clear (VSC = 0), and the open reading was  $1666.90 \mu\text{mol m}^{-2} \text{s}^{-1}$ . Readings were taken from 12:50 to 13:21. There were no significant meteorological notes. April 1, 2014 (Day 91, Figure 31) was partly cloudy with a VSC of 3. Readings were taken between 11:37 and 12:07, and the open reading PAR was  $1196.40 \mu\text{mol m}^{-2} \text{s}^{-1}$ . March 23, 2014 (Day 82, Figure 31) is the representative overcast day for this phenoseason. Visual sky condition was completely overcast with a VSC of 8. Measurements were collected between 12:08 and 12:30 and the open reading PAR value was  $716.50 \mu\text{mol m}^{-2} \text{s}^{-1}$ . Distributions of PAR values for these three days have the greatest ranges in the clear and partly cloudy sky conditions, and the smallest range with disconnected values during the fully overcast sky condition.

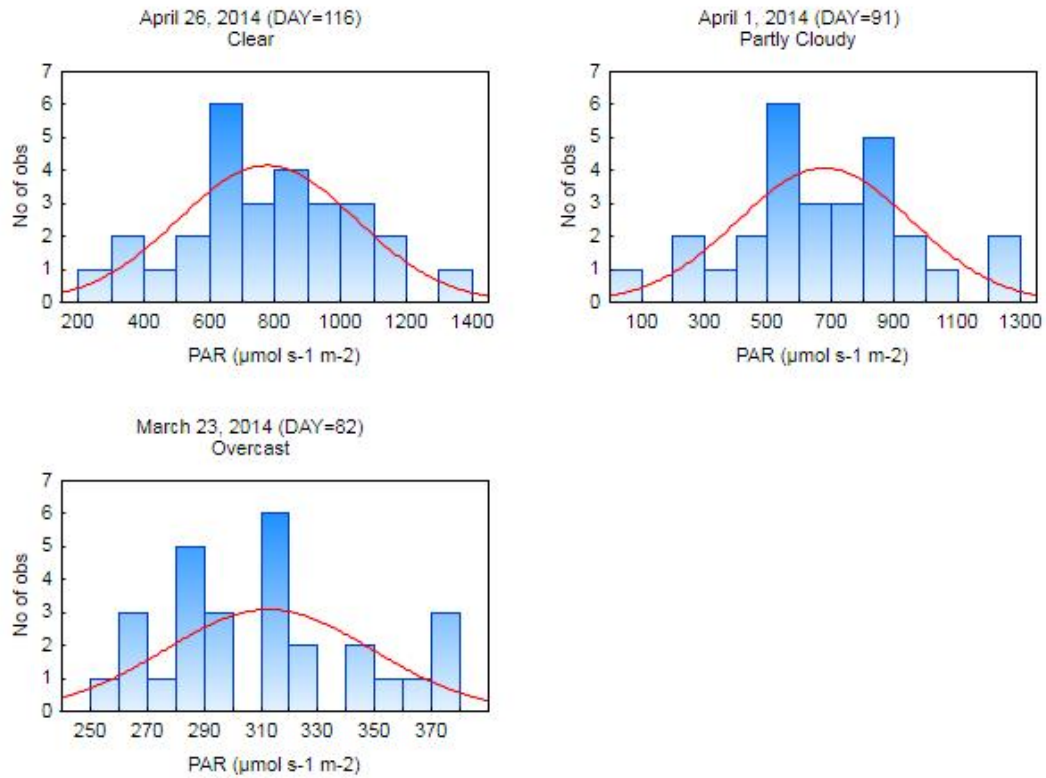


Figure 31: Distribution of PAR values for three sky conditions during the spring leafing phenoseason.

#### 5.1.4 Summer Leafing Phenoseason (May to June)

The summer leafing phenoseason had a total of 406 non-tiered readings, 50.0% of which had days with cloud cover greater than 4 oktas and 14.5% of which were fully overcast. The range of the open PAR values is greater, while the mean of subcanopy readings falls to  $105.45 \mu\text{mol m}^{-2} \text{s}^{-1}$ , median subcanopy readings fall from 341 to  $26.47 \mu\text{mol m}^{-2} \text{s}^{-1}$ , and the upper quartile range of all subcanopy readings drops to  $98.3 \mu\text{mol m}^{-2} \text{s}^{-1}$ . The number of extreme outliers also increases for this

phenoseason. For a graphical representation of PAR for the summer leafing phenoseason by location, see Figure 32.

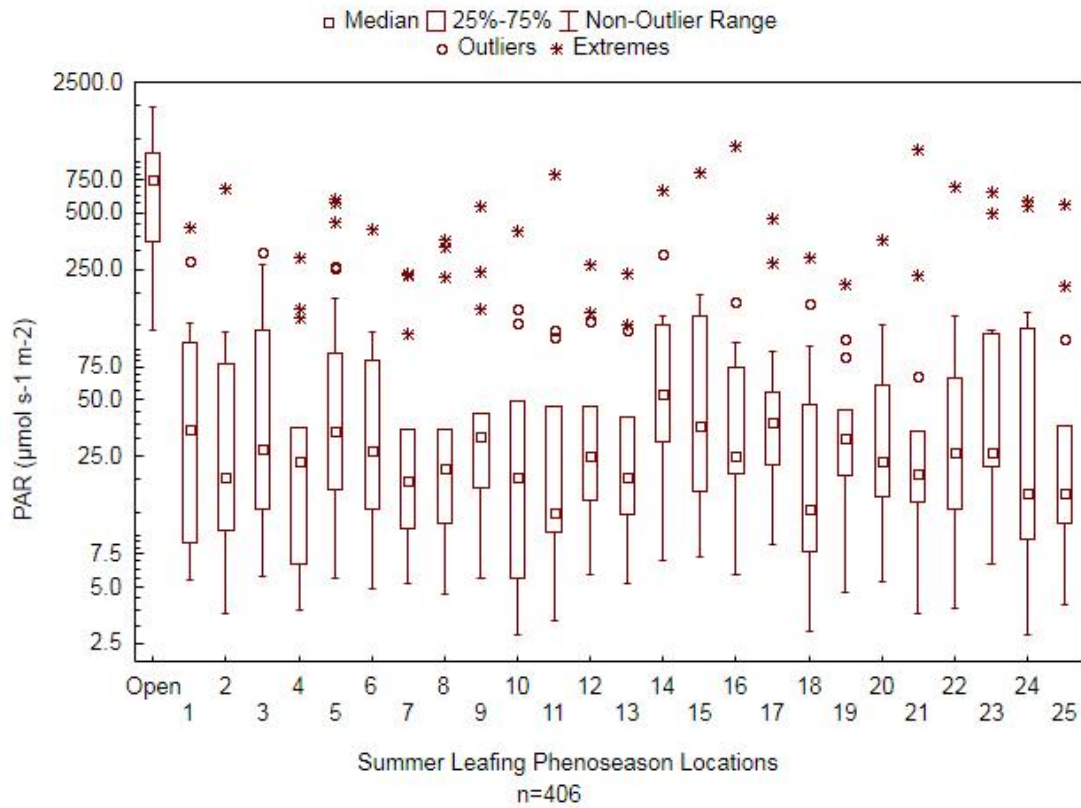


Figure 32: Box plot of PAR values at each location for the summer leafing phenoseason.

#### 5.1.4.1 Selected Days

Days selected to highlight variability for the summer leafing phenoseason were May 3, 4, and 26, 2014. A summary of the descriptive statistics for these days can be found in Table 9.

Table 9: Summary descriptive statistics of PAR ( $\mu\text{mol m}^{-2} \text{s}^{-1}$ ) for selected days of the summer leafing phenoseason.

Day	Mean	Median	Minimum	Maximum	Lower (Quartile)	Upper (Quartile)	Std.Dev.
123	499.56	435.40	208.40	1143.50	289.65	627.90	248.24
124	128.91	117.89	67.02	245.10	95.33	147.20	44.64
146	32.04	20.48	7.81	104.05	12.70	40.43	28.98

May 26, 2014 (Day 146, Figure 33) represents the clear day for the summer leafing phenoseason. The closest clear day reading to solar noon had a VSC of 1, and the readings took place between 15:09 and 15:38. The open reading PAR value for this day was  $1084.70 \mu\text{mol m}^{-2} \text{s}^{-1}$ . May 3, 2014 (Day 123, Figure 33) is the partly cloudy day for this phenoseason, with a VSC of 5. Readings were taken from 12:14 to 12:46. The open reading PAR value was  $1051.30 \mu\text{mol m}^{-2} \text{s}^{-1}$ , and there were no significant meteorological notes. May 4, 2014 (Day 124, Figure 33) was an overcast day on which the VSC ranged from 7.5 to 8. Readings were collected between 10:43 and 11:14. Open reading PAR was  $398.80 \mu\text{mol m}^{-2} \text{s}^{-1}$ . Distributions for all sky conditions show many more values on the lower energy side, which can be expected as the canopy closes with leaf-out. The timing of these days as far as canopy closure can also be seen in these distributions. May 3<sup>rd</sup> and May 4<sup>th</sup> both have higher max values of PAR than the May 26<sup>th</sup> reading, regardless of sky condition, due to the completion of canopy closure as the month progresses.

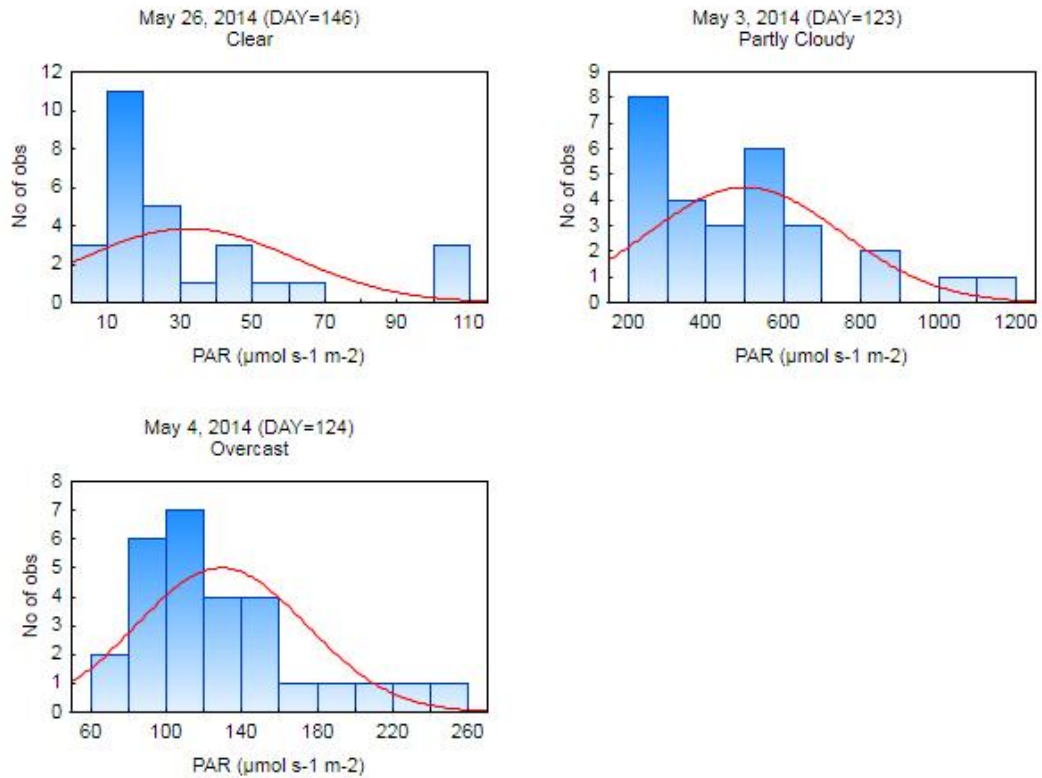


Figure 33: Distributions of PAR values for three sky conditions during the summer leafing phenoseason.

### 5.1.5 Summer Fully-leafed Phenoseason (June to August)

The summer fully-leafed phenoseason had a total of 637 non-tiered readings, 45.5% of which had days with cloud cover greater than 4 oktas. 16.9% of days were completely overcast. Mean and range of open PAR values increase. Median values are lowest for this phenoseason, at  $10.77 \mu\text{mol m}^{-2} \text{s}^{-1}$ . Mean and range of subcanopy readings decrease even farther, to a mean of  $56.81 \mu\text{mol m}^{-2} \text{s}^{-1}$ . Even readings of  $100 \mu\text{mol m}^{-2} \text{s}^{-1}$  are considered ‘extreme’ outliers, with the upper quartile being  $18.82 \mu\text{mol m}^{-2} \text{s}^{-1}$ . For a graphical representation of PAR for the summer fully-leafed

phenoseason by location, see Figure 34. This figure is presented with a log scale to facilitate ease of visualization.

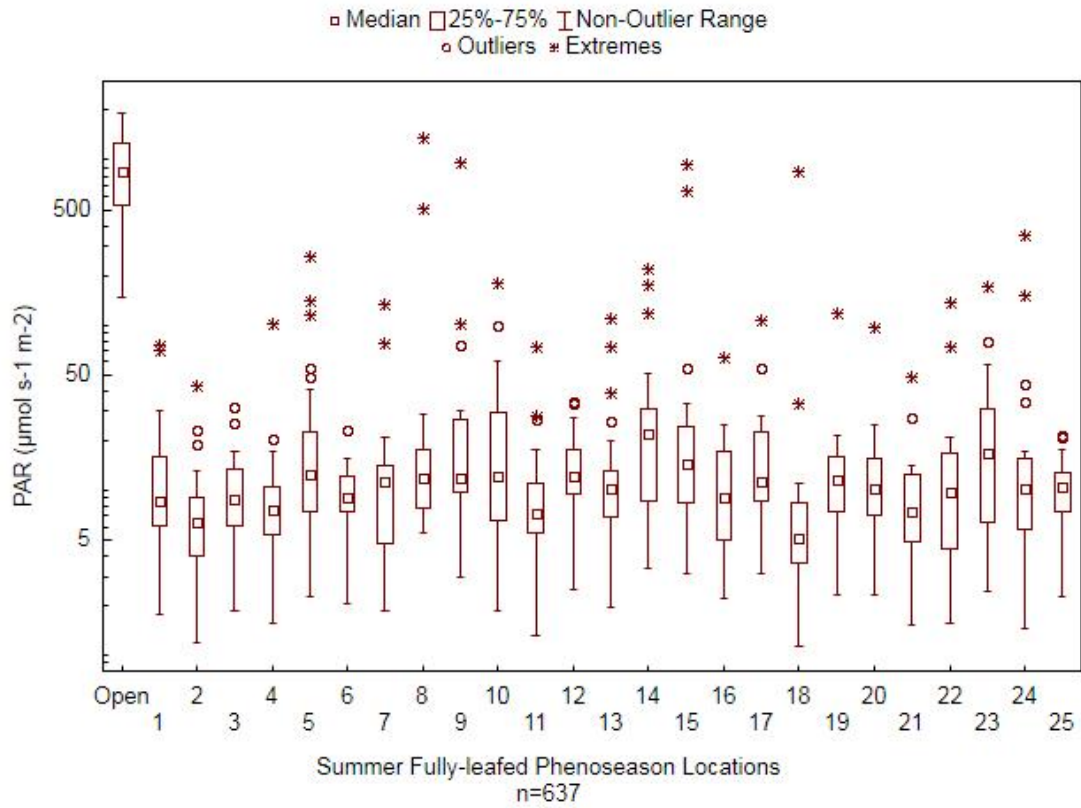


Figure 34: Box plot of PAR values on a log scale at each location for the summer fully-leaved phenoseason.



Figure 35: Canopy on June 29, 2014

### 5.1.5.1 Selected Days

Days selected to highlight variability for the summer leafing phenoseason were June 8 and 26, and July 5, 2014. A summary of the descriptive statistics for these days can be found in Table 10.

Table 10: Summary descriptive statistics of PAR ( $\mu\text{mol m}^{-2} \text{s}^{-1}$ ) for selected days of the summer fully-leafed phenoseason.

Day	Mean	Median	Minimum	Maximum	Lower (Quartile)	Upper (Quartile)	Std.Dev.
159	20.35	14.65	8.36	55.25	11.86	25.04	13.58
186	23.21	7.42	4.70	169.02	6.94	11.88	38.68
207	6.72	6.25	3.87	12.52	4.67	7.38	2.50

July 5, 2014 (Day 186, Figure 36) was a clear day with a VSC of 0. Readings were collected from 11:50 to 12:12, and the open reading PAR was 1694.9  $\mu\text{mol m}^{-2}\text{s}^{-1}$ . These readings took place after the weather system associated with Hurricane Arthur. There was some leaf and branch fall, mostly from *L. tulipifera*. There was no apparent impact on PAR. Partly cloudy readings were obtained on June 8, 2014 (Day 159, Figure 36). The visual sky condition was 3.5. Readings were collected between 13:21 and 13:47, and the open reading was 1269.00  $\mu\text{mol m}^{-2} \text{s}^{-1}$ . There were no significant meteorological notes for this day. July 26, 2014 (Day 207, Figure 36) was selected as the representative overcast for the summer fully-leafed phenoseason. This day was completely overcast (VSC=8). Measurements were taken from 11:49 to 12:14 and the open reading was 186.81  $\mu\text{mol m}^{-2} \text{s}^{-1}$ . There were no significant meteorological notes. Distributions show values and skewness greatly reduced by overcast conditions and all sky conditions are right skewed.

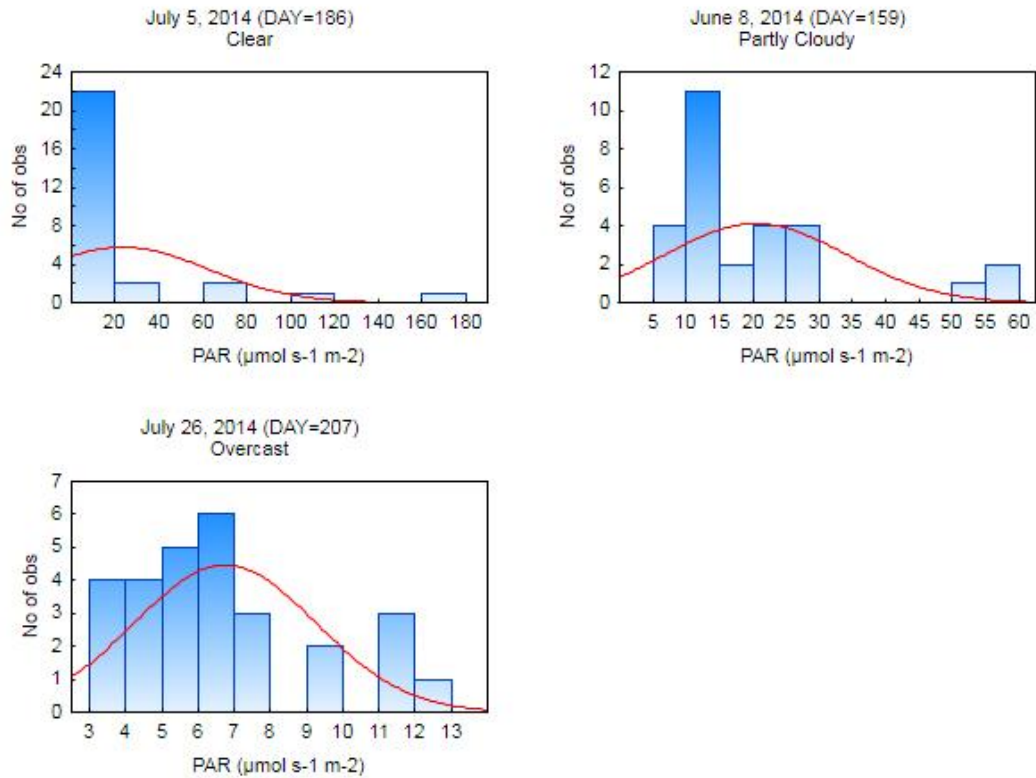


Figure 36: Distribution of PAR values for three sky conditions during the summer fully-leafed phenoseason.

### 5.1.6 Autumnal Fully-Leafed Phenoseason (August to October)

The autumnal fully-leafed phenoseason was similar to the summer fully-leafed phenoseason, but the mean and range of open PAR decreased. A total of 493 non-tiered readings were collected, 32.3% of which had days with cloud cover greater than 4 oktas. 25.4% of days were completely overcast. The mean of all subcanopy readings was  $47.14 \mu\text{mol m}^{-2} \text{s}^{-1}$ . The median of all subcanopy readings was  $11.06 \mu\text{mol m}^{-2} \text{s}^{-1}$ . Mean and minimum values were lowest for this phenoseason. There were many fewer extreme outliers while mean subcanopy PAR remained low. For a graphical

representation of PAR for the autumnal fully-leafed phenoseason by location, see Figure 37.

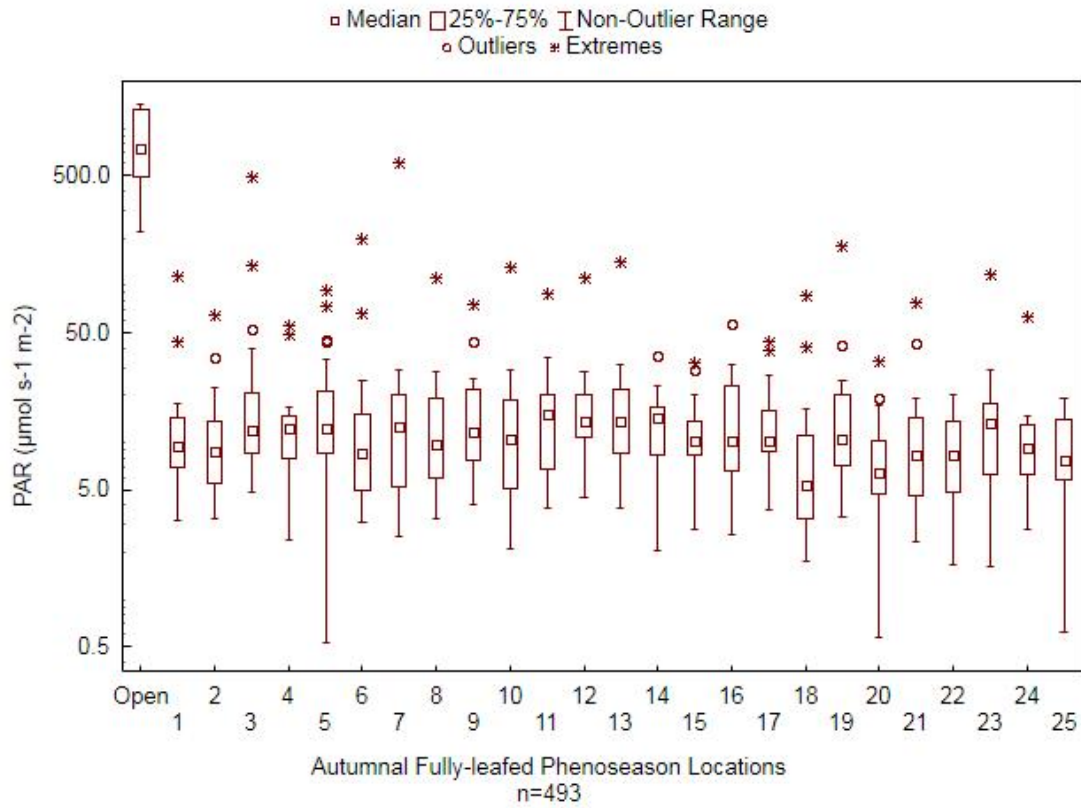


Figure 37: Box plot of PAR values on a log scale at each location for the autumnal fully-leafed phenoseason.



Figure 38: Canopy on September 20, 2014

### 5.1.6.1 Selected Days

Days selected to highlight variability for the summer leafing phenoseason were August 18, August 21, and September 4, 2014. A summary of the descriptive statistics for these days can be found in Table 11.

Table 11: Summary descriptive statistics of PAR ( $\mu\text{mol m}^{-2} \text{s}^{-1}$ ) for selected days of the autumnal fully-leafed phenoseason.

Day	Mean	Median	Minimum	Maximum	Lower (Quartile)	Upper (Quartile)	Std.Dev.
230	31.20	18.26	0.61	195.96	11.99	32.99	38.20
233	20.03	20.27	8.85	35.55	14.32	23.16	6.59
247	21.95	18.18	6.83	115.29	13.62	22.94	19.83

August 18, 2014 (Day 230, Figure 39) was selected as the representative clear day for the autumnal fully-leafed phenoseason. Cloud cover was less than 1% with a few high thin clouds and measurements were taken from 11:12 to 11:37. The open reading PAR was  $1402.30 \mu\text{mol m}^{-2} \text{s}^{-1}$ . September 4, 2014 (Day 247, Figure 39) was partly cloudy with a VSC of 3 described as large fluffy variable clouds. There were no partly cloudy readings during the solar noon timeframe so selected readings were taken from 14:57 to 15:26. The open reading PAR was  $1392.20 \mu\text{mol m}^{-2} \text{s}^{-1}$ . August 21, 2014 (Day 233, Figure 39) had a VSC of 8, and was ‘mostly cloudy’. Readings were taken from 12:28 to 12:55, with an open reading value of  $729.00 \mu\text{mol m}^{-2} \text{s}^{-1}$ . Clear and partly cloudy day distributions are right skewed, while the overcast day is less so. Hot spots are also present for clear and partly cloudy days and this hot spot is greater on the clear day than the partly cloudy day.

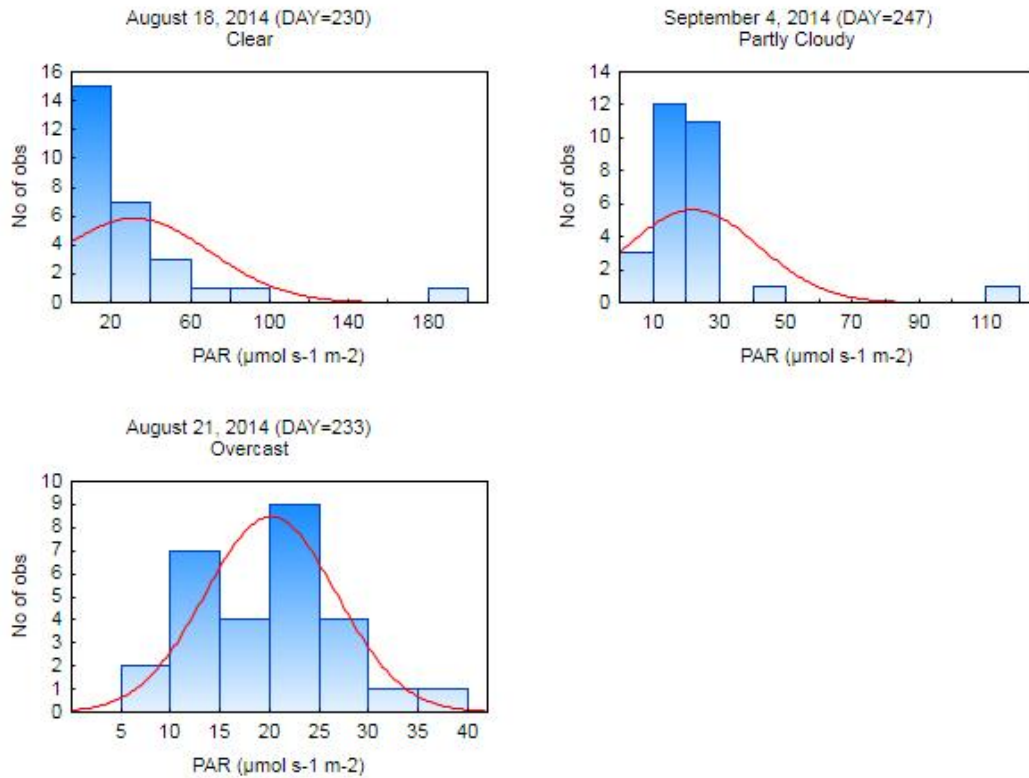


Figure 39: Distribution of PAR values for three sky conditions during the autumnal fully-leaved phenoseason.

### 5.1.7 Autumnal Partially-Leafed Phenoseason (October to November)

The autumnal partially-leafed phenoseason had a total of 397 observations, not including tiered readings. 58.4% of days had cloud cover greater than 4 oktas. 20.9% of days observed were fully overcast. Mean and range of open PAR values continued to decrease. Subcanopy means increase to  $77.04 \mu\text{mol m}^{-2} \text{s}^{-1}$ , subcanopy median increases to  $44.91 \mu\text{mol m}^{-2} \text{s}^{-1}$  and ranges at all locations begin to spread, but remain below  $200 \mu\text{mol m}^{-2} \text{s}^{-1}$ , the upper quartile measurement being at  $85.08 \mu\text{mol m}^{-2} \text{s}^{-1}$ . For a graphical representation of PAR for the autumnal partially-leafed phenoseason by location, see Figure 40.

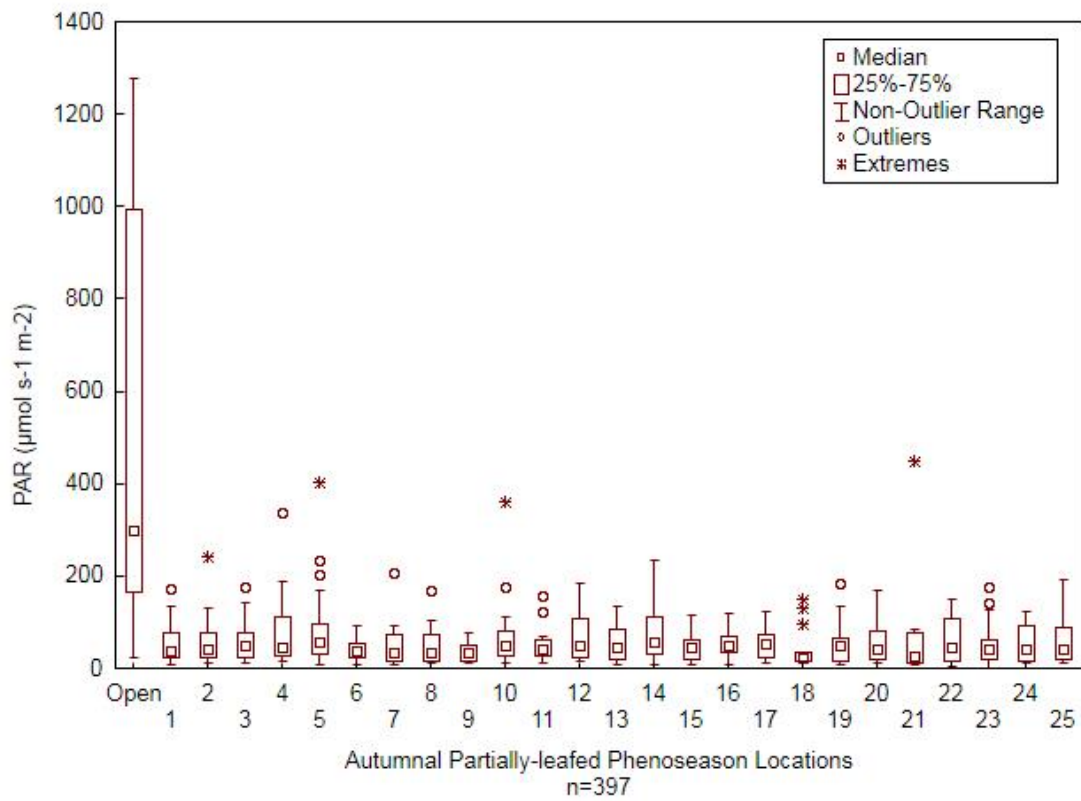


Figure 40: Box plot of PAR values at each location for the autumnal partially-leaved phenoseason.



Figure 41: Canopy on November 2, 2014

### 5.1.7.1 Selected Days

Days selected to highlight variability for the summer leafing phenoseason were October 26<sup>th</sup>, November 7<sup>th</sup>, and November 11<sup>th</sup>, 2014. A summary of the descriptive statistics for these days can be found in Table 12.

Table 12: Summary descriptive statistics of PAR ( $\mu\text{mol m}^{-2} \text{s}^{-1}$ ) for selected days of the autumnal partially-leafed phenoseason.

Day	Mean	Median	Minimum	Maximum	Lower (Quartile)	Upper (Quartile)	Std.Dev.
299	75.17	53.98	19.79	362.00	32.75	80.59	65.54
311	51.39	44.87	22.47	124.91	35.94	57.85	24.87
315	80.45	65.95	0.61	338.50	41.76	111.07	55.16

October 26, 2014 (Day 299, Figure 42) was a clear day with a VSC of 0. Measurements were taken between 11:53 and 12:28. The open reading PAR value was  $1140.40 \mu\text{mol m}^{-2} \text{s}^{-1}$ . The week before these measurements were collected, a fire occurred at the Fair Hill Nature Center barns and readings had been missed due to area closure. Unfortunately, this took place during a large portion of the beginning of leaf fall. Drupes on *L. benzoin* were mostly gone when we returned to the site, and leaves on *L. benzoin* were senescing and falling. November 11, 2014 (Day 315, Figure 42) was selected as the representative partly cloudy day with a VSC of 4 and open reading PAR value of  $281.7 \mu\text{mol m}^{-2} \text{s}^{-1}$ . Readings were collected between 13:15 and 13:40. Clouds were large and alternating with large gaps. November 7, 2014 (Day 311, Figure 42) was overcast with visual sky conditions decreasing from 8 to 7.5. No solar noon fully overcast values were recorded, these measurements took place from 09:20 to 09:49. The open reading PAR value was  $139.42 \mu\text{mol m}^{-2} \text{s}^{-1}$ . By this point in the season, some understory plants were still green, but all *L. benzoin* had lost 80% or

more of leaves. Similar to the autumnal fully-leafed phenoseason, the clear and partly cloudy day subcanopy readings have higher maximum values and are more right-skewed than the fully overcast day.

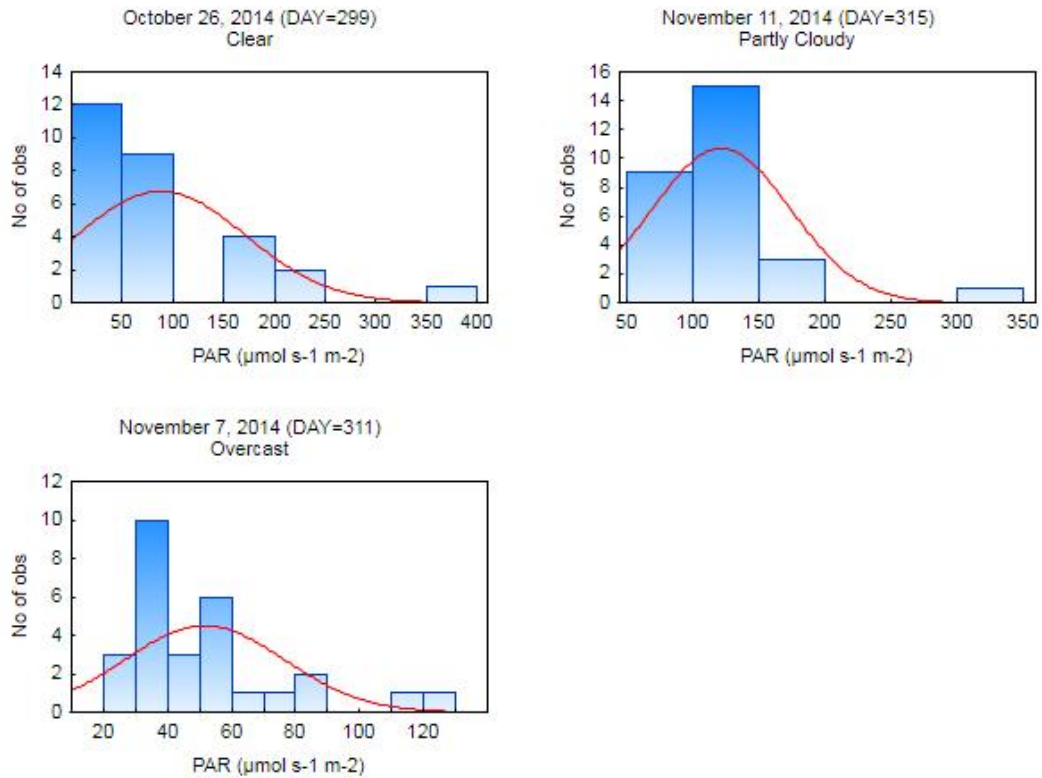


Figure 42: Distribution of PAR values for three sky conditions during the autumnal partially-leafed phenoseason.

### 5.1.8 Shrub Layer

At the five locations within the site where *L. benzoin* was abundant, 1160 observations were made both within and below *L. benzoin* canopy. Table 13 shows the mean PAR for the open, understory PAR above the *L. benzoin* canopy, within the *L. benzoin* canopy (shrub mid-level), and below the *L. benzoin* canopy (shrub low-level). This table also shows the PAR value as a percent of the open PAR value. For the

spring leafless and summer leafing phenoseasons only, mean shrub mid-level PAR was just slightly higher than the understory PAR. The spring leafing phenoseason has the most variation between levels. Percentage means vary within 6% between the three heights. Figure 43 shows how PAR values change between the three layers when compared with the open.

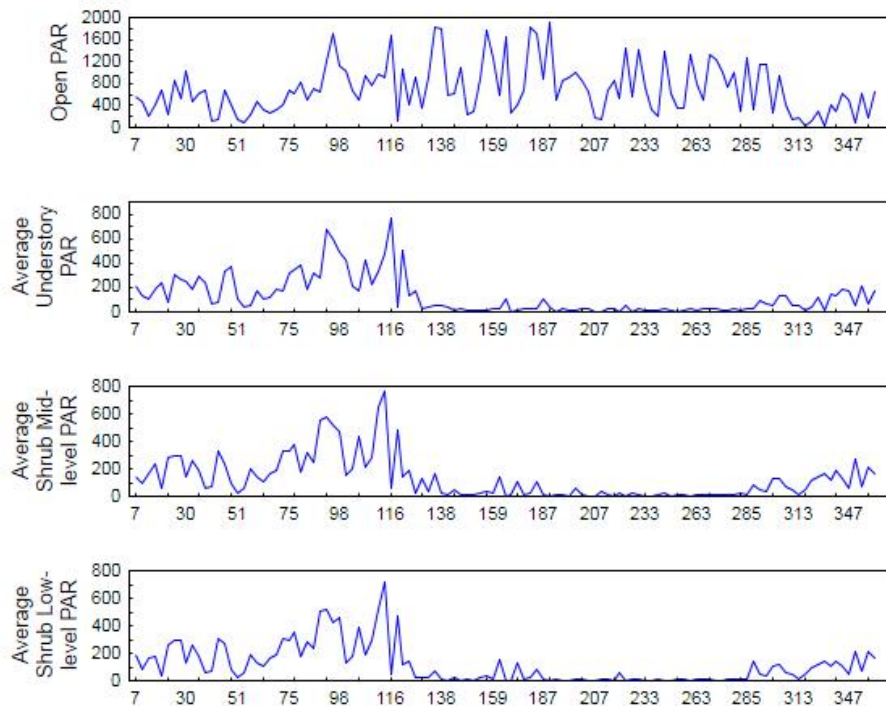


Figure 43: Mean annual PAR (by day of the year in  $\mu\text{mol m}^{-2} \text{s}^{-1}$ ) in the open and at three levels beneath the canopy.

Figure 44 shows the means and confidence intervals for all levels. Results of an ANOVA with phenoseason as the effect suggests that all but 24% of the variance

between levels is explained by phenoseason (Wilks =.24253, F (18, 303.13)=10.948,  $p=0.0000$ ). This result is significant at the=.05 level.

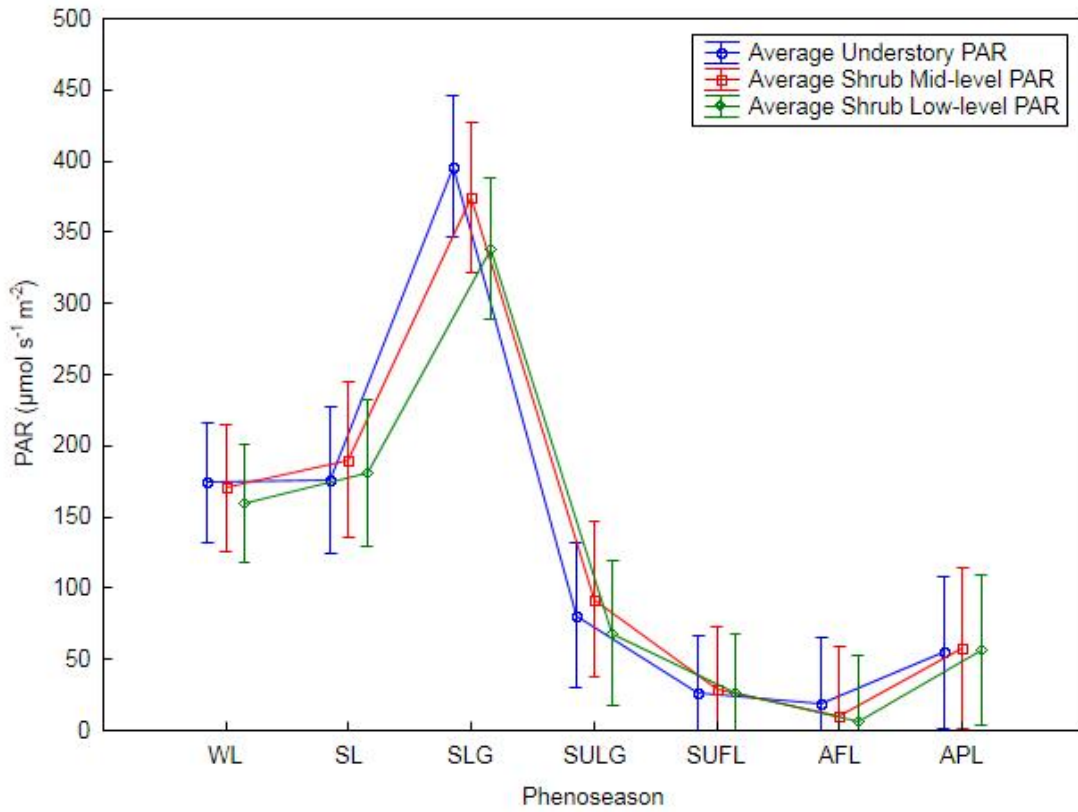


Figure 44: Results of an ANOVA of mean PAR by phenoseason; means and confidence intervals (95%) of understory, shrub mid-level and shrub low-level PAR.

Table 13: Descriptive statistics of PAR by phenoseason.

Phenoseason		Valid N	Mean	Minimum	Maximum	Std.Dev.	Mean as a % of Open PAR
Winter Leafless	Open PAR ( $\mu\text{mol m}^{-2} \text{ s}^{-1}$ )	21	478.83	42.88	1017.90	245.82	
	Average Understory PAR ( $\mu\text{mol m}^{-2} \text{ s}^{-1}$ )	21	174.30	12.31	299.55	79.52	36.40%
	Average Shrub Mid-level PAR ( $\mu\text{mol m}^{-2} \text{ s}^{-1}$ )	21	170.69	55.06	298.64	79.39	35.65%
	Average Shrub Low-level PAR ( $\mu\text{mol m}^{-2} \text{ s}^{-1}$ )	21	159.80	37.51	299.79	78.51	33.37%
Spring Leafless	Open PAR ( $\mu\text{mol m}^{-2} \text{ s}^{-1}$ )	13	346.69	83.97	682.10	210.11	
	Average Understory PAR ( $\mu\text{mol m}^{-2} \text{ s}^{-1}$ )	14	176.12	37.05	371.25	117.84	50.80%
	Average Shrub Mid-level PAR ( $\mu\text{mol m}^{-2} \text{ s}^{-1}$ )	14	190.05	29.06	373.00	113.14	54.82%
	Average Shrub Low-level PAR ( $\mu\text{mol m}^{-2} \text{ s}^{-1}$ )	14	180.90	26.01	348.60	107.88	52.18%
Spring Leafing	Open PAR ( $\mu\text{mol m}^{-2} \text{ s}^{-1}$ )	15	943.94	491.00	1704.70	364.24	
	Average Understory PAR ( $\mu\text{mol m}^{-2} \text{ s}^{-1}$ )	15	396.28	167.64	772.28	181.53	41.98%
	Average Shrub Mid-level PAR ( $\mu\text{mol m}^{-2} \text{ s}^{-1}$ )	15	374.11	59.18	761.76	206.91	39.63%
	Average Shrub Low-level PAR ( $\mu\text{mol m}^{-2} \text{ s}^{-1}$ )	15	338.34	52.42	713.77	184.73	35.84%
Summer Leafing	Open PAR ( $\mu\text{mol m}^{-2} \text{ s}^{-1}$ )	14	792.55	117.08	1839.00	536.51	
	Average Understory PAR ( $\mu\text{mol m}^{-2} \text{ s}^{-1}$ )	14	80.91	9.31	499.56	128.74	10.21%
	Average Shrub Mid-level PAR ( $\mu\text{mol m}^{-2} \text{ s}^{-1}$ )	14	92.32	8.00	480.94	128.30	11.65%
	Average Shrub Low-level PAR ( $\mu\text{mol m}^{-2} \text{ s}^{-1}$ )	14	68.32	3.62	471.36	124.20	8.62%
Summer Fully-leafed	Open PAR ( $\mu\text{mol m}^{-2} \text{ s}^{-1}$ )	22	916.39	146.61	1913.30	545.76	
	Average Understory PAR ( $\mu\text{mol m}^{-2} \text{ s}^{-1}$ )	22	26.19	2.25	107.49	27.02	2.86%
	Average Shrub Mid-level PAR ( $\mu\text{mol m}^{-2} \text{ s}^{-1}$ )	22	29.37	1.64	146.99	39.40	3.21%
	Average Shrub Low-level PAR ( $\mu\text{mol m}^{-2} \text{ s}^{-1}$ )	22	26.57	1.08	151.46	41.99	2.90%
Autumnal Fully-leafed	Open PAR ( $\mu\text{mol m}^{-2} \text{ s}^{-1}$ )	17	841.90	221.50	1428.00	431.87	
	Average Understory PAR ( $\mu\text{mol m}^{-2} \text{ s}^{-1}$ )	17	18.76	5.40	49.89	11.82	2.23%
	Average Shrub Mid-level PAR ( $\mu\text{mol m}^{-2} \text{ s}^{-1}$ )	17	9.48	1.66	27.43	6.69	1.13%
	Average Shrub Low-level PAR ( $\mu\text{mol m}^{-2} \text{ s}^{-1}$ )	17	6.32	2.20	10.26	2.74	0.75%
Autumnal Partially-leafed	Open PAR ( $\mu\text{mol m}^{-2} \text{ s}^{-1}$ )	14	536.77	23.78	1278.80	453.34	
	Average Understory PAR ( $\mu\text{mol m}^{-2} \text{ s}^{-1}$ )	14	59.19	11.76	136.77	42.55	11.03%
	Average Shrub Mid-level PAR ( $\mu\text{mol m}^{-2} \text{ s}^{-1}$ )	13	57.53	8.54	134.56	44.19	10.72%
	Average Shrub Low-level PAR ( $\mu\text{mol m}^{-2} \text{ s}^{-1}$ )	13	56.49	7.56	141.52	45.45	10.52%

### **5.1.9 Comparative analysis of PAR across phenoseasons**

Similar to Hutchison and Matt (1977), mean PAR values in the open for this study gradually increase through the spring, and reach their maximum in the spring leafing phenoseason, and remaining fairly constant until after the summer solstice, after which they decline again. The spring leafless and early spring leafing phases have lower open PAR values than the summer phenoseason, higher overall subcanopy PAR values, and more subcanopy variation. Late summer leafing and fully-leafed phenoseasons have PAR values that are higher in the open, lower subcanopy PAR values, less overall variation, and definite hot-spots (or sunflecks) at times based on canopy and sky conditions and the position of the Sun.

Figure 45 shows the mean PAR contours by phenoseason at a given height from ground level as it is attenuated by the canopy. Open values are assigned above the canopy and values between the open and 2 m are interpolated. The highest radiation values are received at the forest floor during the spring leafless phenoseason, before leaf-out of the canopy trees but just as the sun begins to climb higher in the sky. Lowest values are found during the summer and autumnal fully-leafed phenophases.

Figure 46 shows PAR by phenoseason. These are the values recorded in the subcanopy, tiered and open readings not included. Here, PAR increases from the winter leafless to the spring leafing phenoseason, declines into the summer and autumnal fully-leafed phenophases, and slightly increases again with leaf-off in the autumnal partially-leafed phenophase.

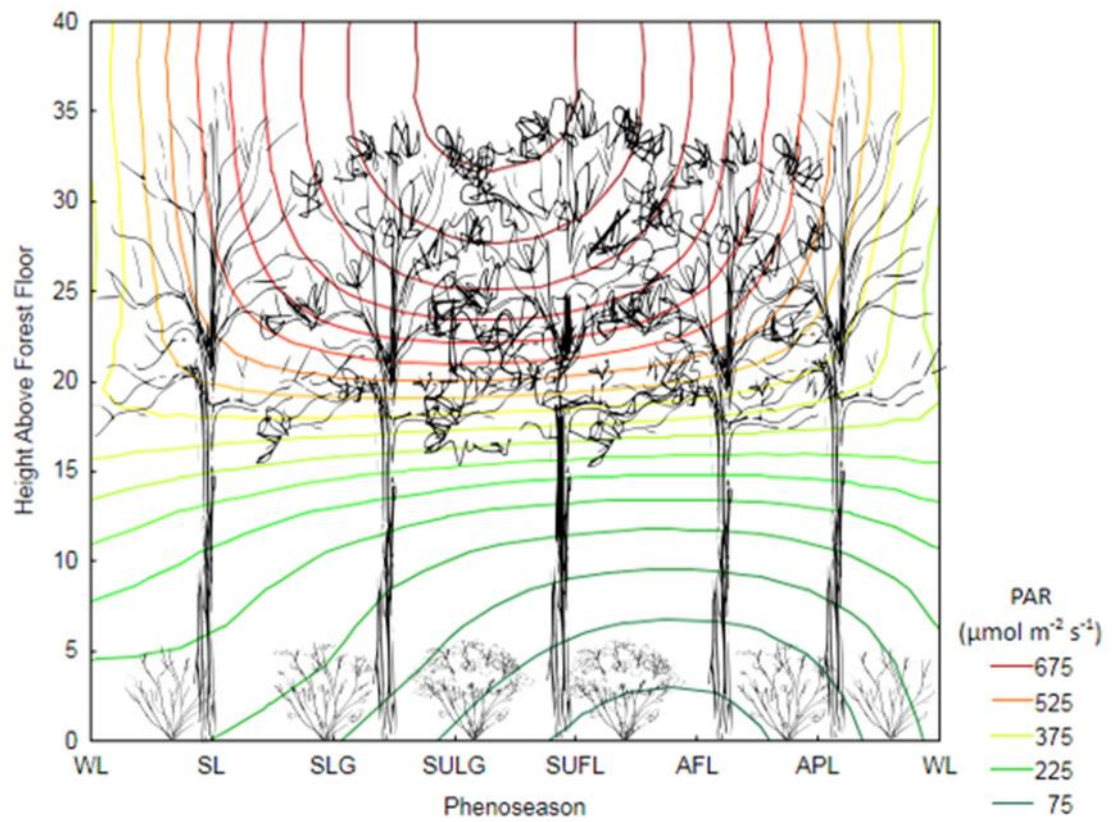


Figure 45: Contour plot of annual course of average daily total PAR received within and above our plot canopy. Contours represent  $\mu\text{mol m}^{-2} \text{s}^{-1}$ .

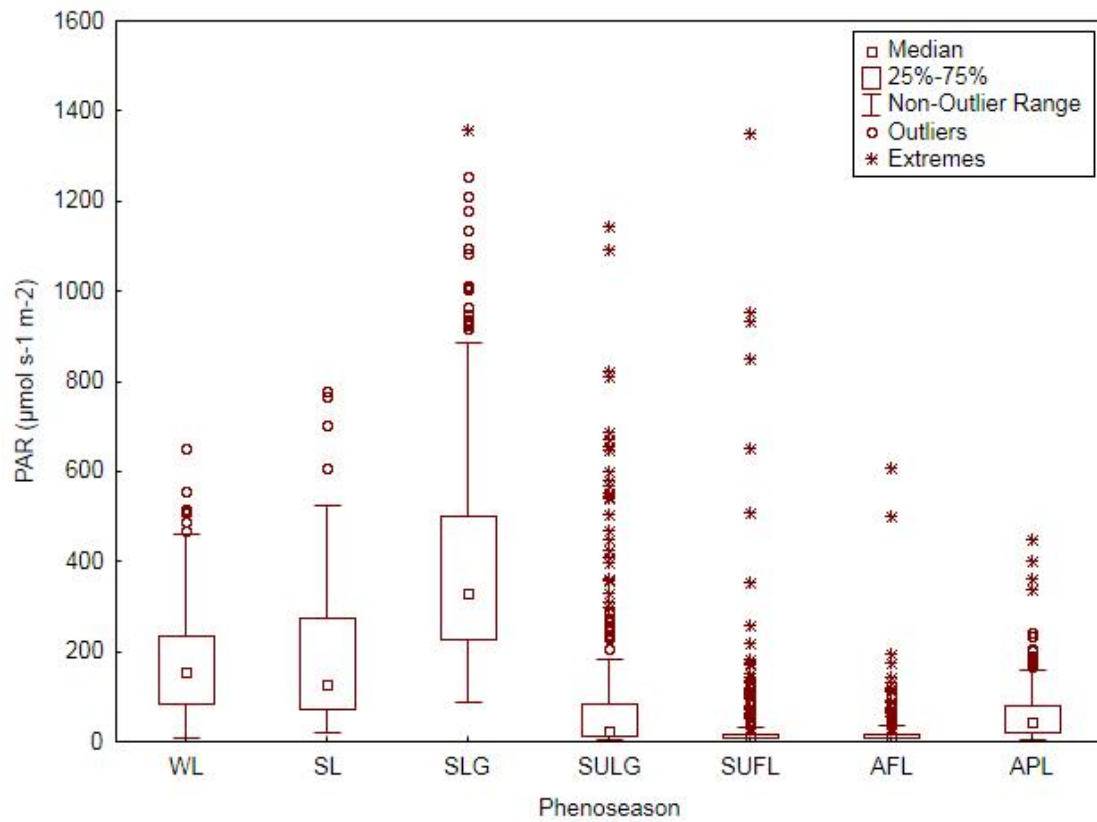


Figure 46: Box plot of PAR by phenoseason.

Hutchison and Matt (1977) also found that winter leafless overcast conditions increase subcanopy radiation, while summer overcast conditions decreased subcanopy radiation. Our findings are in agreement with this (Table 14).

Table 14: Comparison of winter and summer clear and overcast days, showing that winter overcast conditions increased subcanopy radiation, while summer overcast conditions decreased subcanopy radiation ( $\mu\text{mol m}^{-2} \text{s}^{-1}$ ).

Phenoseason	VSC (Oktas)	Valid N	Mean	Min	Max	Std. Dev.
WL	0	145	243.57	57.58	1017.90	147.66
WL	8	80	62.04	8.43	157.28	48.29
AFL	0	29	78.48	.61	1402.30	257.36
AFL	8	125	30.14	.57	729.00	95.29

### 5.1.10 Comparative analysis of PAR among locations

It is also important to represent the results of the study from the perspective of each individual location within the plot. The open location has the highest annual values of PAR. Ranked by mean, the next highest values of PAR in descending order can be found at the following locations respectively: 15, 8, 21, 23, 9, 14, 22, 17, 5, 7, 24, 16, 13, 4, 25, 1, 3, 20, 19, 11, 10, 6, 12, 18, and 2. Additionally, the following figures show box plots of PAR ( $\mu\text{mol m}^{-2} \text{s}^{-1}$ ) for the winter leafless (WL), spring leafless (SL), spring leafing (SLG), summer leafing (SULG), summer fully-leafed (SUFL), autumnal fully-leafed (AFL), and autumnal partially-leafed (APL) phenoseasons, grouped by location. For each location except the open, a similar pattern can be seen: an increase from winter leafless to spring leafing, a large decrease for the summer leafing as well as an increase in the number of extreme values, a further decrease for summer and autumnal fully-leafed before a slight increase for autumnal partially leafed. Table 15 lists descriptive statistics of annual PAR for each location of the study, with locations having large populations of *L. benzoin* marked in red. Figures 47 through 53 show box plots of PAR (on a logarithmic scale) for each phenoseason, grouped by location.

Table 15: Descriptive statistics of annual PAR ( $\mu\text{mol m}^{-2} \text{s}^{-1}$ ) for each location.\*

Location	Valid N	Mean	Median	Min	Max	Lower q	Upper q	Std. Dev.
Open	118	699.10	616.95	23.78	1913.30	332.10	949.00	461.59
1	118	123.76	65.47	1.78	883.60	10.30	163.69	165.81
2	118	109.70	47.94	1.18	671.60	9.10	164.03	134.67
3	118	122.22	58.69	1.85	606.50	12.40	184.95	145.63
4	118	125.00	55.84	1.56	875.50	11.51	191.40	162.31
5	474	132.87	63.25	0.53	1357.40	16.40	181.21	184.51
6	119	115.60	44.24	2.06	933.80	11.66	186.54	152.37
7	119	132.56	50.21	1.86	916.60	11.83	192.17	183.23
8	119	140.74	44.42	3.29	1351.70	13.90	202.00	195.84
9	119	136.39	48.89	2.94	1210.30	14.65	176.92	209.90
10	118	115.66	56.65	1.86	649.00	13.24	173.98	140.70
11	118	116.36	46.79	1.32	812.00	11.49	143.87	164.88
12	119	112.16	52.14	2.47	645.60	16.51	157.14	134.05
13	119	126.79	64.46	1.95	886.60	12.98	184.75	166.82
14	118	134.23	73.40	2.07	737.40	20.25	184.11	163.59
15	118	144.93	61.66	2.83	1135.00	15.30	200.20	198.60
16	118	131.34	56.36	2.22	1143.50	14.53	173.98	187.75
17	118	133.87	58.71	3.11	877.80	15.44	207.00	167.94
18	118	110.31	43.13	1.12	878.80	7.81	148.26	160.42
19	118	118.37	55.22	2.29	1096.90	14.10	176.55	165.75
20	119	121.70	52.61	0.57	845.40	11.38	177.96	165.00
21	119	140.69	43.03	1.54	1254.50	11.70	212.80	218.06
22	118	134.13	62.18	1.55	1084.40	12.02	175.47	193.95
23	118	137.76	64.43	0.61	796.50	17.00	216.90	165.96
24	119	132.07	52.84	1.44	1007.10	11.06	189.44	168.40
25	119	124.48	41.23	0.61	924.70	11.07	192.65	173.40

\*Locations with growth of *L. benzoin* are highlighted in red

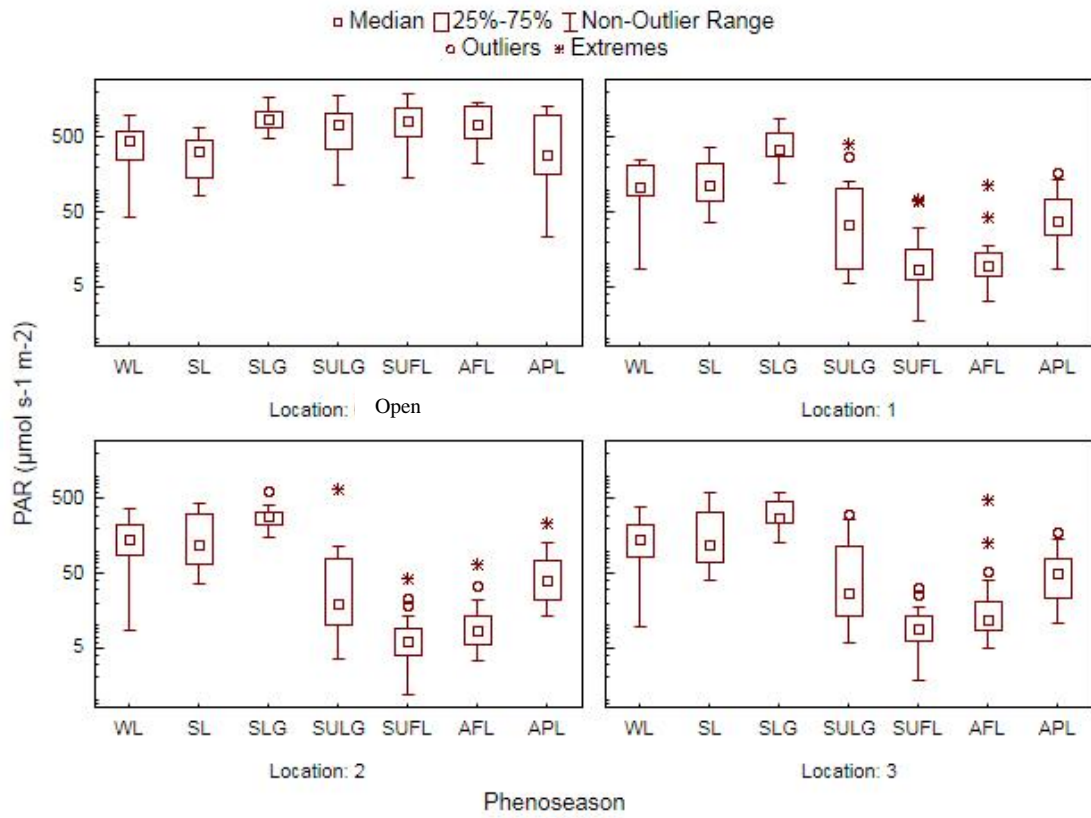


Figure 47: PAR ( $\mu\text{mol m}^{-2} \text{s}^{-1}$ ) on a log scale by phenoseason for locations 0 (open), 1, 2, and 3.

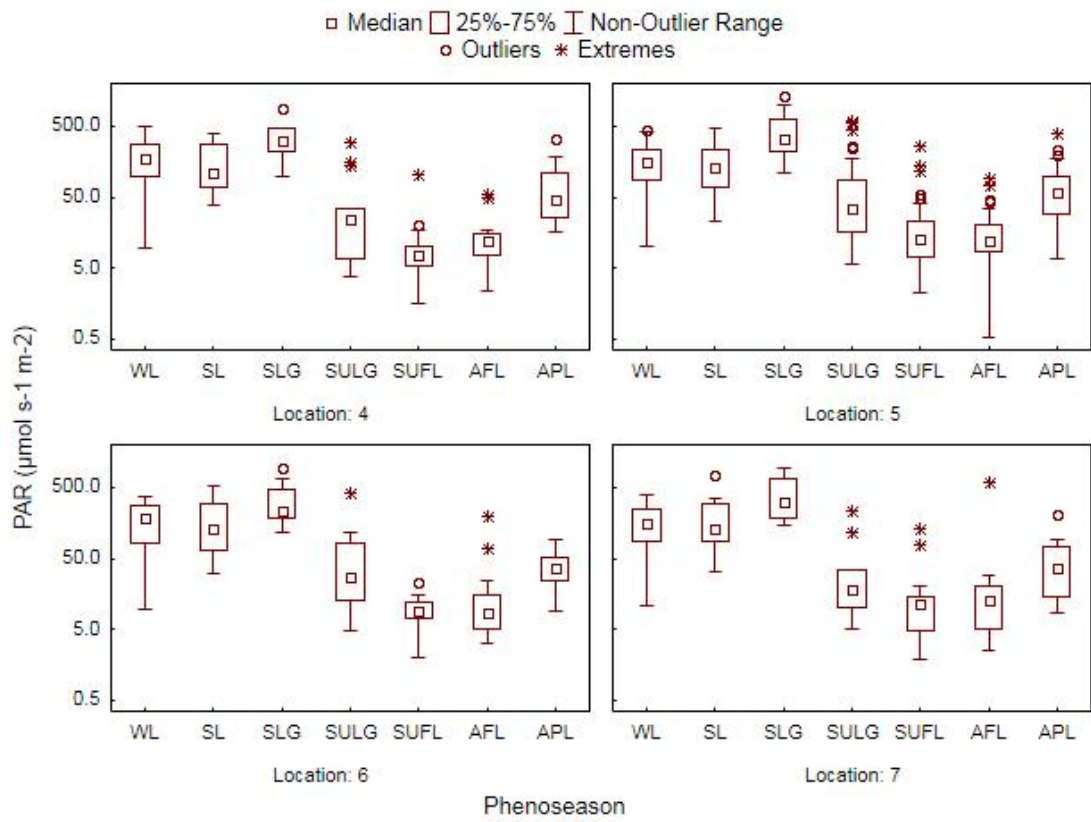


Figure 48: PAR ( $\mu\text{mol m}^{-2} \text{s}^{-1}$ ) on a log scale by phenoseason for locations 4, 5, 6, and 7.

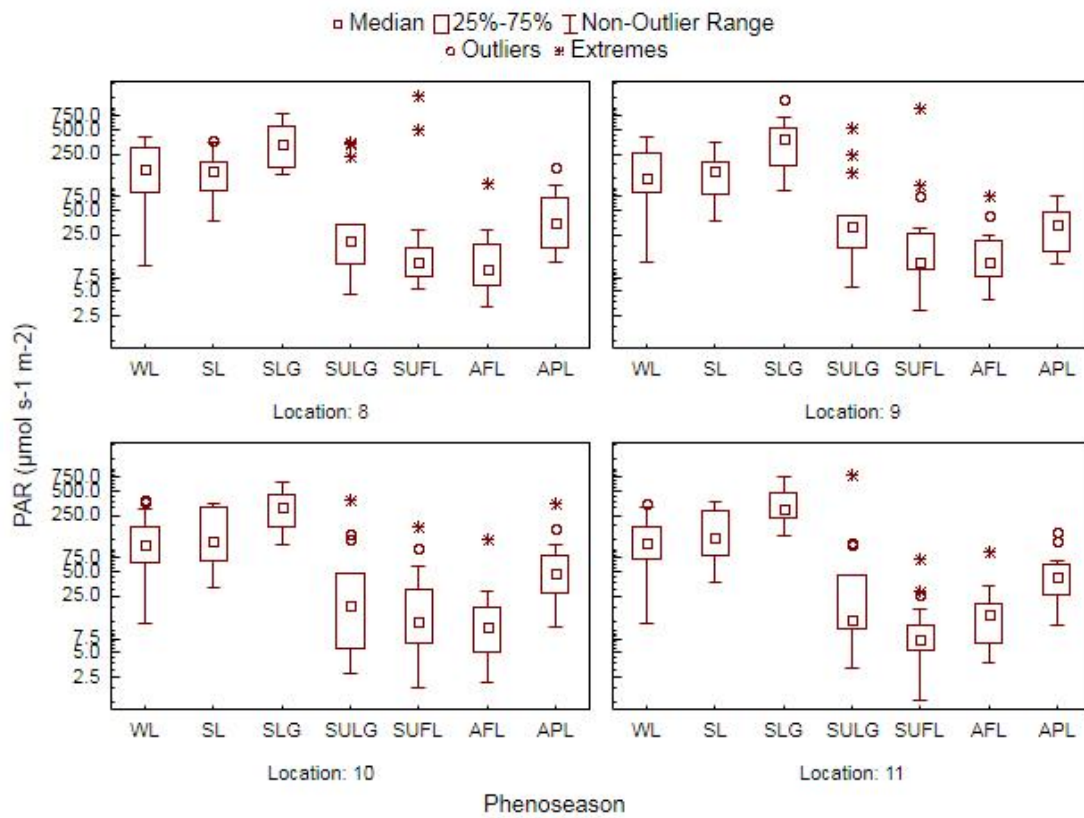


Figure 49: PAR ( $\mu\text{mol m}^{-2} \text{s}^{-1}$ ) on a log scale by phenoseason for locations 8, 9, 10, and 11.

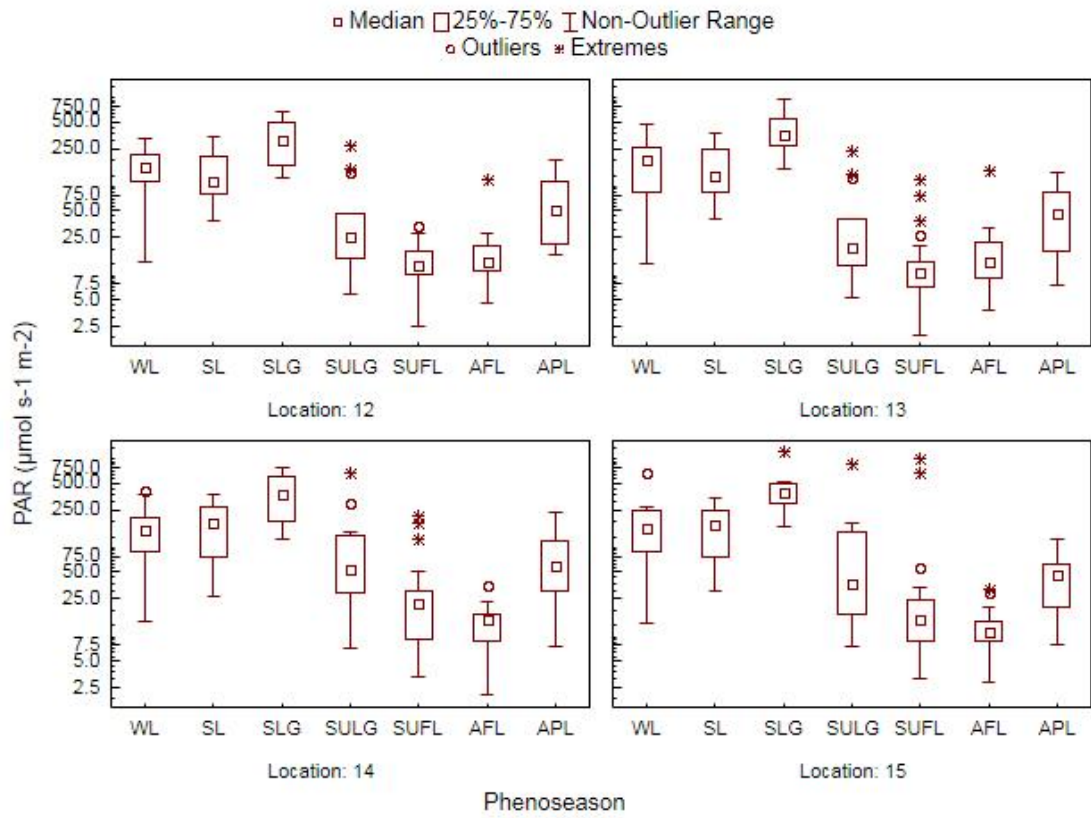


Figure 50: PAR ( $\mu\text{mol m}^{-2} \text{s}^{-1}$ ) one a log scale by phenoseason for locations 12, 13, 14, and 15.

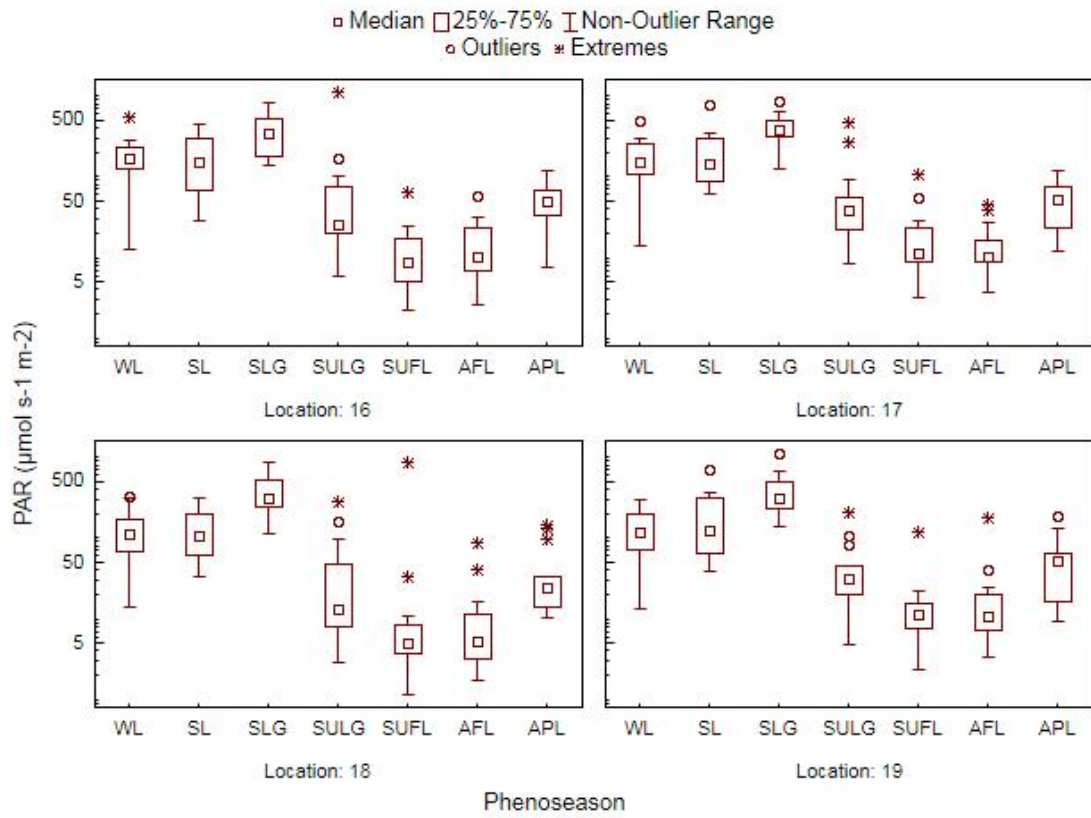


Figure 51: PAR ( $\mu\text{mol m}^{-2} \text{s}^{-1}$ ) on a log scale by phenoseason for locations 16, 17, 18, and 19.

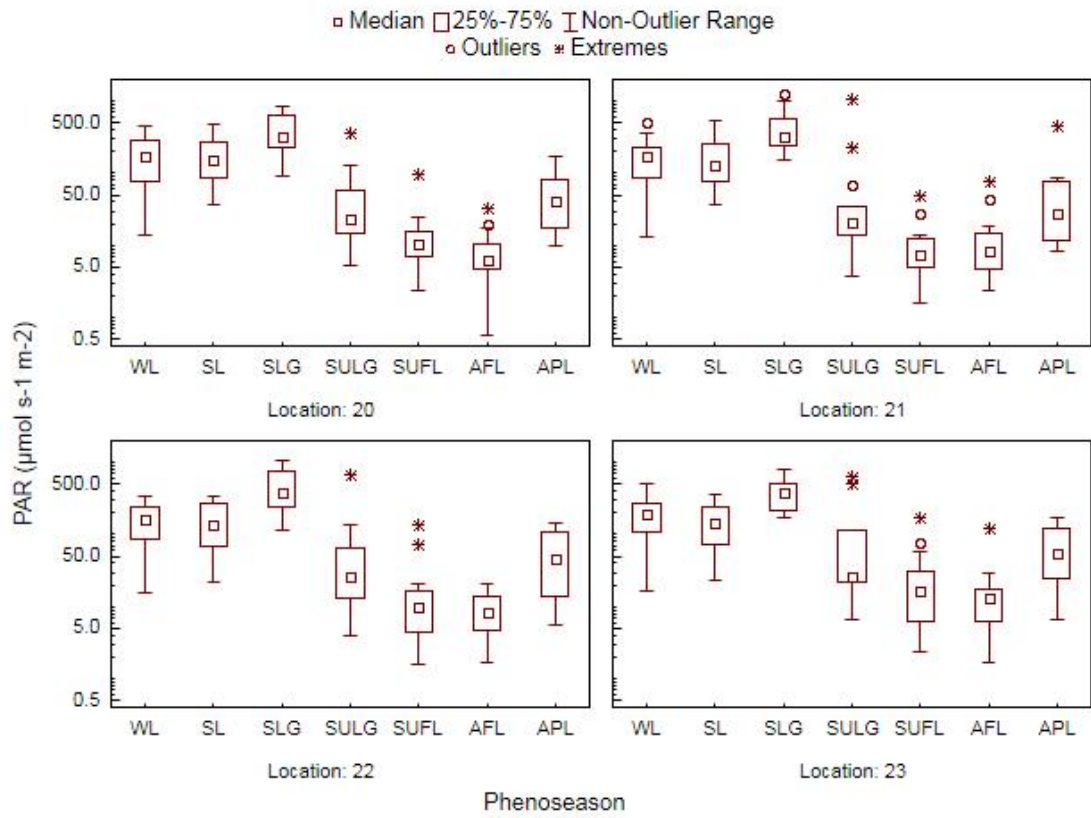


Figure 52: PAR ( $\mu\text{mol m}^{-2} \text{s}^{-1}$ ) on a log scale by phenoseason for locations 20, 21, 22, and 23.

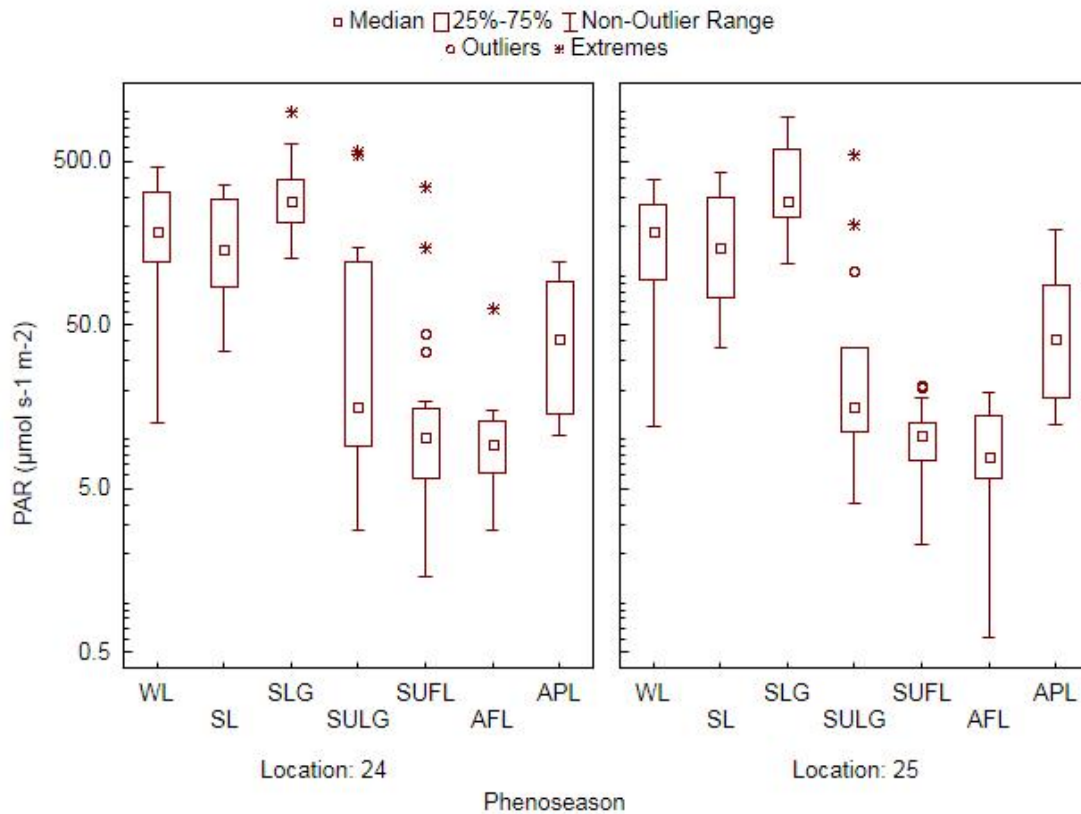


Figure 53: PAR ( $\mu\text{mol m}^{-2} \text{s}^{-1}$ ) on a log scale by phenoseason for locations 24 and 25.

### 5.1.11 Temporal variation in PAR over the course of an afternoon

During the autumnal fully-leafed phenoseason, on September 26<sup>th</sup> of 2014, a field methods class assisted with the collection of four consecutive hours of PAR values at the field site. Visual sky conditions were almost completely clear (.05 oktas). Figure 54 shows the large decrease in the open PAR as the day progresses and the sun elevation drops (in essence, the arc of the sun with time), while the subcanopy PAR decrease is far less dramatic as the solar elevation drops. Most of the extreme subcanopy values occur during the hour between 13:55 and 14:55. Solar noon on this

day would occur at 12:54. These extreme values occur at locations 3, 12, 13, and 19 (Table 16).

Table 16: Descriptive statistics of PAR in  $\mu\text{mol m}^{-2} \text{s}^{-1}$  for each location during four consecutive hours on September 26, 2014.

<b>Location</b>	<b>Valid N</b>	<b>Mean</b>	<b>Median</b>	<b>Minimum</b>	<b>Maximum</b>	<b>Std. Dev.</b>
Open	4	1074.93	1117.45	741.10	1323.70	258.95
1	4	9.05	9.60	4.94	12.04	3.08
2	4	31.48	28.80	3.54	64.76	25.72
3	4	131.44	11.21	4.83	498.50	244.73
4	4	22.05	15.10	9.24	48.76	18.03
5	16	19.36	12.79	5.13	92.88	21.17
6	4	5.71	5.09	4.00	8.64	2.09
7	4	12.17	9.42	3.99	25.86	9.85
8	4	8.76	7.16	4.32	16.39	5.36
9	4	25.32	9.48	6.69	75.63	33.61
10	4	4.93	4.72	3.12	7.17	1.82
11	4	33.90	21.67	3.85	88.42	38.74
12	4	33.52	8.20	4.52	113.16	53.16
13	4	47.09	20.59	4.70	142.49	64.66
14	4	10.13	8.94	6.04	16.61	4.55
15	4	8.78	9.00	6.76	10.35	1.49
16	4	18.22	17.52	6.30	31.52	12.49
17	4	17.00	10.28	8.71	38.74	14.51
18	4	4.00	4.21	2.20	5.39	1.64
19	4	48.63	7.29	3.39	176.55	85.30
20	4	5.97	5.86	4.34	7.83	1.45
21	4	11.10	10.42	4.61	18.97	6.40
22	4	6.48	6.86	3.66	8.53	2.10
23	4	9.36	8.25	5.63	15.31	4.16
24	4	6.06	6.12	4.30	7.70	1.82
25	4	5.70	5.71	3.67	7.71	1.68

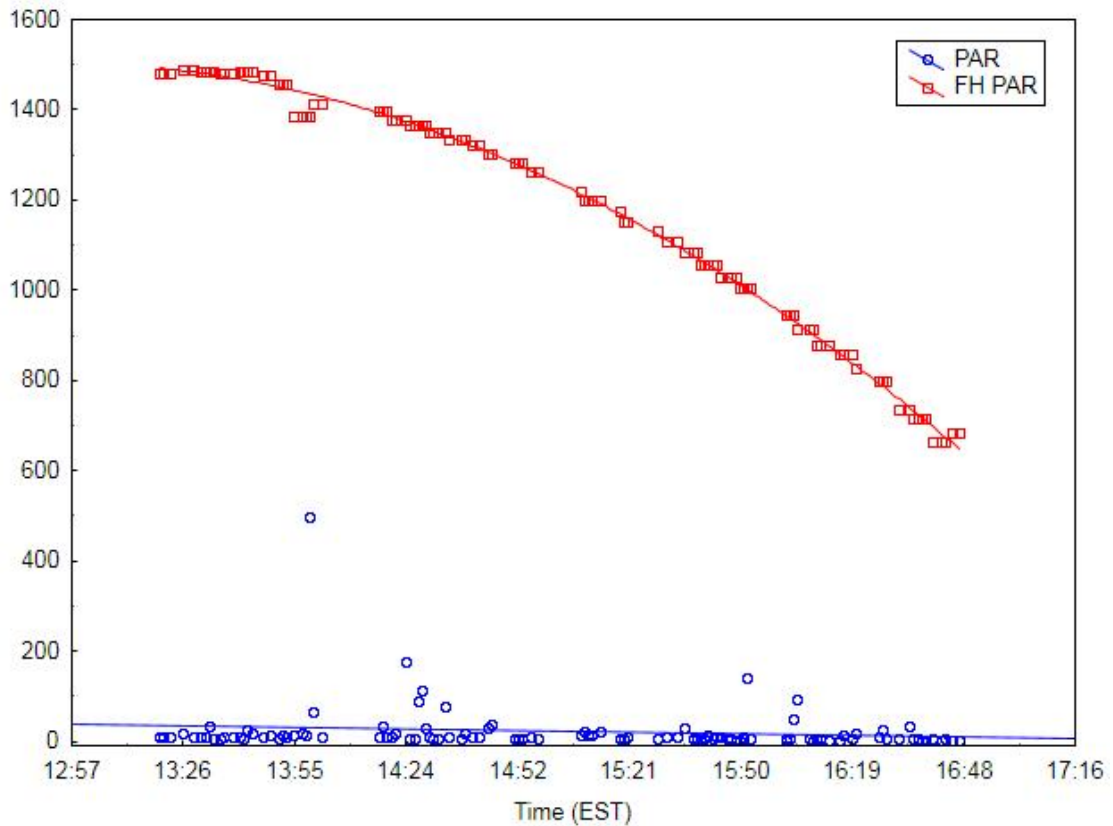


Figure 54: Scatterplot of subcanopy PAR and the adjusted PAR from the Fair Hill DEOS station PAR (adjusted) in the open over a 4 hour period, showing the “arc” of the sun across the sky and the only slight decrease in subcanopy PAR.

## 5.2 Ecological Survey

The ecological survey conducted in October of 2014 provided the following insights to understory and canopy plant growth. A total of 682 *L. benzoin* with height greater than 45cm (~ 2 years of age) were marked as waypoints within the plot. There are 42 trees within the plot: 3 red maple, 4 hickory species, 28 American beech, 5 yellow poplar, one oak species, and one miscellaneous species (Table 17).

Table 17: Trees and shrubs in the Fair Hill NRMA plot.

<b>Species</b>	<b>Total Surveyed</b>	<b>Mean DBH (cm)</b>	<b>Standard Deviation</b>
<i>L. benzoin</i>	682	-	-
<i>A. rubrum</i>	3	60.5	40.1
<i>Carya</i> spp.	4	48.4	8.3
<i>F. grandifolia</i>	28	24.8	14.4
<i>L. tulipifera</i>	5	87.6	10.9
<i>Quercus</i> spp.	1	102.8	-
Miscellaneous	1	48.2	-
Tree Total	42	39.5	28.8

Visual analysis of Figure 55 seems to suggest that, even with a 2m cell (fairly representative of the canopy of a cluster of *L. benzoin*) the *L. benzoin* thrives in areas where canopy edges of the trees appear to overlap. Ripley's K Function did show that *L. benzoin* does grow in clusters, in fact, significantly so (Figure 56).



Figure 55: Tree locations with respect to *L. benzoin* locations represented as a binary “present” or “not present” using 2m cells.

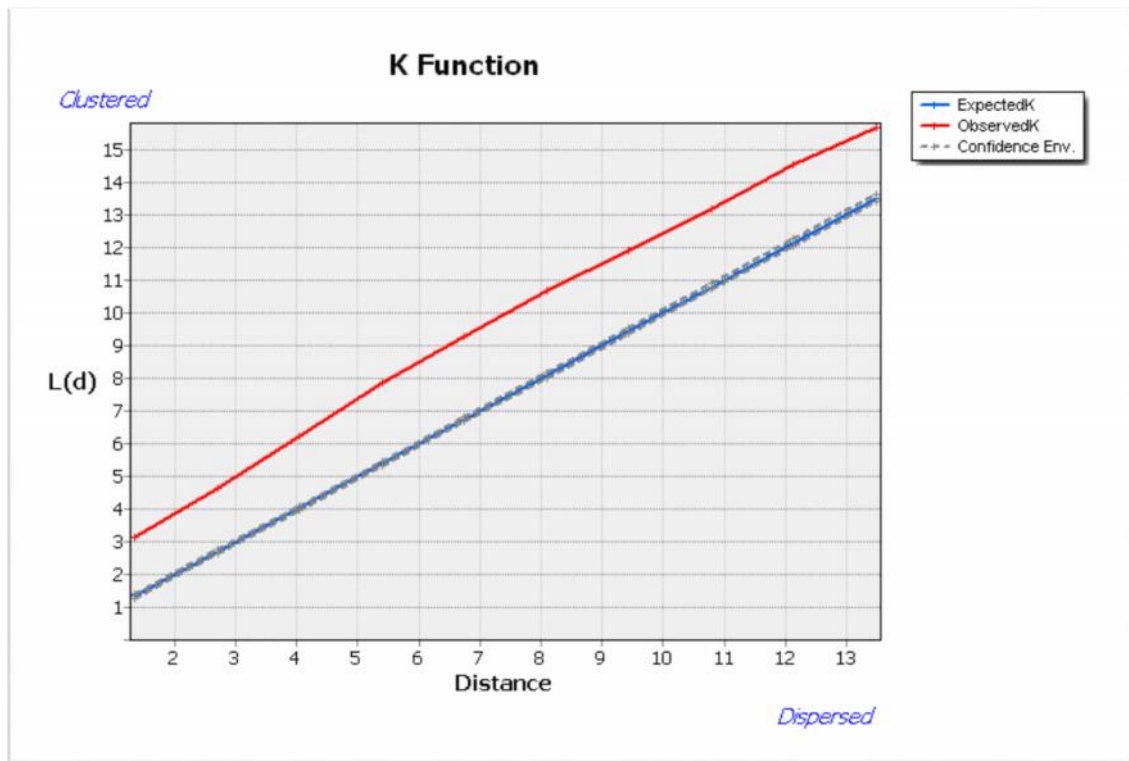


Figure 56: Results of a Ripley’s K analysis, showing the observed significant clustering of *L. benzoin* within the plot.

### 5.3 *Lindera benzoin* Treatments

The purpose of these treatments was to determine how changes in light growth environment would impact leaf pigments and overall plant health. Overall PAR for Experiment 1 was  $350 \mu\text{mol m}^{-2}\text{s}^{-1}$ , with  $517.9 \mu\text{mol m}^{-2}\text{s}^{-1}$  as the incident PAR for the upper treatment or “sun” environment and  $366 \mu\text{mol m}^{-2}\text{s}^{-1}$  as the incident PAR for the lower treatment or “shade” environment. Overall PAR for Experiment 2 was set to  $150 \mu\text{mol m}^{-2}\text{s}^{-1}$ , making the upper and lower treatments  $164.5 \mu\text{mol m}^{-2}\text{s}^{-1}$  and  $118.06 \mu\text{mol m}^{-2}\text{s}^{-1}$ . For more information see 4.3 Methods, *Lindera benzoin* Treatments.

Visually, the plants from Experiment 2, which were grown under lower PAR conditions ( $150 \mu\text{mol m}^{-2}\text{s}^{-1}$ ) did much better than the plants from Experiment 1 with an average PAR of  $350 \mu\text{mol m}^{-2}\text{s}^{-1}$ . Mean total weight of plants from Experiment 1 was nearly half that for Experiment 2. Plants from Experiment 1 grew taller, with more nodes, but had fewer leaves and did not grow as broad as those from Experiment 2. Additionally, all results for Experiment 1 should be considered carefully, as this set of plants contracted a viral infection during their time in the growth chamber.

### **5.3.1 Physical Results**

The measured physical variables were number of nodes (#NODES), internodal distance (IND), total node height (TNH), initial stomatal conductance (SC1), secondary stomatal conductance (SC2), the difference between initial and secondary stomatal conductance (SCDIFF), root weight (RW), shoot weight (SW), root to shoot ratio (R/S RATIO), total weight (TW), leaf weights (L1W, L2W), root and shoot dry weights (RDW, SDW), root to shoot dry weight ratio (R/S DW RATIO), and total dry weight (TDW). Physical results were normally distributed. Descriptive statistics for these variables can be found in Table 18.

Table 18: Descriptive statistics of measured physical characteristics by experiment.

	<b>Exp.</b>	<b>Valid N</b>	<b>Mean</b>	<b>Minimum</b>	<b>Maximum</b>	<b>Std.Dev.</b>
#NODES	1	13	4.00	1.00	6.00	1.41
IND (cm)	1	13	1.47	0.50	2.35	0.60
TNH (cm)	1	13	7.33	1.50	14.10	4.16
SC1 (mmol m <sup>-2</sup> s <sup>-1</sup> )	1	12	108.59	54.27	192.58	49.21
SC2 (mmol m <sup>-2</sup> s <sup>-1</sup> )	1	12	63.00	31.22	161.90	37.35
SCDIFF (mmol m <sup>-2</sup> s <sup>-1</sup> )	1	12	45.59	4.80	133.75	40.00
RW (g)	1	13	0.94	0.21	1.91	0.58
SW (g)	1	13	0.98	0.38	2.00	0.55
R/S RATIO	1	13	0.93	0.46	1.37	0.30
TW (g)	1	13	1.93	0.60	3.70	1.11
L1W (g)	1	13	0.14	0.06	0.30	0.07
L2W (g)	1	13	0.13	0.04	0.30	0.08
RDW (g)	1	13	0.16	0.04	0.38	0.11
SDW (g)	1	13	0.22	0.07	0.50	0.13
R/S DW RATIO	1	13	0.71	0.48	0.91	0.14
TDW (g)	1	13	0.38	0.12	0.88	0.24
#NODES	2	7	2.43	1.00	4.00	1.13
IND (cm)	2	7	1.48	1.00	2.17	0.49
TNH (cm)	2	7	3.68	1.00	7.00	2.30
SC1 (mmol m <sup>-2</sup> s <sup>-1</sup> )	2	7	117.82	57.84	189.90	44.26
SC2 (mmol m <sup>-2</sup> s <sup>-1</sup> )	2	7	50.37	39.19	71.87	11.25
SCDIFF (mmol m <sup>-2</sup> s <sup>-1</sup> )	2	7	67.46	13.94	137.97	46.31
RW (g)	2	7	2.58	1.18	4.11	1.24
SW (g)	2	7	1.66	1.05	3.17	0.74
R/S RATIO	2	7	1.56	1.04	2.72	0.58
TW (g)	2	7	4.24	2.23	7.28	1.86
L1W (g)	2	7	0.19	0.09	0.43	0.12
L2W (g)	2	7	0.16	0.07	0.35	0.09
RDW (g)	2	7	0.42	0.18	0.70	0.20
SDW (g)	2	7	0.44	0.25	0.90	0.23
R/S DW RATIO	2	7	0.99	0.59	1.92	0.45
TDW (g)	2	7	0.86	0.44	1.60	0.41

For the following sections, results from all Tukey-Kramer Honest Significant Difference test and Each Pair Student's t test at  $\alpha=0.05$  were analogous and therefore used interchangeably.

### 5.3.1.1 Comparison of plants grown at $350 \mu\text{mol m}^{-2} \text{s}^{-1}$

Overall PAR for the growth chamber was  $350 \mu\text{mol m}^{-2} \text{s}^{-1}$ . The PAR for the upper set of plants was measured at  $517.9 \mu\text{mol m}^{-2} \text{s}^{-1}$ , while the PAR for the lower set of plants was measured at  $366 \mu\text{mol m}^{-2} \text{s}^{-1}$ . Using Tukey-Kramer Honest Significant Difference test (correcting for type I errors) at  $\alpha=0.05$ , means of the root-shoot ratios, initial stomatal conductance of the Upper and Lower PAR sets for Experiment 1 were significantly different. Using the same test, means of biomass and secondary stomatal conductance were not significantly different.



Figure 57: Subset of plants grown for experiment 1, with lower level PAR plants shown on the left, and upper level PAR plants shown on the right.

### 5.3.1.2 Comparison of plants grown at $150 \mu\text{mol m}^{-2} \text{s}^{-1}$

Overall PAR for the growth chamber was  $150 \mu\text{mol m}^{-2} \text{s}^{-1}$ . The PAR for the upper set of plants was measured at  $164.5 \mu\text{mol m}^{-2} \text{s}^{-1}$ , while the PAR for the lower set of plants was measured at  $118.06 \mu\text{mol m}^{-2} \text{s}^{-1}$ . Using Tukey-Kramer Honest Significant Difference test (correcting for type I errors) at  $\alpha=0.05$ , means of the root-to-shoot ratios, biomass, secondary stomatal conductance of the Upper and Lower PAR sets for Experiment 2 were not significantly different. Initial stomatal conductance means were significantly different.



Figure 58: Subset of plants grown for experiment 1, with upper level PAR plants shown on the left, and lower level PAR plants shown on the right.

### 5.3.1.3 Comparison of all plants from Experiments 1 and 2

Using Each Pair Student's t test, there is a significant difference for root-to-shoot ratio between plants grown on the upper level of Experiment 1 (highest) and plants grown on the lower level of Experiment 2 (lowest;  $p=0.0130$ ) (Figure 59). Each Pair Student's t test for the biomass variable (total dry weight) also found significant

differences between both upper ( $p=0.0007$ ) and lower ( $p=0.0082$ ) treatments of Experiment 1 when paired with the upper treatment Experiment 2. The upper treatment of Experiment 2 had significantly higher biomass than either level from Experiment 1. There is no significant difference between the upper and lower levels of Experiment 2 (Figure 60).

For initial stomatal conductance, using Each Pair Student's t test, significant differences are found between the upper and lower treatments of Experiment 1 when paired with the upper and lower treatments of Experiment 2. (2L-1U,  $p=0.0022$ ; 2L-2U,  $p=0.0121$ ; 1L-1U,  $p=0.0021$ ; 1L-2U,  $p=0.0177$ ). In other words, there was a significant difference between the stomatal conductivity of plants grown in the  $350 \mu\text{mol m}^{-2}\text{s}^{-1}$  light environment and the plants grown in the  $150 \mu\text{mol m}^{-2}\text{s}^{-1}$  light environment (Figure 61). No significant differences are found for the secondary stomatal conductance results (Figure 62).

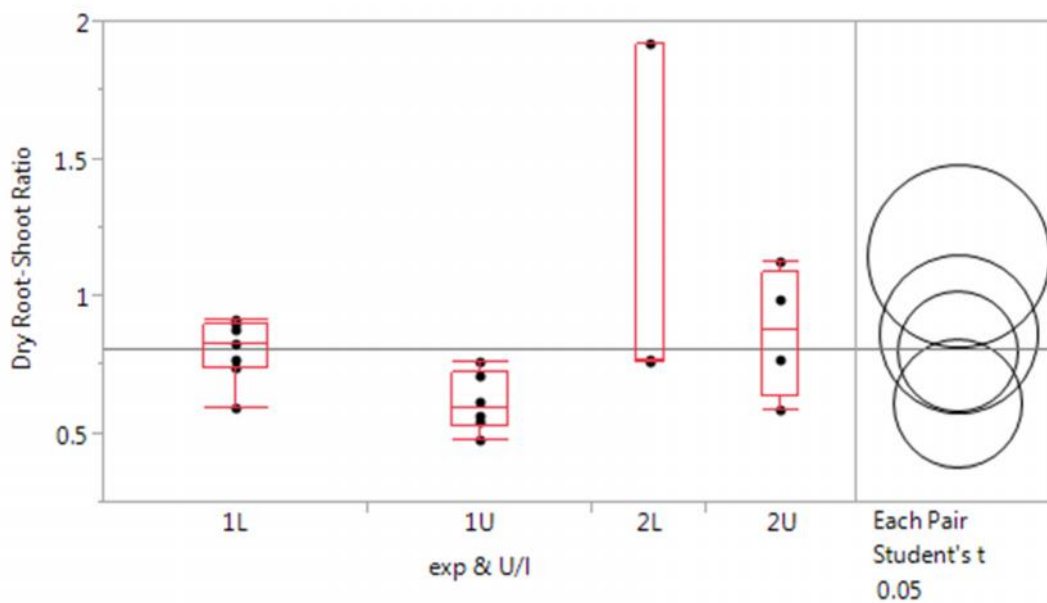


Figure 59: Box plot of means of dry root-shoot ratios for all experiments

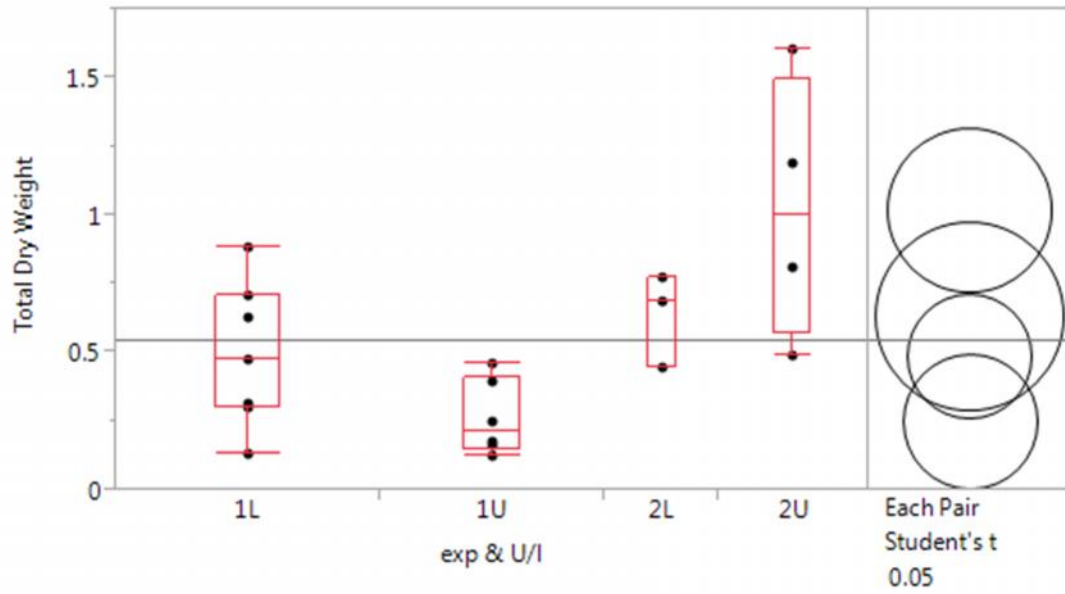


Figure 60: Box plot of means of total dry weight (mg) for all experiments.

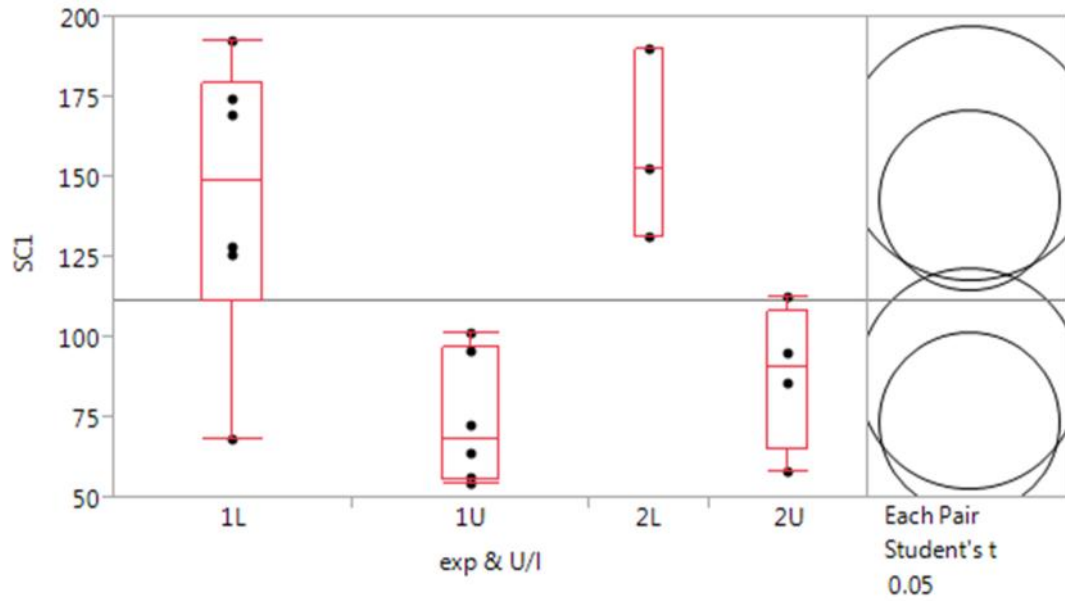


Figure 61: Box plot of means of initial stomatal conductance ( $\text{mmol m}^{-2} \text{s}^{-1}$ ) for all experiments

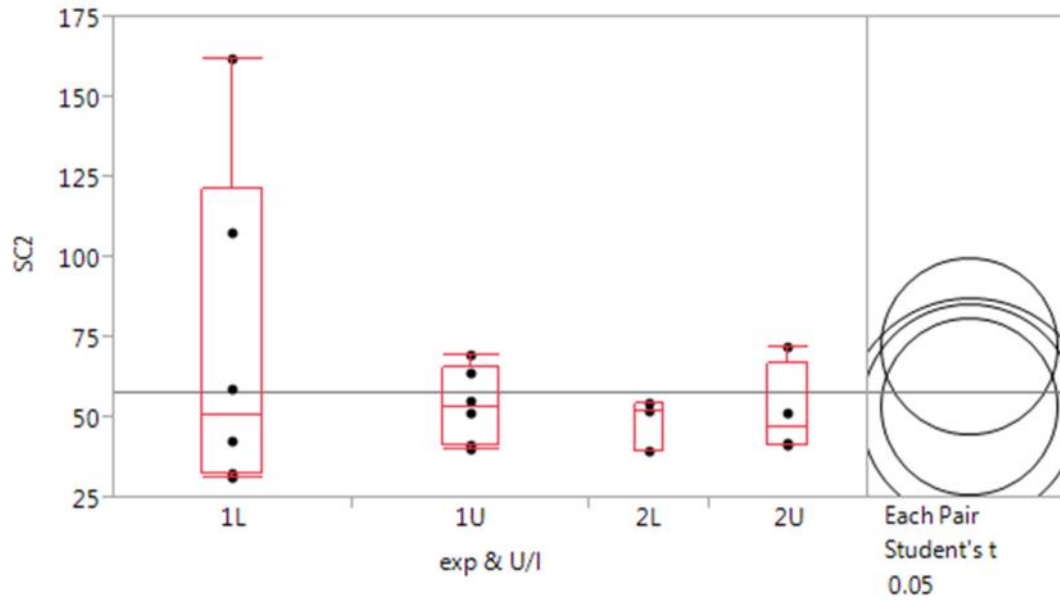


Figure 62: Box plot of means of secondary stomatal conductance ( $\text{mmol m}^{-2} \text{s}^{-1}$ ) for all experiments

For the physical attributes, a stepwise discriminant function of the non-collinear variables (SC1, TDW, R/S DW Ratio, SC2, #NODES, IND, and TNH) was conducted. SC1, TDW, and R/S DW R were found to significantly contribute to the functions. IND and TNH were not included in the model. Mahalanobis distances (or units of standard deviation) show the means of the data quite far from their centroids, or less tightly grouped (Table 21). Results of a Chi-square test suggest we can interpret two canonical roots: the first being weighted most heavily by SC1, R/S DW R, and SC2, the second being most heavily weighted by TDW (see standardized coefficients in Table 19). The first function accounts for 70% of the variance and discriminates mostly between plants from 2L and the other plants. The second function accounts for another 27.5% of the variance and discriminates mostly between plants from 2U and other plants. To summarize, the higher the SC1 and R/S DW ratio,

and the lower the SC2, the more likely that plant is to belong to group 2L. You can view the classification functions that might be used for new cases in Table 20.

Posterior probabilities or, the likelihood a case belongs to a group can be found in Table 22. As is, the functions correctly grouped 89.47% of the cases. A scatter plot of the canonical scores for roots 1 and 2 can be seen in Figure 63. Note that plants from group 2L are clustered to the right, indicative of higher SC1 and R/S DW ratio.

Table 19: Standardized coefficients for canonical variables of physical attributes.

	ROOT 1	ROOT 2	ROOT 3
SC1	1.559009	0.31042	0.208458
TDW	-0.497356	-1.10889	0.284450
R/S DW RATIO	1.072197	0.07072	-0.511281
SC2	-0.948399	-0.70929	0.707977
#NODES	-0.382685	0.68732	0.163885
EIGENVAL	5.609885	2.19434	0.199133
CUM. PROP.	0.700941	0.97512	1.000000

Table 20: Classification functions of measured physical attributes.

	1L	1U	2U	2L
	p=.31579	p=.31579	p=.21053	p=1.5789
SC1	0.2758	0.1291	0.1364	0.4059
TDW	-5.1318	-4.0139	8.7814	-10.5578
R/S DW RATIO	23.4396	13.1845	15.2976	36.3142
SC2	-0.1142	-0.0583	0.0005	-0.2209
#NODES	0.0400	1.3112	-0.7907	-1.0071
Constant	-24.8415	-10.5085	-17.7926	-44.7562

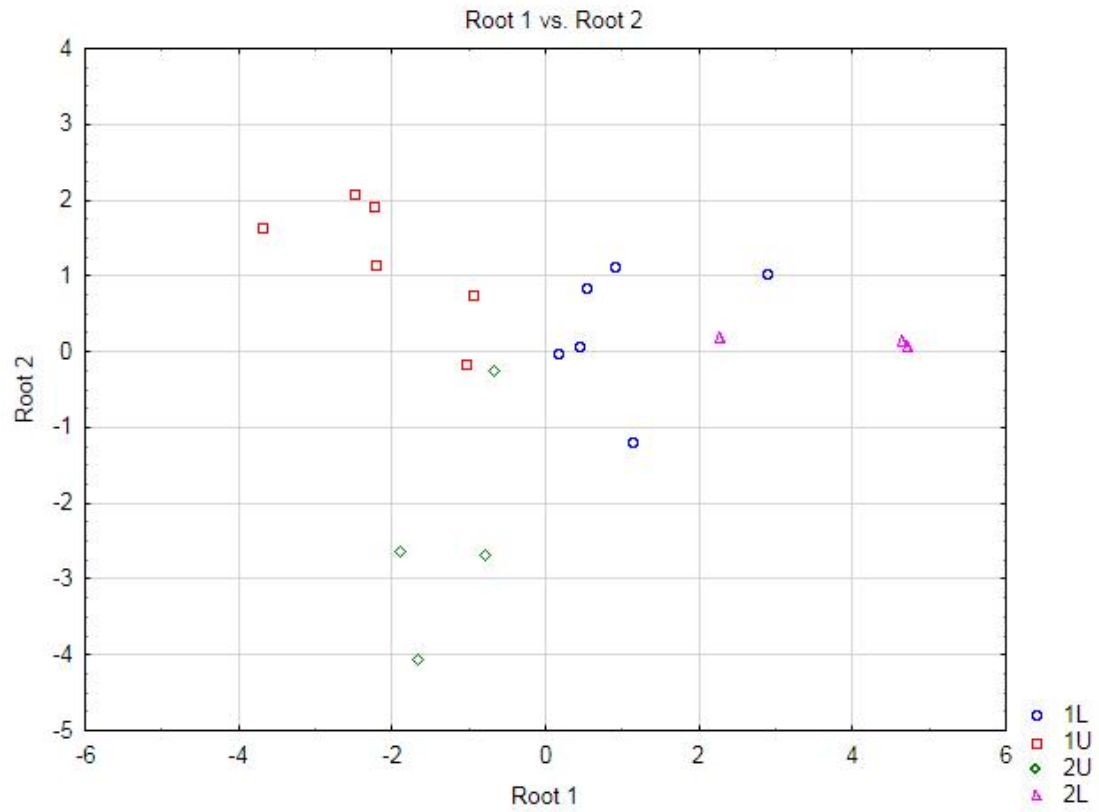


Figure 63: Scatterplot of the canonical scores of the physical attributes.

Table 21: Mahalanobis distances between groups.

	1L	1U	2U	2L
1L	0.00000	11.12168	12.89625	9.47389
1U	11.12168	0.00000	13.98676	37.14956
2U	12.89625	13.98676	0.00000	33.01352
2L	9.47389	37.14956	33.01352	0.00000

Table 22: Posterior probabilities of cases of physical attributes. Incorrectly classified cases are marked with a \*.

Observed Classification	1L p=.31579	1U p=.31579	2U p=.21053	2L p=1.5789	
1	1L	0.989836	0.006822	0.003141	0.000201
2	1L	0.992590	0.007037	0.000231	0.000142
3	1L	0.976742	0.017387	0.000206	0.005665
5	1L	0.667431	0.000010	0.000001	0.332558
6	1L	0.786067	0.156424	0.054263	0.003247
7	1L	0.906877	0.001098	0.073549	0.018476
8	1U	0.001019	0.998939	0.000042	0.000000
9	1U	0.001828	0.997503	0.000669	0.000000
10	1U	0.220032	0.772501	0.007462	0.000005
11	1U	0.000572	0.999408	0.000020	0.000000
12	1U	0.278422	0.573369	0.148203	0.000006
13	1U	0.000022	0.999941	0.000037	0.000000
14	2U	0.000197	0.001107	0.998696	0.000000
15	2U	0.002992	0.000352	0.996656	0.000000
16*	2U	0.459705	0.370702	0.169548	0.000046
17	2U	0.000020	0.000004	0.999976	0.000000
18	2L	0.000454	0.000000	0.000000	0.999546
19	2L	0.003674	0.000000	0.000000	0.996326
20*	2L	0.762712	0.000078	0.000094	0.237116

### 5.3.2 Spectrophotometry Results

The measured spectrophotometry variables were chlorophyll a (chl a mg/ml), chlorophyll b (chl b mg/ml), total chlorophyll (tot chl mg/ml), the ratio of chlorophyll a to chlorophyll b (chla/b), total carotenoid (tot car %), and the ratio of chlorophyll to carotenoid (car/chl). Spectrophotometry variables were normally distributed.

Descriptive statistics of spectrophotometry results can be found in Table 23.

Additionally, foliar weights can be found in Table 24.

Table 23: Descriptive statistics for chemical attribute variables.

	Valid N	Mean	Median	Min	Max	Lower Quartile	Upper Quartile	Std. Dev.
<i>Chl a mg/ml</i>	80	6.09	6.04	2.48	16.04	4.35	7.22	2.41
<i>Chl b mg/ml</i>	80	4.70	4.73	1.85	9.57	3.65	5.64	1.44
<i>Tot Chl mg/ml</i>	80	10.79	10.60	4.61	25.62	8.28	13.15	3.74
<i>chl a/b</i>	80	1.29	1.34	0.78	1.77	1.09	1.47	0.23
<i>tot car %</i>	80	0.07	0.07	0.03	0.17	0.06	0.09	0.03
<i>car/chl</i>	80	0.54	0.49	0.32	1.05	0.38	0.64	0.18

Table 24: Foliar sample weights used for spectrophotometry

<b>Experiment</b>	<b>Treatment</b>	<b>Plant ID</b>	<b>Leaf Sample Weight (mg)</b>
1	UPPER	U1-1	27
1	UPPER	U1-2	28.4
1	UPPER	U1-3	29.9
1	UPPER	U1-4	28.2
1	UPPER	U3-1	23
1	UPPER	U3-2	20.8
1	UPPER	U3-3	12.3
1	UPPER	U3-4	15.1
1	UPPER	U4-1	34.6
1	UPPER	U4-2	28.5
1	UPPER	U4-3	27.4
1	UPPER	U4-4	35.3
1	UPPER	U6-1	30
1	UPPER	U6-2	29.1
1	UPPER	U6-3	28.9
1	UPPER	U6-4	29.6
1	UPPER	U7-1	22.7
1	UPPER	U7-2	31.2
1	UPPER	U7-3	27.6
1	UPPER	U7-4	26.6
1	UPPER	U9-1	16.9
1	UPPER	U9-2	18.6
1	UPPER	U9-3	13.8

1	UPPER	U9-4	17.6
1	LOWER	L2-1	31.6
1	LOWER	L2-2	31.7
1	LOWER	L2-3	28.2
1	LOWER	L2-4	25
1	LOWER	L3-1	32.8
1	LOWER	L3-2	28.6
1	LOWER	L3-3	26.1
1	LOWER	L3-4	23.1
1	LOWER	L4-1	24.3
1	LOWER	L4-2	25.2
1	LOWER	L4-3	27.8
1	LOWER	L4-4	29
1	LOWER	L5-1	22.6
1	LOWER	L5-2	25.5
1	LOWER	L5-3	26
1	LOWER	L5-4	28.6
1	LOWER	L6-1	29.4
1	LOWER	L6-2	28.1
1	LOWER	L6-3	25.8
1	LOWER	L6-4	23.6
1	LOWER	L7-1	28.4
1	LOWER	L7-2	28.9
1	LOWER	L7-3	25.5
1	LOWER	L7-4	25.8
1	LOWER	L8-1	25.7
1	LOWER	L8-2	28.6
1	LOWER	L8-3	21
1	LOWER	L8-4	25.1
2	UPPER	U1-1	33
2	UPPER	U1-2	36
2	UPPER	U1-3	31
2	UPPER	U1-4	32
2	UPPER	U3-1	27
2	UPPER	U3-2	19
2	UPPER	U3-3	24
2	UPPER	U3-4	22
2	UPPER	U4-1	30
2	UPPER	U4-2	31

2	UPPER	U4-3	29
2	UPPER	U4-4	30
2	LOWER	L1-1	24
2	LOWER	L1-2	16
2	LOWER	L1-3	31
2	LOWER	L1-4	33
2	LOWER	L2-1	31
2	LOWER	L2-2	30
2	LOWER	L2-3	29
2	LOWER	L2-4	32
2	LOWER	L3-1	31
2	LOWER	L3-2	35
2	LOWER	L3-3	23
2	LOWER	L3-4	25
3	FIELD	F1-1	31
3	FIELD	F1-2	34
3	FIELD	F1-3	33
3	FIELD	F1-4	31

---

### 5.3.2.1 Comparison of plants grown at 350 $\mu\text{mol m}^{-2} \text{s}^{-1}$

Student's T tests ( $\alpha=0.05$ ) showed significant differences in the means for chlorophyll a (prob  $> |t| = 0.0053$ ), chlorophyll-carotenoid ratio (prob  $> |t| = <0.0001$ ), and ratio of chlorophyll a to chlorophyll b (prob  $> |t| = <0.0001$ ) between the upper and lower sets of experiment 1. While there were differences in chlorophyll b and total carotenoid, they were not significant at  $\alpha=0.05$ .

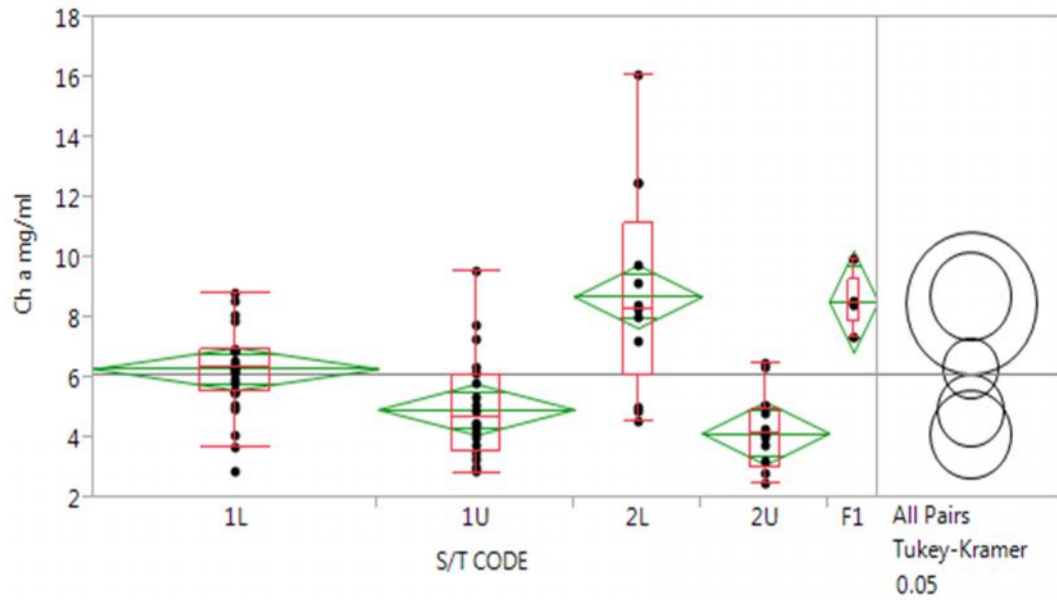
### 5.3.2.2 Comparison of plants grown at 150 $\mu\text{mol m}^{-2} \text{s}^{-1}$

Student's T tests ( $\alpha=0.05$ ) showed significant differences in the means for chlorophyll a (prob  $> |t| = 0.0001$ ), chlorophyll b (prob  $|t| = <0.0001$ ), total carotenoid (prob  $|t| = 0.0004$ ), and ratio of chlorophyll a to chlorophyll b (prob  $> |t| = 0.0017$ ) for

the upper and lower sets of experiment 2. While there were differences in chlorophyll-carotenoid ratio, they were not significant at  $\alpha=0.05$ .

### 5.3.2.3 Comparison of all plants from Experiments 1 and 2, and Field Plant

Chlorophyll a and b pigments were highest, and most similar, for plants from Experiment 2 Lower, and the field plant. Carotenoids were highest for plants from Experiment 2 Lower. The chlorophyll a to chlorophyll b ratio was lowest for the plants grown in the most intense conditions, and the ratio of total carotenoids to chlorophylls was highest for plants grown in the less intense conditions. Significant differences in chlorophyll A content were found between the upper set of each experiment, the lower set of the second experiment and the field plant, and the lower experiment of the first set (Figure 64). Most significant were the differences between 2L and 2U ( $p < 0.0001$ ), and 2L and 1U ( $p < 0.0001$ ). Significant differences in chlorophyll b content were found between 2U and all other sets (2U-F1,  $p = 0.0003$ ; 2U-2L,  $p < 0.0001$ ; 2U-1U,  $p = 0.0003$ ; 2U-1L,  $p = 0.0025$ ; Figure 65). Significant differences in total carotenoid were found between 2L and 1L ( $p = 0.0001$ ), 2L and 1U ( $p = 0.0039$ ), and 2L and 1L ( $p = 0.0450$ ) (Figure 66). For the ratio of carotenoid to chlorophylls, significant differences were found between 1L and all other sets (2U,  $p < 0.0001$ ; 2L,  $p < 0.0001$ ; F1,  $p = 0.0011$ ; 1U,  $p < 0.0001$ ), as well as between 1U and 2U ( $p < 0.0001$ ) (Figure 67). Ratio of chlorophyll a to b showed significant differences between 1U and all other sets (2L,  $p < 0.0001$ ; F1,  $p < 0.0001$ ; 1L,  $p < 0.0001$ ; 2U,  $p < 0.0001$ ) as well as between 2L and 2U ( $p = 0.0090$ ), and 2L and 1L ( $p = 0.0276$ ) (Figure 68).



Ordered Differences Report						
Level	- Level	Difference	Std Err Dif	Lower CL	Upper CL	p-Value
2L	2U	4.551462	0.7453022	2.46816	6.634768	<.0001*
F1	2U	4.381892	0.9999278	1.58684	7.176941	0.0004*
2L	1U	3.756969	0.6769543	1.86471	5.649226	<.0001*
F1	1U	3.587400	0.9500776	0.93170	6.243105	0.0029*
2L	1L	2.405873	0.6342246	0.63306	4.178689	0.0027*
F1	1L	2.236303	0.9201201	-0.33566	4.808270	0.1185
1L	2U	2.145589	0.6342246	0.37277	3.918405	0.0098*
1L	1U	1.351097	0.5522976	-0.19271	2.894906	0.1144
1U	2U	0.794492	0.6769543	-1.09776	2.686749	0.7663
2L	F1	0.169569	0.9999278	-2.62548	2.964618	0.9998

Figure 64: Graphical representation of the results of the Tukey-Kramer All Pairs test of significance for chlorophyll a, and its associated ordered differences report.

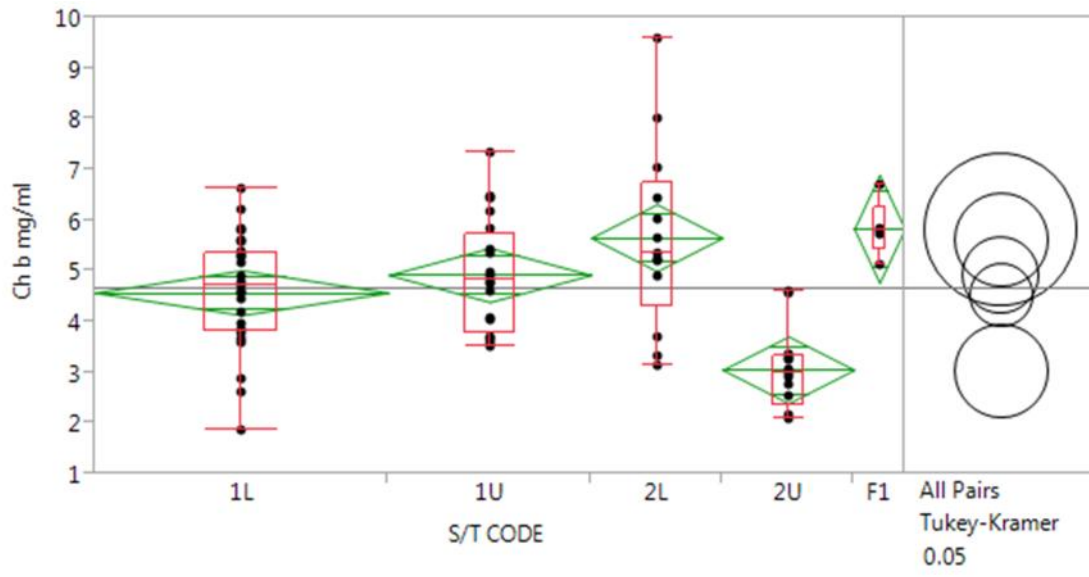


Figure 65: Box plot and mean diamonds of chlorophyll b results for all experiments.

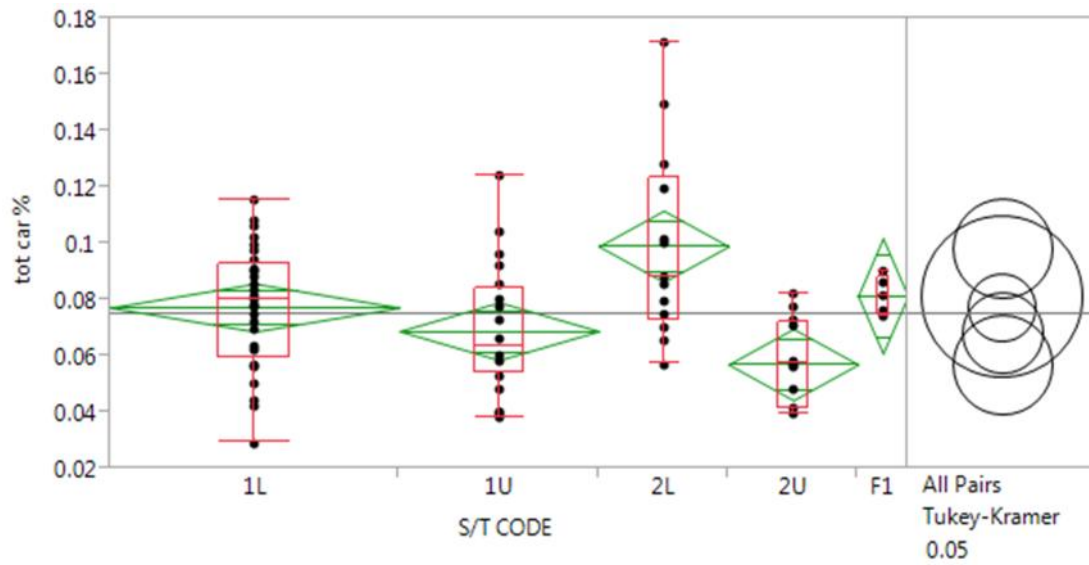


Figure 66: Box plot and mean diamonds of total carotenoid (%) results for all experiments.

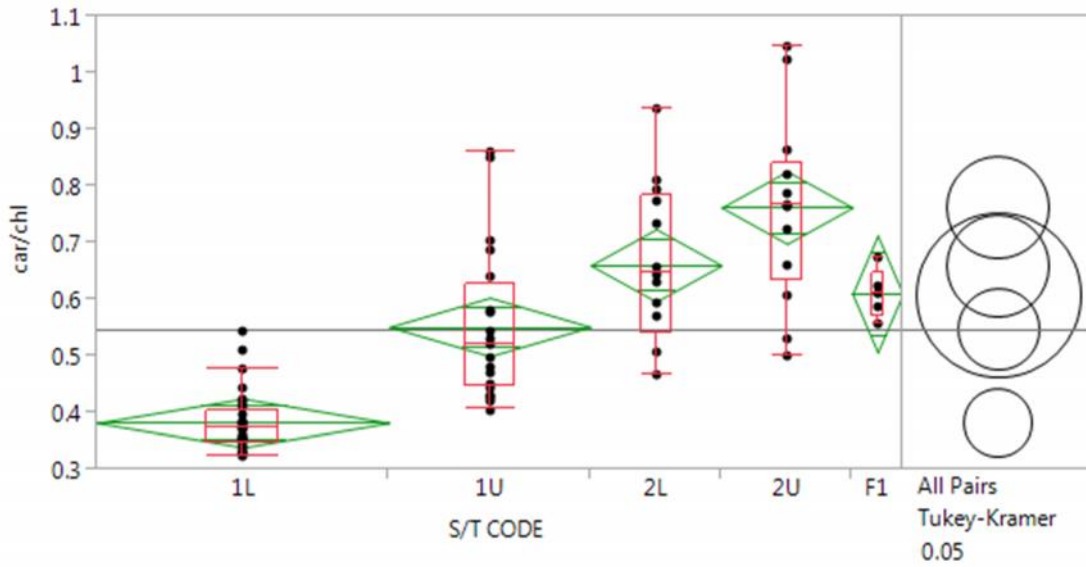


Figure 67: Box plot and mean diamonds of carotenoid to chlorophyll ratio for all experiments.

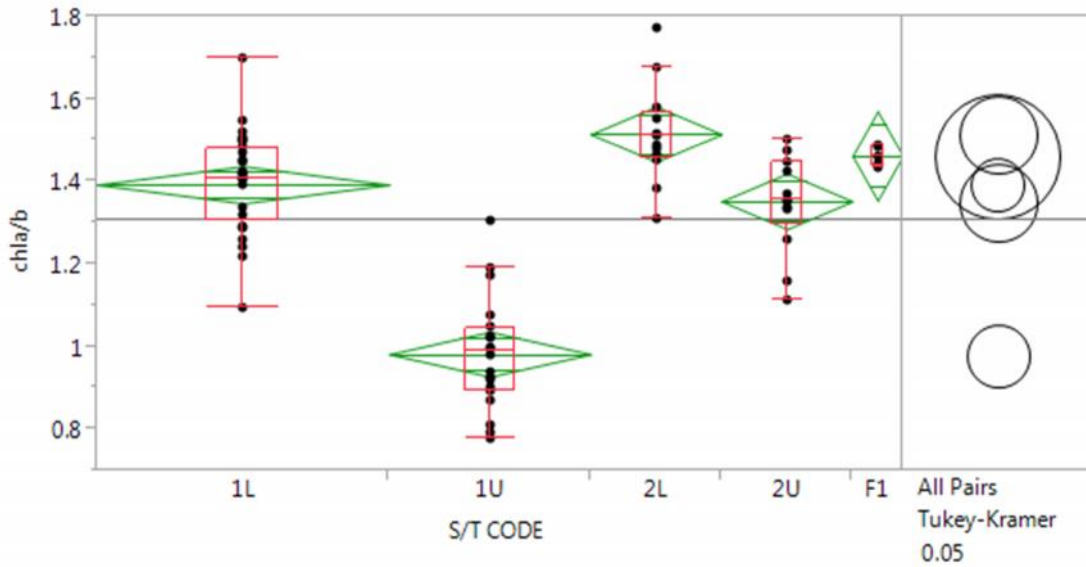


Figure 68: Box plots and mean diamonds for chlorophyll a to b ratio results for all experiments.

For the chemical attributes, a stepwise discriminant function of the non-collinear variables (chlorophyll a mg/ml, chlorophyll b mg/ml, chl a/b ratio, total carotenoid %, and carotenoid/chlorophyll ratio) was conducted. Car/chl was found to significantly contribute to the functions. All selected variables were included in the model. Mahalanobis distances (or units standard deviation) show the means of the data overall not too far from their centroids, or somewhat tightly grouped (Table 26). Results of a Chi-square test suggest we can interpret three canonical roots: the first function being weighted most heavily by chlorophyll a mg/ml and chlorophyll b mg/ml, the second being most heavily weighted by car/chl, chlorophyll a mg/ml, and chl a/b, and the third being weighted almost solely by chlorophyll a mg/ml (see standardized coefficients in Table 24). The first function accounts for 69% of the variance and discriminates mostly between plants from 1U (negatively), 2L, and F (positively) and the other plants. The second function accounts for another 22% of the variance and discriminates mostly between plants from 1L and other plants. The final function accounts for only 8% of the variance and discriminates mostly between plants from 2U and other plants. To summarize, the higher the chl a mg/ml, the more likely that plant is to belong to group 2L or F. Plants with a very high chl/car ratio are likely to be from group 1L. You can view the classification functions that might be used for new cases in Table 25. Posterior probabilities or, the likelihood a case belongs to a group can be found in Table 27. As is, the functions correctly grouped 80% of the cases. Four of the incorrectly grouped cases were those of the field plant, which were grouped with 2L. Scatter plots of the canonical scores for roots 1, 2, and 3 against each other can be seen in Figures 69 (1vs2), 70 (1vs3), and 71 (2vs3).

Table 25: Standardized coefficients for canonical variables of chemical attributes.

	ROOT 1	ROOT 2	ROOT 3	ROOT 4
chla/b	0.45	-0.55	-0.36	-0.53
car/chl	0.72	0.87	-0.06	-0.03
Chl a mg/ml	2.10	0.60	1.22	0.74
tot car %	-0.31	-0.09	0.00	1.30
Chl b mg/ml	-1.63	-0.03	-0.13	-1.50
Eigenval	4.08	1.31	0.47	0.04
Cum.Prop	0.69	0.91	0.99	1.00

Table 26: Classification functions of measured chemical attributes.

	1U p=.3	1L p=.35	2U p=.15	2L p=.15	F p=.05
chla/b	363.36	382.48	383.51	380.57	382.93
car/chl	87.54	83.74	114.38	117.19	112.23
Chl a mg/ml	-67.65	-66.06	-63.86	-61.35	-62.56
tot car %	205.79	185.60	147.05	150.34	102.15
Chl b mg/ml	96.59	93.67	91.02	89.18	91.41
Constant	-281.90	-296.51	-315.10	-321.31	-320.78

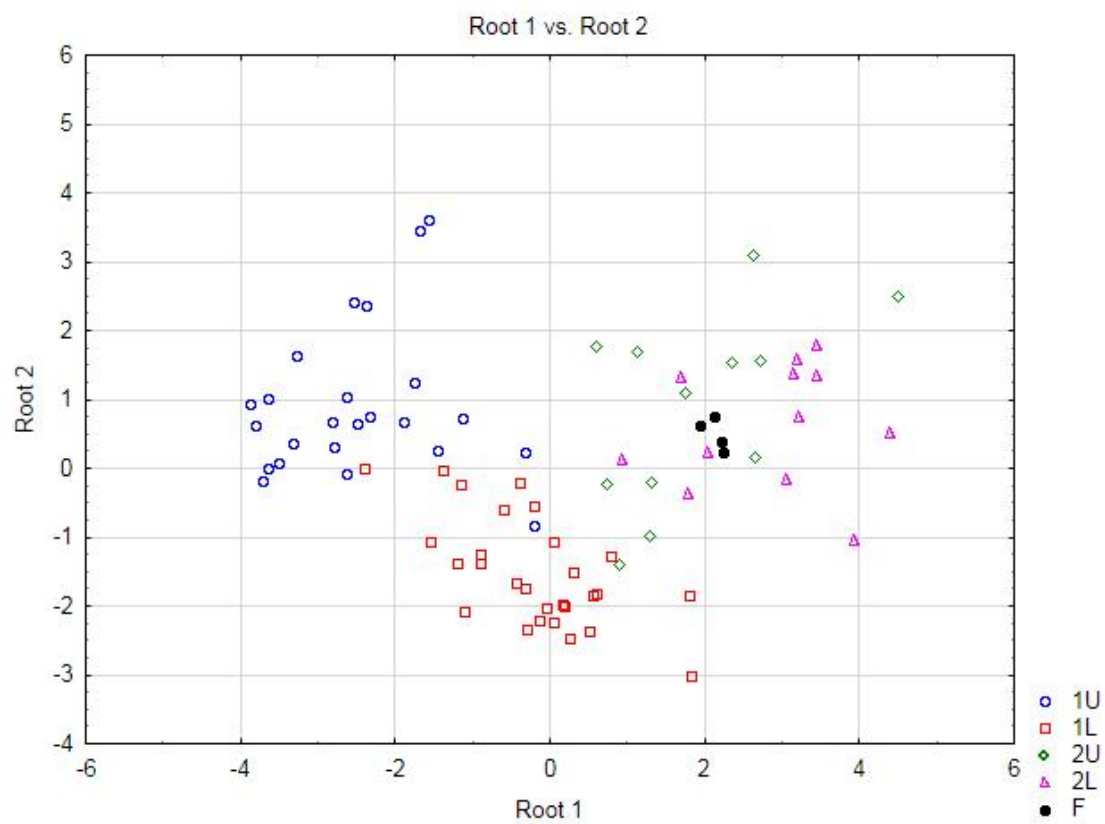


Figure 69: Scatterplot of the canonical scores of the chemical attributes for Root 1 vs Root 2.

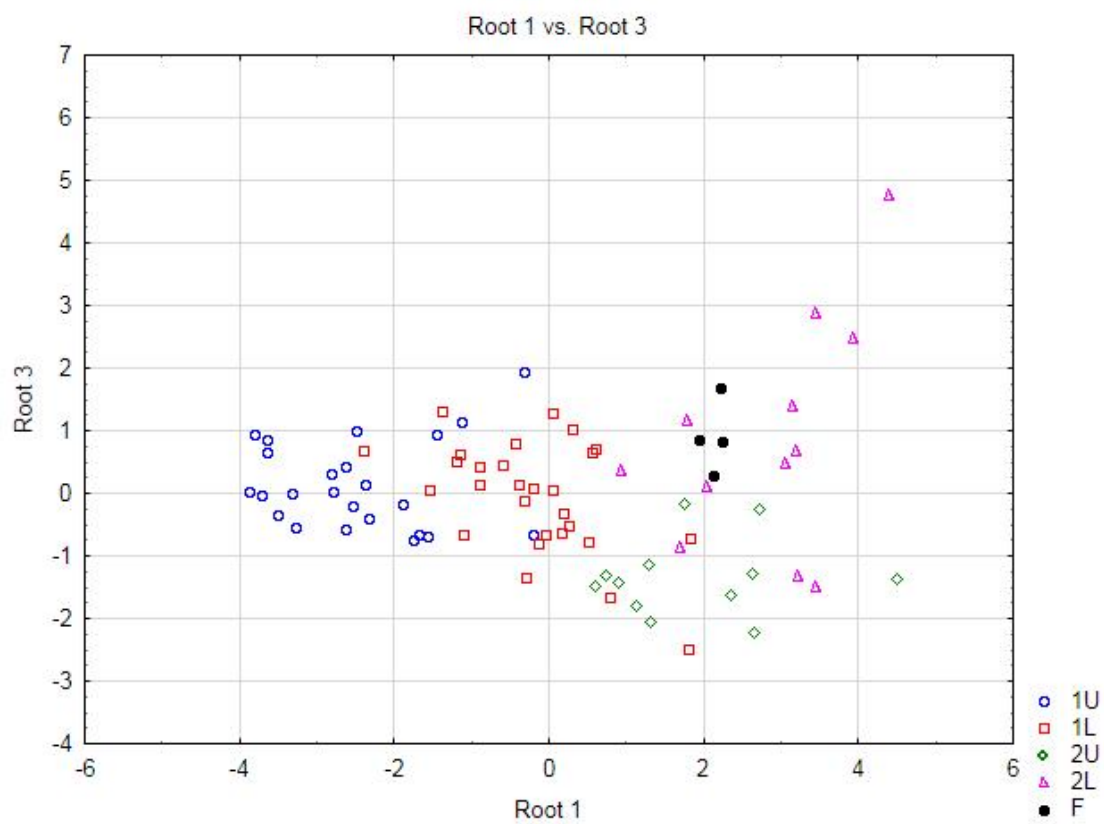


Figure 70: Scatter plot of the canonical scores of the chemical attributes for Root 1 vs Root 3.

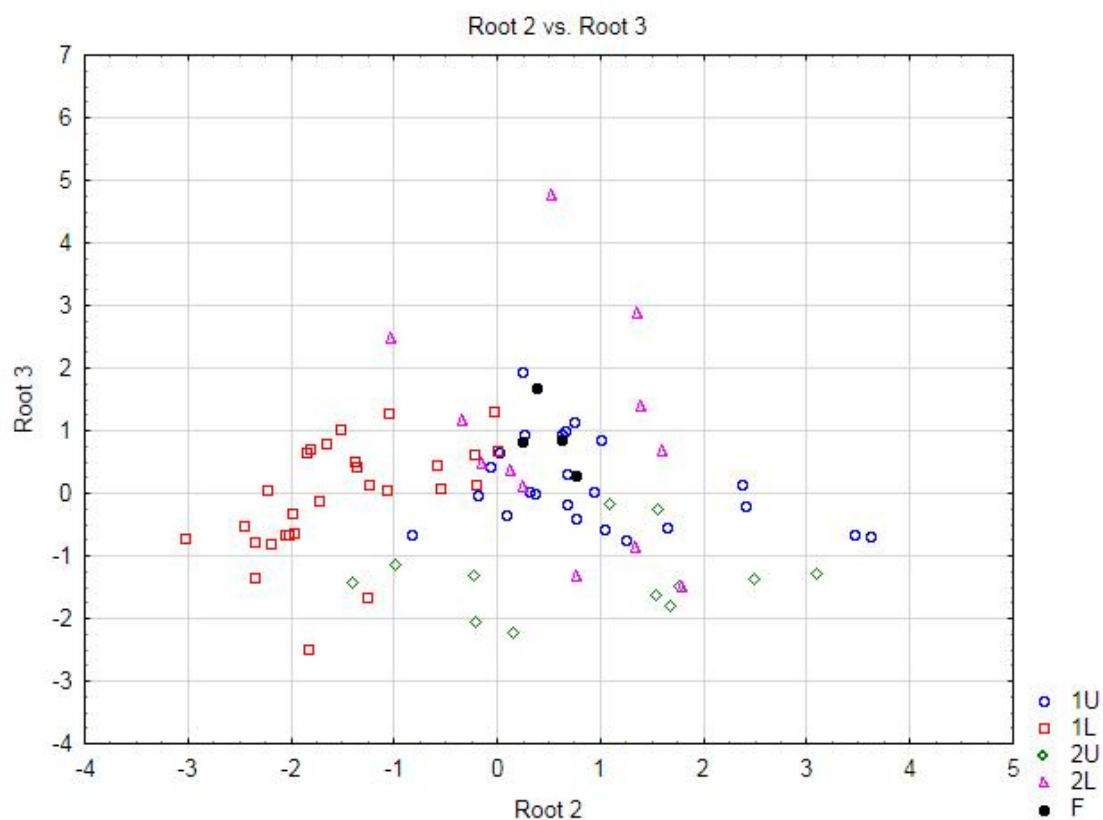


Figure 71: Scatter plot of the canonical scores of the chemical attributes for Root 2 vs Root 3.

Table 27: Squared Mahalanobis distances from group centroid for chemical attribute discriminant analysis. Incorrectly classified cases are marked with a \*.

		1U	1L	2U	2L	F
		p=.3	p=.35	p=.15	p=.15	p=.05
1	1U	5.86078	17.10108	37.25805	48.35053	37.41908
2	1U	4.58378	14.75436	28.40795	33.08226	23.69757
3*	1U	11.79700	3.77781	10.66249	17.50814	11.34077
4	1U	1.14608	8.13800	16.16709	24.44909	17.84989
5	1U	7.70675	23.64776	42.83352	50.03533	39.80611
6	1U	8.79866	25.81527	42.29124	49.07260	41.50821
7	1U	13.20405	25.39794	46.24748	52.38380	49.16968
8	1U	6.62611	24.01040	39.81205	49.88495	45.61699
9	1U	11.86166	31.47955	22.90458	33.77143	30.79811

10	1U	10.48748	29.93724	22.65720	33.25577	31.16887
11	1U	2.76437	21.16896	23.65392	33.64207	28.83094
12	1U	3.54427	21.13774	23.93156	32.56746	25.65362
13	1U	2.91537	15.01919	30.97940	41.36329	31.32314
14	1U	1.34233	12.76436	25.86897	34.07904	25.00670
15	1U	7.81809	25.64626	33.96919	46.63912	39.82061
16	1U	5.46798	17.50884	25.94476	37.43276	30.59642
17	1U	1.81089	8.83096	25.08927	31.91945	23.33663
18	1U	5.42422	8.90952	19.89327	22.73188	13.95809
19	1U	4.98277	9.43063	17.35073	18.44151	12.19263
20*	1U	10.52956	9.21923	18.11184	14.13211	7.78335
21	1U	4.26583	15.66919	32.91411	44.19567	37.38930
22	1U	0.77181	10.27675	24.46067	32.89988	27.02368
23	1U	8.16671	17.59217	26.64559	35.17753	34.84656
24	1U	5.41766	14.41216	17.82138	27.41559	25.97099
25	1L	17.49762	1.63849	13.38790	11.56041	8.20469
26	1L	11.76013	2.34633	14.37908	10.99371	8.65523
27	1L	14.96128	1.95999	14.41166	11.28459	9.70677
28	1L	18.95174	3.06612	15.08345	12.72525	12.75953
29	1L	10.85431	4.52247	11.96521	15.89814	8.79880
30	1L	7.00613	3.19091	9.97679	13.78225	7.74448
31	1L	34.96719	12.23330	10.78629	21.51279	17.83105
32	1L	19.38519	4.29747	6.55618	15.33957	11.74730
33	1L	7.13192	2.49717	12.75379	15.31217	8.99612
34*	1L	5.84685	7.80186	20.86167	21.62850	13.59920
35	1L	5.51783	5.16452	16.41897	19.64825	11.79271
36*	1L	4.29561	10.73124	26.33867	32.02562	21.83792
37	1L	17.36139	1.68234	16.10574	17.38184	15.95279
38	1L	11.72548	1.26700	16.93339	16.26804	13.54417
39	1L	35.20557	7.35016	16.10092	17.46613	16.32096
40	1L	16.27358	1.26133	14.03692	20.14011	16.03830
41	1L	5.06608	2.21663	17.79844	22.96446	18.42891
42	1L	8.02657	0.98768	16.15640	18.31304	14.68353
43	1L	16.47096	1.12166	12.85412	15.77454	14.11775
44	1L	16.53638	2.05192	14.05517	18.76549	17.53242
45	1L	16.02014	0.76428	11.71056	16.26717	13.55359
46	1L	7.53357	0.99499	14.87719	18.29556	14.97092
47	1L	12.64325	1.03841	14.24140	17.19225	15.27101
48	1L	7.71868	2.02742	18.87071	21.05628	17.55690

49	1L	17.89990	2.67786	15.48207	24.14598	20.22518
50	1L	20.50340	1.78794	12.64866	17.28307	14.17398
51	1L	12.58108	2.66067	19.29421	26.09885	23.13002
52	1L	19.40301	1.39503	14.55412	18.21207	15.34138
53*	2U	28.40035	18.87480	3.20077	3.06742	4.53809
54	2U	56.37482	42.92243	12.47942	14.41417	18.75030
55	2U	18.26203	10.86536	1.73636	2.97000	2.53898
56	2U	33.90472	31.78870	6.56773	11.58624	14.77257
57*	2U	20.39225	4.60545	4.80086	10.65794	7.25069
58*	2U	19.30320	3.14691	6.20434	13.46141	11.01012
59	2U	20.89333	8.34819	2.33304	12.25923	10.59605
60*	2U	13.86796	4.24582	2.69604	10.22003	8.52673
61	2U	33.42161	16.59453	2.72689	11.28159	10.66699
62	2U	16.13741	16.66449	5.81797	15.29731	14.04808
63	2U	20.46376	18.07256	4.53432	14.37635	13.97995
64	2U	26.77100	18.30267	0.80364	7.45494	8.46905
65	2L	78.37806	58.31857	53.58892	27.03674	31.03794
66	2L	59.51774	33.08157	31.95840	14.39581	22.70458
67*	2L	39.91568	27.75157	4.91258	8.86126	11.77897
68	2L	33.77793	22.65524	7.28216	1.90249	4.43578
69	2L	42.84220	30.31187	20.80149	5.00609	7.48279
70	2L	34.30686	22.68788	10.49657	1.65631	4.90043
71	2L	21.01797	8.35347	2.78881	1.83754	0.99793
72	2L	32.84021	13.76422	6.78078	2.41466	1.53227
73*	2L	35.51173	19.50751	2.90853	6.36744	7.60914
74*	2L	18.60851	12.40087	0.61494	5.32553	4.21229
75	2L	20.85981	6.84537	7.89192	2.21218	1.63154
76*	2L	12.41057	4.28387	4.53888	4.40267	2.64507
77*	F	25.75883	13.51466	10.46219	2.57271	0.72878
78*	F	21.86663	11.28433	3.27460	1.84990	0.53823
79*	F	24.29522	11.03607	6.41311	2.29591	0.18472
80*	F	20.53213	10.35552	5.24934	1.44866	0.19879

---

Table 28: Posterior probabilities for cases from chemical attribute discriminant analysis. Incorrectly classified cases are marked with a \*.

		1U	1L	2U	2L	F
		p=.3	p=.35	p=.15	p=.15	p=.05
1	1U	0.995790	0.004210	0.000000	0.000000	0.000000
2	1U	0.992818	0.007166	0.000003	0.000000	0.000012
3*	1U	0.015053	0.968090	0.013272	0.000433	0.003152
4	1U	0.965540	0.034154	0.000264	0.000004	0.000038
5	1U	0.999597	0.000403	0.000000	0.000000	0.000000
6	1U	0.999765	0.000235	0.000000	0.000000	0.000000
7	1U	0.997382	0.002618	0.000000	0.000000	0.000000
8	1U	0.999804	0.000196	0.000000	0.000000	0.000000
9	1U	0.997919	0.000064	0.001996	0.000009	0.000013
10	1U	0.998782	0.000070	0.001137	0.000006	0.000005
11	1U	0.999867	0.000118	0.000015	0.000000	0.000000
12	1U	0.999802	0.000176	0.000019	0.000000	0.000003
13	1U	0.997261	0.002738	0.000000	0.000000	0.000000
14	1U	0.996150	0.003846	0.000002	0.000000	0.000001
15	1U	0.999842	0.000157	0.000001	0.000000	0.000000
16	1U	0.997156	0.002825	0.000018	0.000000	0.000001
17	1U	0.966290	0.033703	0.000004	0.000000	0.000003
18	1U	0.828489	0.169204	0.000299	0.000072	0.001937
19	1U	0.883100	0.111460	0.000911	0.000528	0.004002
20*	1U	0.250117	0.561855	0.002823	0.020646	0.164560
21	1U	0.996118	0.003882	0.000000	0.000000	0.000000
22	1U	0.990028	0.009968	0.000004	0.000000	0.000000
23	1U	0.989583	0.010368	0.000048	0.000001	0.000000
24	1U	0.986171	0.012816	0.000999	0.000008	0.000006
25	1L	0.000306	0.990222	0.001192	0.002973	0.005306
26	1L	0.007586	0.979853	0.001024	0.005565	0.005972
27	1L	0.001276	0.990930	0.000840	0.004011	0.002943
28	1L	0.000303	0.994131	0.001047	0.003404	0.001115
29	1L	0.033950	0.939133	0.009740	0.001363	0.015814
30	1L	0.109828	0.863229	0.012434	0.001855	0.012654
31	1L	0.000005	0.527312	0.465914	0.002183	0.004586
32	1L	0.000397	0.874015	0.121079	0.001499	0.003011
33	1L	0.077253	0.914708	0.002323	0.000646	0.005069
34*	1L	0.693061	0.304225	0.000190	0.000130	0.002395

35	1L	0.416338	0.579580	0.000894	0.000178	0.003011
36*	1L	0.955337	0.044630	0.000008	0.000000	0.000025
37	1L	0.000337	0.999066	0.000316	0.000167	0.000114
38	1L	0.004568	0.994721	0.000169	0.000236	0.000307
39	1L	0.000001	0.990365	0.005341	0.002699	0.001595
40	1L	0.000471	0.998687	0.000720	0.000034	0.000088
41	1L	0.170922	0.828884	0.000147	0.000011	0.000036
42	1L	0.024746	0.974822	0.000212	0.000072	0.000148
43	1L	0.000397	0.997895	0.001212	0.000281	0.000215
44	1L	0.000612	0.998167	0.001059	0.000100	0.000062
45	1L	0.000416	0.997368	0.001794	0.000184	0.000238
46	1L	0.031552	0.967847	0.000401	0.000073	0.000128
47	1L	0.002580	0.996592	0.000580	0.000133	0.000116
48	1L	0.047427	0.952395	0.000090	0.000030	0.000058
49	1L	0.000424	0.998835	0.000710	0.000009	0.000022
50	1L	0.000074	0.997577	0.001873	0.000185	0.000291
51	1L	0.005973	0.993914	0.000104	0.000003	0.000005
52	1L	0.000105	0.999071	0.000595	0.000095	0.000134
53*	2U	0.000003	0.000411	0.446294	0.477065	0.076226
54	2U	0.000000	0.000000	0.717065	0.272541	0.010393
55	2U	0.000289	0.013594	0.559402	0.301886	0.124829
56	2U	0.000002	0.000007	0.920090	0.074830	0.005071
57*	2U	0.000221	0.690682	0.268453	0.014356	0.026289
58*	2U	0.000242	0.910369	0.084592	0.002246	0.002551
59	2U	0.000165	0.102226	0.886663	0.006199	0.004746
60*	2U	0.003531	0.506190	0.470834	0.010941	0.008504
61	2U	0.000000	0.002223	0.978049	0.013575	0.006153
62	2U	0.011088	0.009939	0.965282	0.008438	0.005253
63	2U	0.000686	0.002644	0.986553	0.007194	0.002924
64	2U	0.000004	0.000354	0.958276	0.034449	0.006916
65	2L	0.000000	0.000000	0.000002	0.956858	0.043140
66	2L	0.000000	0.000203	0.000153	0.994441	0.005203
67*	2L	0.000000	0.000022	0.869838	0.120779	0.009360
68	2L	0.000000	0.000063	0.058433	0.860666	0.080838
69	2L	0.000000	0.000007	0.000339	0.911577	0.088077
70	2L	0.000000	0.000059	0.011163	0.927707	0.061072
71	2L	0.000062	0.040456	0.280127	0.450734	0.228622
72	2L	0.000000	0.004885	0.068764	0.610168	0.316182
73*	2L	0.000000	0.000480	0.826623	0.146627	0.026270

74*	2L	0.000214	0.005565	0.864511	0.082012	0.047697
75	2L	0.000103	0.132667	0.033692	0.576596	0.256942
76*	2L	0.006951	0.471693	0.177954	0.190497	0.152906
77*	F	0.000010	0.005257	0.010366	0.535542	0.448825
78*	F	0.000042	0.009686	0.227744	0.464319	0.298210
79*	F	0.000016	0.013956	0.060344	0.472796	0.452889
80*	F	0.000080	0.015091	0.083087	0.555702	0.346040

---

## Chapter 6

### DISCUSSION AND CONCLUSION

#### 6.1 Spatial and temporal distribution of PAR in the field

Broadly, this research was an attempt to understand (1) how PAR varies spatially and temporally within and among phenoseasons in a mid-Atlantic deciduous forest; and (2) how this PAR variability might affect woody understory shrubs, specifically *Lindera benzoin* L. Blume (northern spicebush), within the same plot. We postulated that as phenoseasons progressed from leafless to fully-leafed, subcanopy PAR would be significantly decreased while PAR in the open increased, and that canopy closure would greatly affect the amount and distribution of PAR by creating sunflecks and sun patches that were temporally variable. Using data collected from 4,592 unique field observations from one full calendar year, we were able to show that leafless subcanopy PAR values were almost 10 times higher than leafed season PAR, with the exception of sunflecks which could be three orders of magnitude higher than the subcanopy mean, in multiple locations, during one afternoon during the leafed season. Using ANOVA, we were able to show that phenoseason (i.e., the combination of canopy state and celestial geometry) is responsible for nearly three-quarters of the variation between levels in this mid-Atlantic deciduous forest. It is likely that the other 24% may be variation caused by sky conditions, slope, aspect, and canopy species distribution. By collecting values in multiple canopy layers, we were able to determine that while understory PAR is typically less than 40% of open PAR, values of PAR in the shrub canopy are often ~5% lower than the subcanopy.

We postulated that the re-distribution of PAR by canopy species would affect the growth and distribution of the shrub *L. benzoin* in the subcanopy by restricting a primary growth-limiting resource. While it was originally thought that we might be able to make some assumptions about the spatial dependency of species within the plot, visual inspection of the data does not justify any further investigation, at least not at this scale. And, because *F. grandifolia* greatly outnumbers any other species in the plot, any spatial statistic would be inherently skewed in favor of it. While we are not able to make conclusions about species dependencies, it does appear that subcanopy locations with higher PAR means do encompass the locations with greater occurrence of *L. benzoin*. Table 15 shows that, when ranked by mean values, 4 of the 5 locations with occurrence of *L. benzoin* are in the top 24%, and all 5 locations are within the top 36% of annual PAR.

### **6.1.1 Discussion of the Spring Leafless phenoseason**

Mean subcanopy PAR should increase with increasing solar elevation angle from December 21, 2013 onward. Results show that mean subcanopy PAR actually decreased for the spring leafless phenoseason. It was initially thought this might be explained by the fact that only 11.9% of observation days in the winter leafless phenoseason were completely overcast, while 42.9% of observation days in the spring leafless phenoseason were completely overcast. Per our findings, in alignment with Hutchison and Matt (1977), regarding winter leafless overcast conditions actually increasing subcanopy radiation, it seems unlikely this is the case. While we acknowledge the result is unusual, we know that mean PAR is not the best indicator of actual PAR values. The two phenoseasons are not significantly different, and the maximum value of PAR does, in fact, increase, for the spring leafless phenoseason.

Another interesting finding, which is also in agreement with the results of Hutchison and Matt (1977) is the amount of light intercepted by woody areas in leafless phenoseasons. Our results show that less 50% of incident PAR ever makes it to the forest floor, even during leafless phenoseasons. This means that more than 50% of the incident PAR is intercepted by woody frames of trees and shrubs in our field site. Without question, woody area index must be considered in models of light attenuation through forest canopies.

## **6.2 *Lindera benzoin* response to changes in PAR**

We also postulated that light quality and quantity would not only affect the growth of *L. benzoin*, but will also affect the health of *L. benzoin* and its ability to thrive. It has been shown that leaves of woody and herbaceous shade adapted species grown in high light conditions often have fewer pigments, and higher chlorophyll a to chlorophyll b ratio (Hallik, Niinemets, and Kull 2012; Kitajima and Hogan 2003). Luken *et al.* (1997) showed that *L. benzoin* had most new stem growth, lower stomatal density, highest photosynthetic rate and lower leaf thickness at light levels between 191 and 391  $\mu\text{mol m}^{-2} \text{s}^{-1}$ .

Experimental plants that showed the most physical success in terms of biomass were from Experiment 2, on the upper level (receiving 164.5  $\mu\text{mol m}^{-2} \text{s}^{-1}$  for 12 hours). While this value is at the low end of what would be considered peak efficiency for this type of plant, it was closer to the most natural scenario than the other photoperiod-photointensity combinations. It is likely that while the lower level set from Experiment 1 experienced photointensity closer to the value of that found to be conducive for peak efficiency (366  $\mu\text{mol m}^{-2} \text{s}^{-1}$ ), they do not likely experience such an intense photon flux for more than a few hours, and especially not for 16 hours

straight, every day for weeks. As Chazdon and Pearcy (1991) suggest it is possible that many plants may experience greater success in the field in terms of carbon gain due to precise temporal light sequences, rather than exposure total alone. That being the case, a sharp rise to a photointensity that remains constant for a full 12 to 16 hours before sharply falling to complete darkness is hardly representative of the highly variable temporal light sequences we now know to be occurring in the field.

While on the topic of plant success, we also know that the spectral composition, or quality of the light plants use to conduct photosynthesis is also key. In field conditions, plants are exposed not only to redistribution of PAR but also spectral filtration (Leuchner 2011). In the end, light quality proved more difficult to address and was thus outside the scope of this study but, it should be stated that it is extremely likely that the spectral output of the bulbs in the growth chamber had some influence on plant health and growth.

Using UV-vis spectrophotometry, we can confirm that *L. benzoin* under lab conditions do significantly alter their pigments and pigment ratios in response to high intensity light conditions. In this case, while the plants grown in high photointensity conditions did have fewer pigments, the chlorophyll a to b ratios were higher than for those plants grown in lower photointensity conditions. These results are in opposition with the literature. It was believed that carotenoid pigments would also be more abundant in plants grown in high intensity conditions as an attempt to use carotenoids as a defense against phototoxicity, restricting photon absorption indicative of light stress. Our results show that opposite is happening. It is believed that these results may be due to both light filtration within the growth chamber due to non-operational wavelengths and the plants from 2L increasing *all* pigments in an attempt to acquire

additional light resources. It is suspected that these results would be different in a natural light experiment with filtration similar to that of canopy trees. Additionally, changes in pigmentation can also result from limitation of nutrients (Kitajima and Hogan 2003). Without fertilization, it is possible that these plants may have been nutrient deprived. Oliphant (2011) showed that leaves of shade tolerant species do not tolerate even short episodes of high intensity light well. To induce physiological change in the experimental plants, this study exposed the plants to very long episodes of unnaturally intense levels of PAR. It is possible that the intense levels of PAR this exposure may have led to the overall decrease in expensive pigments as well as the weakened plant metabolic and physiological state. It could be argued that plants exposed to intense levels of PAR in Experiment 1 may have allocated resources to tackle abiotic stress, and viral infection contracted by the plants of Experiment 1 as the plants allocated resources to defend against light or heat poisoning, rather than other using crucial resources for primary metabolic functions.



Figure 72: Photograph of plant “U6”, a plant on the upper level of Experiment 1, showing evidence of viral infection.

In our study plot, *L. benzoin* began to bloom in the first week of April, while canopy trees did not begin bud burst until the end of April. Other understory plants in the plot begin later in the season, some reaching full bloom as late as mid-May. In a natural setting, *L. benzoin* have a distinct advantage by blooming early. They take advantage of the high amounts of PAR reaching the forest floor during the spring leafless and early spring leafing phenophases. Biologically, an understory species must make the most of this peak in annual energy, as this is the time for germination and reproduction, activities which require the most energy. This early bloom is also beneficial for early pollinators, who may have access to limited resources so early in the season.

### **6.3 Future research & factors not considered**

This is a large, multifaceted dataset with plenty of opportunity for additional research. We know that the success of plants, while highly dependent upon solar radiation, is not solely limited by solar radiation. When looking at spatial relationships between canopy and understory species and considering physiological changes plants make to acquire defenses, nutrition, and water, it would be remiss to not consider the addition of impacts of soil, nutrient availability, and microbial communities. It is necessary to expand the study area to allow for proper analysis of spatial relationships. One might include other wavelengths during spectrophotometry to look at other pigments and include the morphogenic range of light (350-800 nm) to more closely evaluate the impacts of light on plant germination and development in the field. The addition of N and the N:Chl ratio as long term indicators of plant change due to nitrogen redistribution over time in varying light environment (Hallik 2011) in future studies would be ideal, as well as the addition of leaf plasticity and leaf age, and fluorescence. Future research may also address gaps in photosynthesis research and modeling and sub-canopy light dynamics, and may be a possible gateway to more thorough interspecies communication research.

## REFERENCES

- Afifi, A., S. May, and V. A. Clark. 2012. *Practical Multivariate Analysis*. Boca Raton: CRC Press.
- Anderson, M.C. 1964. "Studies of the Woodland Light Climate: II. Seasonal Variation in the Light Climate." *Journal of Ecology* 52(3): 643–63.
- Andersson, T. 1991. "Influence of Stemflow and Throughfall from Common Oak ( *Quercus Robur* ) on Soil Chemistry and Vegetation Patterns." *Canadian Journal of Forest Research* 21: 917–24.
- Baldocchi, D., B. Hutchison, D. Matt, and R. McMillen. 1984. "Seasonal Variations in the Radiation Regime within an Oak-Hickory Forest." *Agricultural and Forest Meteorology* 33(84): 177–91.
- Canham, C.D., K.D. Coates, P. Bartemucci, and S. Quaglia. 1999. "Measurement and Modeling of Spatially Explicit Variation in Light Transmission through Interior Cedar-Hemlock Forests of British Columbia." *Canadian Journal of Forest Research* 29(11): 1775–83.
- Dale, M.R.T. 1999. *Spatial Pattern Analysis in Plant Ecology*. Cambridge: Cambridge University Press.
- De Castro, F. 2000. "Light Spectral Composition in a Tropical Forest: Measurements and Model." *Tree Physiology* 20: 49–56.
- Chazdon, R.L. 1988. "Sunflecks and Their Importance to Forest Understorey Plants." *Advances in Ecological Research* 18: 1–63.
- Chazdon, R.L., and R.W. Pearcy. 1991. "The Importance of Sunflecks for Forest Understorey Plants." *BioScience* 41(11): 760–66.
- Dietze, M.C. 2014. "Gaps in Knowledge and Data Driving Uncertainty in Models of Photosynthesis." *Photosynthesis Research* 119(1-2): 3–14.
- Federer, C.A. 1971. "Solar Radiation Absorption by Leafless Hardwood Forests." *Agricultural Meteorology* 9: 3–20.

- Gendron, F., C. Messier, and P.G. Comeau. 2001. "Temporal Variations in the Understorey Photosynthetic Photon Flux Density of a Deciduous Stand: The Effects of Canopy Development, Solar Elevation, and Sky Conditions." *Agricultural and Forest Meteorology* 106(1): 23–40.
- Gholz, H.L., S.A. Vogel, W.P. Cropper Jr., K. McKelvey, K.C. Ewel, R.O. Teskey, and P.J. Curran. 1991. "Dynamics of Canopy Structure and Light Interception in *Pinus Elliottii* Stands, North Florida." *Ecological Monographs* 61(1): 33–51.
- Gross, L.J. 1982. "Photosynthetic Dynamics in Varying Light Environments: A Model and Its Application to Whole Leaf Carbon Gain." *Ecology* 63(1): 84–93.
- Hair Jr., J.F., R.E. Anderson, and R.L. Tatham. 1987. *Multivariate Data Analysis*. New York: Macmillan.
- Hallik, L., U. Niinemets, and O. Kull. 2012. "Photosynthetic Acclimation to Light in Woody and Herbaceous Species: A Comparison of Leaf Structure, Pigment Content and Chlorophyll Fluorescence Characteristics Measured in the Field." *Plant Biology* 14(1): 88–99.
- Hanson, P.J., and S.D. Wullschleger, eds. 2003. *North American Temperate Deciduous Forest Responses to Changing Precipitation Regimes*. Springer: New York.
- Hojjati, S.M., A. Hagen-Thorn, and N.P. Lamersdorf. 2008. "Canopy Composition as a Measure to Identify Patterns of Nutrient Input in a Mixed European Beech and Norway Spruce Forest in Central Europe." *European Journal of Forest Research* 128(1): 13–25.
- Holst, T., S. Hauser, A. Kirchgässner, A. Matzarakis, H. Mayer, and D. Schindler. 2004. "Measuring and Modelling Plant Area Index in Beech Stands." *International Journal of Biometeorology* 48(4): 192–201.
- Horn, H.S. 1971. *The Adaptive Geometry of Trees*. Princeton: Princeton University Press.
- Hutchison, B.A., and D.R. Matt. 1977. "The Distribution of Solar Radiation within a Deciduous Forest." *Ecological Monographs* 47(2): 185–207.
- Kinerson, R.S. 1973. "Fluxes of Visible and Net Radiation within a Forest Canopy." *Journal of Applied Ecology* 10(2): 657–60.

- Kitajima, K., and K.P. Hogan. 2003. "Increases of Chlorophyll A/b Ratios during Acclimation of Tropical Woody Seedlings to Nitrogen Limitation and High Light." *Plant, Cell and Environment* 26(6): 857–65.
- Kuuluvainen, T., and T. Pukkala. 1987. "Effect of Crown Shape and Tree Distribution on the Spatial Distribution of Shade." *Agricultural and Forest Meteorology* 40: 215–31.
- Leuchner, M., C. Hertel, and A. Menzel. 2011. "Spatial Variability of Photosynthetically Active Radiation in European Beech and Norway Spruce." *Agricultural and Forest Meteorology* 151(9): 1226–32.
- Leuchner, M., A. Menzel, and H. Werner. 2007. "Quantifying the Relationship between Light Quality and Light Availability at Different Phenological Stages within a Mature Mixed Forest." *Agricultural and Forest Meteorology* 142(1): 35–44.
- Levia, D.F., and S.R. Herwitz. 2005. "Interspecific Variation of Bark Water Storage Capacity of Three Deciduous Tree Species in Relation to Stemflow Yield and Solute Flux to Forest Soils." *Catena* 64(1): 117–37.
- Levia, D.F., J.T. Van Stan, S.M. Mage, and P.W. Kelley-Hauske. 2010. "Temporal Variability of Stemflow Volume in a Beech-Yellow Poplar Forest in Relation to Tree Species and Size." *Journal of Hydrology* 380(1-2): 112–20.
- Levia, D.F., and S.R. Herwitz. 2002. "Winter Chemical Leaching from Deciduous Tree Branches as a Function of Branch Inclination Angle in Central Massachusetts." *Hydrological Processes* 16(14): 2867–79.
- Levia Jr., D.F., and S.R. Herwitz. 2000. "Physical Properties of Water in Relation to Stemflow Leachate Dynamics: Implications for Nutrient Cycling." *Canadian Journal of Forest Research* 30(4): 662–66.
- Luken, J.O., L.M. Kuddes, T.C. Tholemeier, and D.M. Haller. 1997. "Comparative Responses of *Lonicera Maackii* (amur Honeysuckle) and *Lindera Benzoin* (spicebush) to Increased Light." *The American Midland Naturalist* 138(2): 331–43.
- Meyer, G.A., and M.C. Witmer. 1998. "Influence of Seed Processing by Frugivorous Birds on Germination Success of Three North American Shrubs." *The American Midland Naturalist* 140(1): 129–39.

- Mooney, E., M. Edwards, and R. Niesenbaum. 2010. "Genetic Differentiation between Sun and Shade Habitats in Populations of *Lindera Benzoin* L." *Population Ecology* 52(3): 417–25.
- Mooney, E.H., and R.A. Niesenbaum. 2012. "Population-Specific Responses to Light Influence Herbivory in the Understory Shrub *Lindera Benzoin*." *Ecology* 93(12): 2683–92.
- Mooney, E.H., E.J. Tiedeken, N.Z. Muth, and R.A. Niesenbaum. 2009. "Differential Induced Response to Generalist and Specialist Herbivores by *Lindera Benzoin* (Lauraceae) in Sun and Shade." *Oikos* 118(8): 1181–89.
- Niesenbaum, R.A. 1992. "Sex Ratio, Components of Reproduction, and Pollen Deposition in *Lindera Benzoin* (Lauraceae)." *American Journal of Botany* 79(5): 495–500.
- Oker-Blom, P., M.R. Kaufmann, and M.G. Ryan. 1991. "Performance of a Canopy Light Interception Model for Conifer Shoots, Trees and Stands." *Tree Physiology* 9(1\_2): 227–43.
- Oliphant, A.J., D. Dragoni, B. Deng, C.S.B. Grimmond, H.-P. Schmid, and S.L. Scott. 2011. "The Role of Sky Conditions on Gross Primary Production in a Mixed Deciduous Forest." *Agricultural and Forest Meteorology* 151(7): 781–91.
- Parker, G.G. 1983. "Throughfall and Stem Flow in the Forest Nutrient Cycle." *Advances in Ecological Research* 13: 57–133.
- Perry, T.O., H.E. Sellers, and C.O. Blanchard. 1969. "Estimation of Photosynthetically Active Radiation under a Forest Canopy with Chlorophyll Extracts and from Basal Area Measurements." *Ecology* 50(1): 39–44.
- Proe, M.F., J.H. Griffiths, and J. Craig. 2002. "Effects of Spacing, Species and Coppicing on Leaf Area, Light Interception and Photosynthesis in Short Rotation Forestry." *Biomass and Bioenergy* 23: 315–26.
- Pukkala, T., P. Becker, T. Kuuluvainen, and P. Oker-Blom. 1991. "Predicting Spatial Distribution of Direct Radiation below Forest Canopies." *Agricultural and Forest Meteorology* 55: 295–307.
- Richardson, A.D., T.F. Keenan, M. Migliavacca, Y. Ryu, O. Sonnentag, and M. Toomey. 2013. "Climate Change, Phenology, and Phenological Control of Vegetation Feedbacks to the Climate System." *Agricultural and Forest Meteorology* 169: 156–73.

- Schuenemeyer, J.H., and L.J. Drew. 2011. *Statistics for Earth and Environmental Scientists*. Hoboken, NJ: John Wiley & Sons, Inc.
- Siegert, C.M., and D.F. Levia. 2014. "Seasonal and Meteorological Effects on Differential Stemflow Funneling Ratios for Two Deciduous Tree Species." *Journal of Hydrology* 519: 446–54.
- Taiz, L., and E. Zeiger. 2010. *Plant Physiology*. Sunderland, MA: Sinauer Associates.
- Du Toit, B. 2008. "Effects of Site Management on Growth, Biomass Partitioning and Light Use Efficiency in a Young Stand of Eucalyptus Grandis in South Africa." *Forest Ecology and Management* 255(7): 2324–36.
- Wilson, J.W. 1967. "Stand Structure and Light Penetration. III. Sunlit Foliage Area." *Journal of Applied Ecology* 4(1): 159–65.

## Appendix A

### FAIR HILL (DFHM) DEOS STATION INSTRUMENTATION

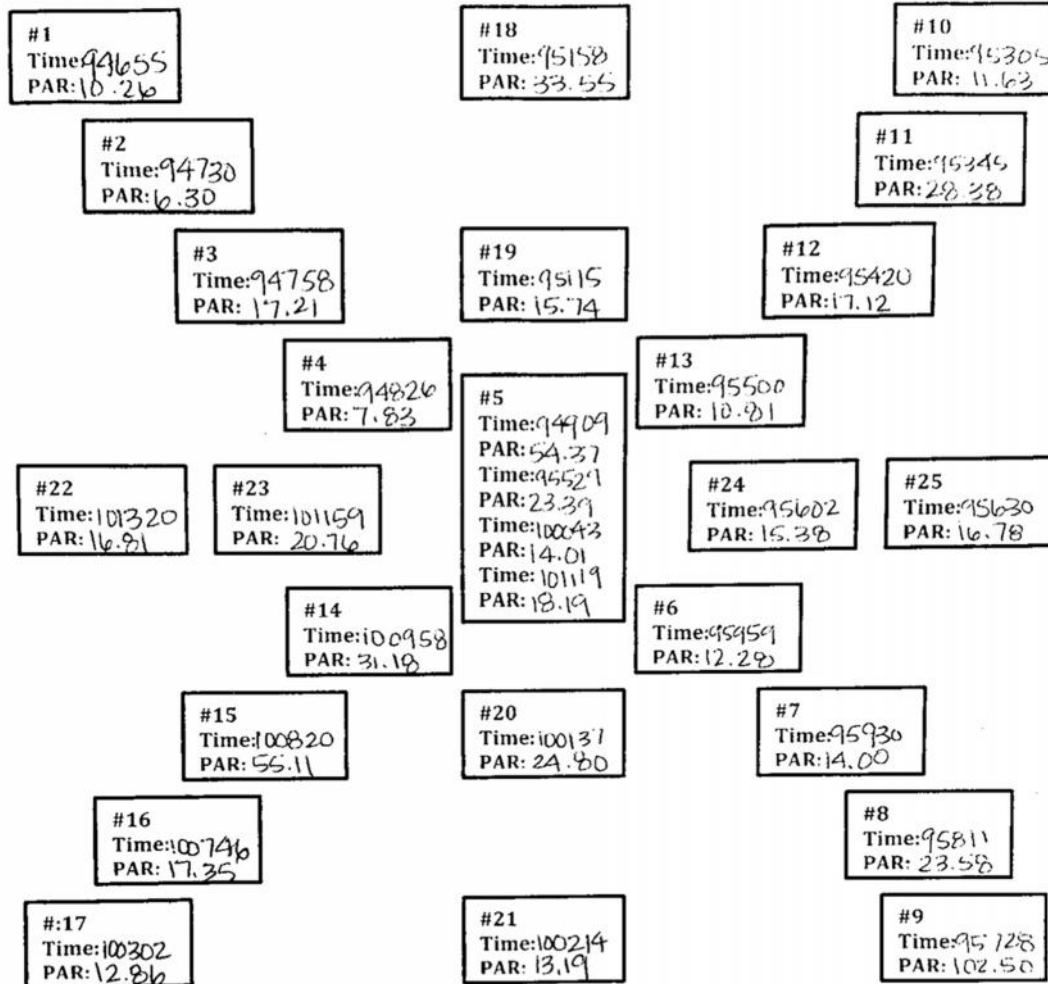
Table 29: Fair Hill (DFHM) DEOS station instrumentation.

Component	Manufacturer	Type	Installation Date
Temperature and relative humidity probe	Campbell Scientific	HMP45C	6/16/2014
Wind Monitor	Campbell Scientific	05103	6/18/2014
Pyranometer	LI-COR	LI-200	4/9/2014
Quantum sensor	LI-COR	LI-190	4/9/2014
Barometer	Campbell Scientific	PTB101B	6/19/2014
Data logger	Campbell Scientific	CR1000	6/18/2014
Tipping bucket rain gage	Texas Electronics	TR525	
All-weather precipitation gauge	GEONOR	T-200B	
Soil moisture probe	Campbell Scientific	CS616	6/18/2014
Soil temperature probe	Campbell Scientific	107-L	6/18/2014

## **Appendix B**

### **COMPLETED FIELD SHEET EXAMPLE**

An example of a completed field sheet used in the completion of this thesis can be found on the following page.



Week: 34 Year: 2014 Month: 07 Day: 26 365 Day: 201

Phenoseason: 5

Visual sky conditions/time: \_\_\_\_\_

NOTES: open: 100528 847.1

5M 94930	204.3	14M 101023	16.78
5B 95012	08.02	14B 101045	13.24
8M 95836	11.86	23M 101219	20.82
8B 95859	13.19	23B 101242	13.26
15M 100845	35.79		
15B 100905	22.71		

OKTA SKY CONDITIONS

0 - CLEAR

1 - 25%

2 - 50%

3 - 75%

4 - 50%

5

6 - 75%

7

8 - OVERCAST

PHENOSEASON

1 - WINTER LEAFLESS

2 - SPRING LEAFLESS

3 - SPRING LEAFING

4 - SUMMER LEAFING

5 - SUMMER FULLY-LEAFED

6 - AUTUMNAL FULLY-LEAFED

7 - AUTUMNAL PARTIALLY LEAFED

## **Appendix C**

### **COPYRIGHT PERMISSIONS**

Permission was obtained through the Copyright Clearinghouse to use images from Hutchison and Matt (1977). The following pages provide that documentation.

Note: Copyright.com supplies permissions but not the copyrighted content itself.

Confirmation Number: 11328053

Order Date: 03/29/2015

#### Order Details

Ecological monographs

Order detail ID: 66589433

Permission Status: Granted

Order License Id: 3598430180980

Permission type: Republish or display content

ISSN: 0012- 9615

Type of use: Republish in a thesis/dissertation

Requestor type: Academic institution

Publication Type: Journal

Publisher: ECOLOGICAL SOCIETY OF AMERICA, ETC.

Author/Editor: ECOLOGICAL SOCIETY OF AMERICA

Format: Print

Portion: image/photo

Number of images/photos: 2 requested

Title or numeric reference of the portion(s): Figure 2, Figure 24

Title of the article or chapter the portion is from: The distribution of solar radiation  
within a deciduous forest

Editor of portion(s): Ecological Society of America

Author of portion(s): Boyd A. Hutchison and Detlef R. Matt

Volume of serial or monograph: 47

Issue, if republishing an article from a serial: 2

Page range of portion: 205, 189

Publication date of portion: 1977

Rights for: Main product

Duration of use: Life of current edition

Creation of copies for the disabled: no

With minor editing privileges: no

For distribution to: Worldwide

In the following language(s): Original language of publication

With incidental promotional use: no

Lifetime unit quantity of new product: Up to 499

Made available in the following markets: Academic

The requesting person/organization: Janice Hudson

Order reference number

Author/Editor: Janice Hudson

The standard identifier: Thesis

The proposed price: 0.00

Title: UNDERSTORY VARIABILITY OF PHOTOSYNTHETICALLY ACTIVE RADIATION IN A MID- ATLANTIC DECIDUOUS FOREST AND ITS EFFECTS ON LINDERA BENZOIN L. BLUME (NORTHERN SPICEBUSH)

Publisher: ProQuest

Expected publication date: May 2015

Estimated size (pages): 200

Note: This item will be invoiced or charged separately through CCC's RightsLink service. More info \$ 0.00

This is not an invoice. Total order items: 1 Order Total: 0.00 USD

Confirmation Number: 11328053

Special Rightsholder Terms & Conditions

The following terms & conditions apply to the specific publication under which they are listed

Ecological monographs

Permission type: Republish or display content

Type of use: Republish in a thesis/dissertation

#### TERMS AND CONDITIONS

The following terms are individual to this publisher:

None

Other Terms and Conditions:

None

#### STANDARD TERMS AND CONDITIONS

1. Description of Service Defined Terms. This Republication License enables the User to obtain licenses for republication of one or more copyrighted works as described in detail on the relevant Order Confirmation (the "Work(s)"). Copyright Clearance Center, Inc. ("CCC") grants licenses through the Service on behalf of the rightsholder identified on the Order Confirmation (the "Rightsholder"). "Republication", as used herein, generally means the inclusion of a Work, in whole or in part, in a new work or works, also as described on the Order Confirmation. "User", as used herein, means the person or entity making such republication.

2. The terms set forth in the relevant Order Confirmation, and any terms set by the Rightsholder with respect to a particular Work, govern the terms of use of Works in connection with the Service. By using the Service, the person transacting for a republication license on behalf of the User represents and warrants that he/she/it (a) has been duly authorized by the User to accept, and hereby does accept, all such terms and conditions on behalf of User, and (b) shall inform User of all such terms and conditions. In the event such person is a "freelancer" or other third party independent of User and CCC, such party shall be deemed jointly a "User" for purposes of these

terms and conditions. In any event, User shall be deemed to have accepted and agreed to all such terms and conditions if User republishes the Work in any fashion.

### 3. Scope of License Limitations and Obligations.

3.1 All Works and all rights therein, including copyright rights, remain the sole and exclusive property of the Rightsholder. The license created by the exchange of an Order Confirmation (and/or any invoice) and payment by User of the full amount set forth on that document includes only those rights expressly set forth in the Order Confirmation and in these terms and conditions, and conveys no other rights in the Work(s) to User. All rights not expressly granted are hereby reserved.

3.2 General Payment Terms: You may pay by credit card or through an account with us payable at the end of the month. If you and we agree that you may establish a standing account with CCC, then the following terms apply: Remit Payment to: Copyright Clearance Center, Dept 001, P.O. Box 843006, Boston, MA 02284- 3006. Payments Due: Invoices are payable upon their delivery to you (or upon our notice to you that they are available to you for downloading). After 30 days, outstanding amounts will be subject to a service charge of 1- 1/2% per month or, if less, the maximum rate allowed by applicable law. Unless otherwise specifically set forth in the Order Confirmation or in a separate written agreement signed by CCC, invoices are due and payable on “net 30” terms. While User may exercise the rights licensed immediately upon issuance of the Order Confirmation, the license is automatically revoked and is null and void, as if it had never been issued, if complete payment for the license is not received on a timely basis either from User directly or through a payment agent, such as a credit card company.

3.3 Unless otherwise provided in the Order Confirmation, any grant of rights to User (i) is “one-time” (including the editions and product family specified in the license), (ii) is non- exclusive and non- transferable and (iii) is subject to any and all limitations and restrictions (such as, but not limited to, limitations on duration of use or circulation) included in the Order Confirmation or invoice and/or in these terms and conditions. Upon completion of the licensed use, User shall either secure a new permission for further use of the Work(s) or immediately cease any new use of the Work(s) and shall render inaccessible (such as by deleting or by removing or severing links or other locators) any further copies of the Work (except for copies printed on paper in accordance with this license and still in User's stock at the end of such period).

3.4 In the event that the material for which a republication license is sought includes third party materials (such as photographs, illustrations, graphs, inserts and similar materials) which are identified in such material as having been used by permission, User is responsible for identifying, and seeking separate licenses (under this Service or otherwise) for, any of such third party materials without a separate license, such third party materials may not be used.

3.5 Use of proper copyright notice for a Work is required as a condition of any license granted under the Service.

Unless otherwise provided in the Order Confirmation, a proper copyright notice will read substantially as follows:

“Republished with permission of [Rightsholder’s name], from [Work’s title, author, volume, edition number and year of copyright] permission conveyed through Copyright Clearance Center, Inc.” Such notice must be provided in a reasonably legible font size and must be placed either immediately adjacent to the Work as used (for example, as part of a by- line or footnote but not as a separate electronic link) or in the place where substantially all other credits or notices for the new work containing the republished Work are located. Failure to include the required notice results in loss to the Rightsholder and CCC, and the User shall be liable to pay liquidated damages for each such failure equal to twice the use fee specified in the Order Confirmation, in addition to the use fee itself and any other fees and charges specified.

3.6 User may only make alterations to the Work if and as expressly set forth in the Order Confirmation. No Work may be used in any way that is defamatory, violates the rights of third parties (including such third parties' rights of copyright, privacy, publicity, or other tangible or intangible property), or is otherwise illegal, sexually explicit or obscene. In addition, User may not conjoin a Work with any other material that may result in damage to the reputation of the Rightsholder. User agrees to inform CCC if it becomes aware of any infringement of any rights in a Work and to cooperate with any reasonable request of CCC or the Rightsholder in connection therewith.

4. Indemnity. User hereby indemnifies and agrees to defend the Rightsholder and CCC, and their respective employees and directors, against all claims, liability, damages, costs and expenses, including legal fees and expenses, arising out of any use of a Work beyond the scope of the rights granted herein, or any use of a Work which has been altered in any unauthorized way by User, including claims of defamation or infringement of rights of copyright, publicity, privacy or other tangible or intangible property.

5. Limitation of Liability. UNDER NO CIRCUMSTANCES WILL CCC OR THE RIGHTSHOLDER BE LIABLE FOR ANY DIRECT, INDIRECT, CONSEQUENTIAL OR INCIDENTAL DAMAGES (INCLUDING WITHOUT LIMITATION DAMAGES FOR LOSS OF BUSINESS PROFITS OR INFORMATION, OR FOR BUSINESS INTERRUPTION) ARISING OUT OF THE USE OR INABILITY TO USE A WORK, EVEN IF ONE OF THEM HAS BEEN ADVISED OF THE POSSIBILITY OF SUCH DAMAGES. In any event, the total liability of the Rightsholder and CCC (including their respective employees and directors) shall not exceed the total amount actually paid by User for this license. User assumes full liability for the actions and omissions of its principals, employees, agents, affiliates, successors and assigns.

6. Limited Warranties. THE WORK(S) AND RIGHT(S) ARE PROVIDED “AS IS”. CCC HAS THE RIGHT TO GRANT TO USER THE RIGHTS GRANTED IN THE ORDER CONFIRMATION DOCUMENT. CCC AND THE RIGHTSHOLDER DISCLAIM

ALL OTHER WARRANTIES RELATING TO THE WORK(S) AND RIGHT(S), EITHER EXPRESS OR IMPLIED, INCLUDING WITHOUT LIMITATION IMPLIED WARRANTIES OF MERCHANTABILITY OR FITNESS FOR A PARTICULAR PURPOSE. ADDITIONAL RIGHTS MAY BE REQUIRED TO USE ILLUSTRATIONS, GRAPHS, PHOTOGRAPHS, ABSTRACTS, INSERTS OR OTHER PORTIONS OF THE WORK (AS OPPOSED TO THE ENTIRE WORK) IN A MANNER CONTEMPLATED BY USER. USER UNDERSTANDS AND AGREES THAT NEITHER CCC NOR THE RIGHTSHOLDER MAY HAVE SUCH ADDITIONAL RIGHTS TO GRANT.

7. Effect of Breach. Any failure by User to pay any amount when due, or any use by User of a Work beyond the scope of the license set forth in the Order Confirmation and/or these terms and conditions, shall be a material breach of the license created by the Order Confirmation and these terms and conditions. Any breach not cured within 30 days of written notice thereof shall result in immediate termination of such license without further notice. Any unauthorized (but licensable) use of a Work that is terminated immediately upon notice thereof may be liquidated by payment of the Rightsholder's ordinary license price therefor. Any unauthorized (and unlicensable) use that is not terminated immediately for any reason (including, for example, because materials containing the Work cannot reasonably be recalled) will be subject to all remedies available at law or in equity, but in no event to a payment of less than three times the Rightsholder's ordinary license price for the most closely analogous licensable use plus Rightsholder's and/or CCC's costs and expenses incurred in collecting such payment.

8. Miscellaneous.

8.1 User acknowledges that CCC may, from time to time, make changes or additions to the Service or to these terms and conditions, and CCC reserves the right to send notice to the User by electronic mail or otherwise for the purposes of notifying User of such changes or additions provided that any such changes or additions shall not apply to permissions already secured and paid for.

8.2 Use of User- related information collected through the Service is governed by CCC's privacy policy, available online here:  
<http://www.copyright.com/content/cc3/en/tools/footer/privacypolicy.html>.

8.3 The licensing transaction described in the Order Confirmation is personal to User. Therefore, User may not assign or transfer to any other person (whether a natural person or an organization of any kind) the license created by the Order Confirmation and these terms and conditions or any rights granted hereunder provided, however, that User may assign such license in its entirety on written notice to CCC in the event of a transfer of all or substantially all of User's rights in the new material which includes the Work(s) licensed under this Service.

8.4 No amendment or waiver of any terms is binding unless set forth in writing and signed by the parties. The Rightsholder and CCC hereby object to any terms contained in any writing prepared by the User or its principals, employees, agents or

affiliates and purporting to govern or otherwise relate to the licensing transaction described in the Order Confirmation, which terms are in any way inconsistent with any terms set forth in the Order Confirmation and/or in these terms and conditions or CCC's standard operating procedures, whether such writing is prepared prior to, simultaneously with or subsequent to the Order Confirmation, and whether such writing appears on a copy of the Order Confirmation or in a separate instrument.

8.5 The licensing transaction described in the Order Confirmation document shall be governed by and construed under the law of the State of New York, USA, without regard to the principles thereof of conflicts of law. Any case, controversy, suit, action, or proceeding arising out of, in connection with, or related to such licensing transaction shall be brought, at CCC's sole discretion, in any federal or state court located in the County of New York, State of New York, USA, or in any federal or state court whose geographical jurisdiction covers the location of the Rightsholder set forth in the Order Confirmation. The parties expressly submit to the personal jurisdiction and venue of each such

Confirmation Number: 11328053

Citation Information

Order Detail ID: 66589433

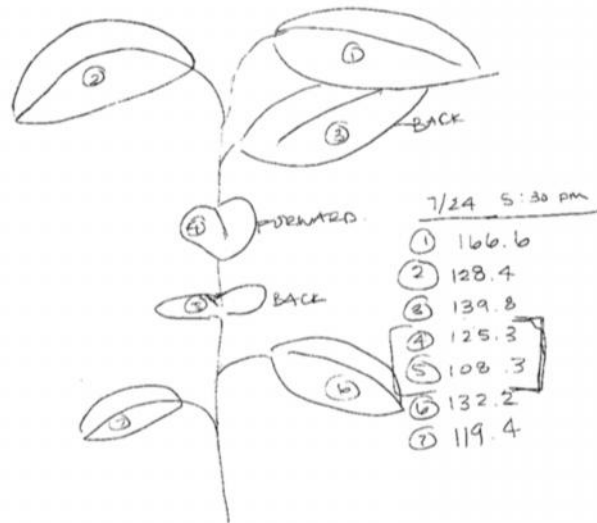
Ecological monographs by ECOLOGICAL SOCIETY OF AMERICA Reproduced with permission of ECOLOGICAL SOCIETY OF AMERICA, ETC. in the format Republish in a thesis/dissertation via Copyright Clearance Center.

## **Appendix D**

### **L. BENZOIN ILLUSTRATION**

An example of illustrations drawn during the lab portion of this thesis can be found on the following page.

L1 - July 24, 2014



node	height (cm)
1	0.5
2	2.3
3	4.5
4	7
1st L	8

8/1 20:00

1	71.3
2	35.2
3	86.4
4	67.9
5	38.7
6	49.5
7	33.3